THE EFFICACY OF UTILISING A GPS-BASED INERTIAL MEASUREMENT UNIT TO CONDUCT BIOMECHANICAL ANALYSIS DURING RUNNING

MICHAEL LAWSON

A thesis submitted in partial fulfilment of the requirement of Staffordshire University for the degree of Doctor of Philosophy

January 2024

Acknowledgements

I would like to acknowledge all of the people who have supported me throughout the process of completing this thesis. Without their direction and advice, the accomplishments of this thesis would not have been possible.

I am especially thankful to my supervisors, Professor Roozbeh Naemi, Dr Robert Needham and Professor Nachi Chockalingam, who have guided and supported me throughout this research. I greatly appreciate their patience and the discussions around the various aspects of the research. I am also grateful for the training I have received during my PhD, which has undoubtedly improved my academic and professional skill set.

I would also like to thank my employers during this time, Shabab Al Ahli F.C, AIK Fotboll and Middlesbrough F.C., for providing me with the opportunity to complete my research.

To my mum and dad, thank you for always believing in me and for providing me with the opportunities to pursue a career in sport.

Finally, none of this would have been possible without the love and support of my wonderful wife, Laura and our daughter, Rae. Their encouragement and belief in me, made completing this thesis possible, and I would not be the person I am today without them.

Peer-reviewed publications relevant to this thesis:

Lawson, M., Naemi, R., Needham, R. A., & Chockalingam, N. (2023). The Effects of Running Kinematics on Peak Upper Trunk GPS-Measured Accelerations during Foot Contact at Different Running Speeds. *Applied Sciences*, 14(1), 63.

Lawson, M., Naemi, R., Needham, R. A., & Chockalingam, N. (2024). Can Machine Learning Predict Running Kinematics Based on Upper Trunk GPS-Based IMU Acceleration? A Novel Method of Conducting Biomechanical Analysis in the Field Using Artificial Neural Networks. *Applied Sciences*, 14(5), 1730.

Book chapter relevant to this thesis:

Needham, R.A., Sinclair, J.K., Lawson, M., Naemi, R. and Chockalingam, N. (2022). 'Gait analysis – kinematics' in Chockalingam, N. (1st) *Technologies and Techniques in Gait Analysis: Past, Present and Future.* Stevenage: Institution of Engineering & Technology, pp: 61-84.

Peer-reviewed conference presentation relevant to this thesis:

Lawson, M., Naemi, R., Needham, R. A., & Chockalingam, N. (2021). The Validity of GPS-Based Accelerometer to Measure Foot Stance Characteristics During Running. *XXVIII Congress of The International Society of Biomechanics.* Stockholm, Sweden.

ABSTRACT

Biomechanical analysis offers detailed insight into an individual's movement strategies. Spatiotemporal variables, segmental peak accelerations and joint kinematics are variables that have been linked to predictors of athletic performance and injury risk. Their inclusion within the monitoring frameworks of team sports athletes could further add to the assessment of an athlete's response to training load and aid in establishing an athlete's physical condition. Therefore, the aim of this thesis was to investigate the capabilities of a Global Positioning System (GPS) based Inertial Measurement Unit (IMU) to measure the running biomechanical variables that can be used within the context of athlete monitoring frameworks.

The first study focused on accurately identifying foot stance characteristics to calculate spatiotemporal variables of running (Chapter 3). Accuracy was running speed dependant and potentially influenced by an individual's running style on the acceleration profile of the GPS-based IMU. To understand this further, an investigation was conducted into the effects of running kinematics on the peak accelerations captured by the GPS-based IMUs (Chapter 4). Results showed that the peak velocities of body segments had, on average, a greater effect than the joint/segment angles. More specifically, the peak velocities of the shank and pelvis during the impact subphase of the foot stance had the largest effect on the resultant peak accelerations captured by the GPS devices. Considering the strengths of these relationships found, a method is developed within Chapter 5 where artificial neural networks (ANN) were utilised to predict running kinematics from GPS-based IMU, anthropometric and running speed data. It was found that sagittal plane kinematics of the trunk, pelvis, hip, thigh and knee could all be estimated with different levels of accuracy.

In this thesis, a series of novel methods to conduct biomechanical analysis of running was developed with GPS devices commonly used by team sports athletes. These newly developed data processing and analysis techniques lay the foundations for increasing the biomechanical understanding of athletes in the field concerning sports performance and injury occurrence.

Table of Contents

Table of Figures

Table of Tables

Table of Equations

List of abbreviations:

ACL	=	Anterior Cruciate Ligament
ANN	=	Artificial Neural Networks
AP	=	Anterior-Posterior
GLMM	=	Generalized Linear Mixed Models
GPS	=	Global Positioning Systems
IFC	=	Initial Foot Contact
IMU	=	Inertial Measurement Units
IOR	=	Istituto Ortopedico Rizzoli
LFF	=	Low-Frequency Fatigue
m/s	=	Meters per second
ML	=	Medial-lateral
MS	=	Midstance
RES	=	Resultant
RMSE	=	Root Mean Squared Error
rRMSE	=	Relative Root Mean Squared Error
TFC	=	Terminal Foot Contact
VT	=	Vertical

Chapter 1: Introduction

1.1. Background:

The inclusion of global positioning systems (GPS) within athlete monitoring frameworks has expanded the capabilities of coaches, sports science and medical practitioners to quantify the field-based workload of athletes. Since the mid-2000s, these devices have been heavily employed in sports teams to track the quantity and rate of an athlete's locomotion through derivatives of distance and speed[1–3]. Application of this data, in theory, aids in the periodisation of training programs to ensure the correct physiological stimulus is provided to the athletes whilst minimising fatigue and reducing injury risk[4–8].

Conversely, in this time, there has been an exponential increase in soft tissue injuries in team sports such as football[9,10]. Causes of soft tissue injuries are multifactorial[11], and there are limitations of monitoring frameworks that have a heavy reliance on GPS data to manage injury risk. GPS variables such as total distance and distance of high-speed running (distance accumulated at speeds >18 km/h) have displayed a limited ability to predict soft tissue injuries[12]. The inclusion of variables such as injury history has increased accuracy in injury forecasting models[13]. However, there is yet to be a consensus on the most effective methodology or choice of variables to utilise in managing injury risk[14,15].

Measuring the quantity and rate of locomotion alone in athlete monitoring does not provide a comprehensive insight into the physical condition of athletes (i.e. neuromuscular fatigue and running economy). Analysis of these variables offers the quantification of training load or 'dose' and thus further information is required to measure an athlete's response to the

training stimulus[16]. Typically, practitioners employ additional assessments of their athletes to measure response[17]. Jump testing[18,19], blood taxonomy[20,21], muscle strength tests[22,23], repeated sprint testing [24,25] and subjective questionnaires[26,27] are popular assessments within the literature employed as measures of response. Albeit, in practice, there are barriers that can prevent the frequent use of these tests within athlete monitoring frameworks including equipment costs, specialised training requirements for staff, athlete/coach buy-in and time constraints[16]. Therefore, there is a need for an additional/alternative assessment of response that can be integrated more conveniently within the team sports environment.

A potential method of measuring response may already be present within GPS devices. In addition to global coordinate data, GPS devices also contain high-frequency tri-axial accelerometers. Inertial measurement units (IMU) such as accelerometers and gyroscopes have been used extensively in both the clinical and sports industries to provide detailed insights into human movement[28–32]. When IMUs are attached to a body segment, they capture the acceleration profile of that segment. During locomotion, time points of key gait events such as initial foot contact (TFC) and terminal foot contact (TFC) can be identified within the acceleration profile, which can be used to measure spatiotemporal variables of walking/running such as step frequency[33,34], stride length[35,36] and stance/flight time[37,38]. Furthermore, methodologies have been developed to measure walking/running style by directly estimating joint kinematics[29,39,40], or indirectly, by measuring the attenuation of ground reaction force to infer kinematic strategies[41–43].

Spatiotemporal variables that quantify running style have been of particular interest in relation to sports performance. Increased step frequency has been associated with reduced injury risk[44], and stance time is an important variable in running performance[45,46], which can also be employed as a proxy measure of neuromuscular fatigue[47]. Recently, van Oeveren et al.[48] suggested that the fundamental differences in running styles can be distinguished by measuring step frequency (normalised to leg length), step length (normalised to leg length), and stance/flight time. These four variables are often associated, in the literature, with biomechanical predictors of performance, such as running economy and force production capabilities[46,49–51]. The authors proposed the 'dual axis' framework that uses these variables to categorise running styles into the following categories: bounce (long flight time and short stance time), stick (short flight time and long stance time), push (large step length and lower step frequency), hop (small step length and higher step frequency) and sit (medium stance/flight time and medium step length/frequency) as indicated in Figure 1.1[48]. The athletes position on the vertical axis (stance vs flight time) is partially descriptive of the lower limb kinematics/kinetics and the position on the horizontal axis (step length vs step frequency) represents the athlete's force production capabilities[48]. They acknowledge that running style is speed-dependent but stipulate that all runners can be grouped into one of the five running styles. The framework intends to allow coaches to distinguish running styles between athletes and provide the basis for future investigations about the most economical running style and associated injury risks[48].

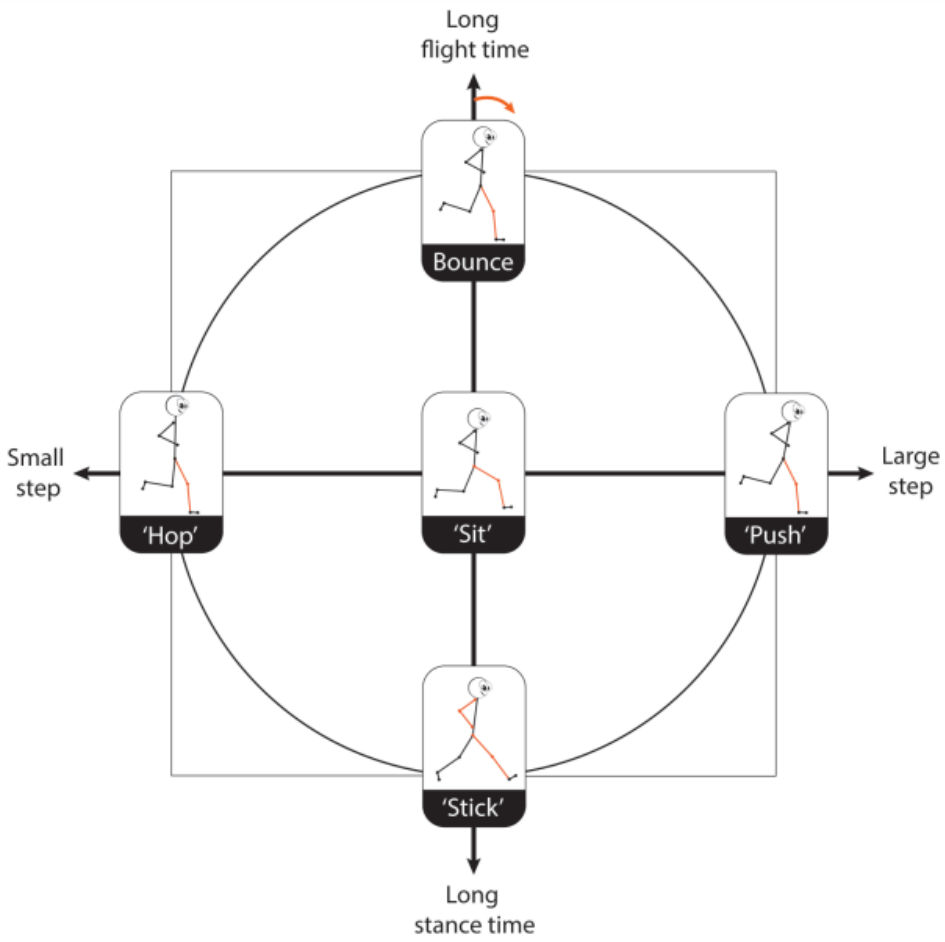

Figure 1.1. Visualisation of the Dual axis framework to characterise the fundamental differences in running styles between individuals. The horizontal axis represents a high stride frequency on the left (hop) and a large stride length on the right (push). The ratio between stance and flight time is represented in the vertical axis with long flight time (bounce) at the top and long stance time (stick) at the bottom. The centre represents medium values of all variables (sit). From "The biomechanics of running and running styles: a synthesis", B.T. van Oeveren, C.J. de Ruiter, P.J. Beek, J.H. van Dieën, 2021, Sports Biomechanics, Published online March 4 2021, 1-39. The dual Axis framework section, Figure 7 (doi:10.1080/14763141.2021.1873411). CC BY-NC-ND 4.0.

In addition, measuring joint angles has been of interest when more specific analysis is required into an individual's running kinematics. Analysing knee joint kinematics provides insights into the rehabilitation progress of athletes who have undergone knee ligament surgery[52]. It can also be useful in assessing the risk of knee ligament injury, as athletes with reduced knee

flexion are at greater risk[53]. However, there is a scarcity of field-based studies that have measured joint kinematics longitudinally with IMUs due to errors associated with sensor misalignment and gyroscopic drift[30,54,55]. Advanced data processing procedures such as machine learning algorithms can overcome these issues, as they can analyse relationships within data sets when the linearity and normality of the data have been skewed[56]. Additionally, they contain training and testing modules whereby the model learns the strengths of the relationships between variables and then tests out the model's ability to estimate the output variables[56]. However, methods utilising deep learning algorithms with IMU data to estimate joint kinematics have only been developed recently[39,57,58]. As a result, most applied field-based studies have indirectly measured running kinematics with IMUs by capturing the peak accelerations of segments. Differences in peak accelerations between two segments in the kinetic chain can provide insights into the shock attenuation properties of the joints between the segments as a more flexed joint angle will result in greater attenuation[59,60]. This methodology has been applied to observing running kinematic alterations during fatigued running[61,62].

Analysing biomechanical variables is valuable in providing insights into the physical condition of athletes and, if applied within team sports, could provide an alternative measure of response within athlete monitoring frameworks. However, measuring spatiotemporal variables and joint angles has yet to be validated with the IMUs contained within GPS devices. Most manufacturers utilise IMU data to quantify external loading placed upon athletes through the sum of all axial accelerations (Playerload^{TM}) or by analysing peak accelerations during contact (either from the ground or an opposition player) as standard[63,64]. Previous

investigations that have measured spatiotemporal variables with GPS devices have either not mounted the sensor in its conventional position[65] (in a standard vest positioning the device between the scapular) or have done so in a single-participant study design[66]. Furthermore, Buttfield (2016) analysed step waveforms from the GPS accelerometer but did not validate their step identification method against a motion capture system[67]. IMU mounting sites can affect the accuracy of measuring spatiotemporal variables with IMU sensors[68], and multiple participants are required to validate accuracy[69]. Despite the existence of considerable developments and research in this field, it remains unclear whether the GPS-based IMU can accurately provide detailed biomechanical insight into the locomotion of athletes.

The potential application of GPS devices to capture biomechanical variables appeals to sports science and medical practitioners. These devices are already commonly employed with athletes and, therefore, would not require investment in additional analysis tools. Many sports teams likely have large amounts of historical data, enabling trends analysis and establishing benchmarks for their cohort of athletes. Moreover, GPS devices have batteries that can last several hours and large data storage capacities, enabling a large window of opportunity to capture an athlete's activity in the field. Given the convenience of collecting data with GPS devices, it is clear that validating a methodology to analyse biomechanical variables would provide practitioners with a practical means to capture an athlete's quality of locomotion in the field, thereby adding value to athlete monitoring frameworks.

In order to measure biomechanical variables with IMUs, it is important to accurately identify key gait events, such as initial foot contact and terminal foot contact, as this allows for the

separation of the stance, swing and flight phases during running[70]. Once these gait events have been identified, spatiotemporal variables such as stance/swing/flight time can be calculated. Additionally, methodologies that utilise IMUs to analyse running kinematics rely on the accurate measurement of the timing of ground contact to evaluate the resulting IMU acceleration profile caused by ground reaction forces[71]. Therefore, the first step to collecting biomechanical variables with GPS devices should be to assess the GPS-based IMU's capabilities to identify the key gait events. In addition, this investigation should be conducted over several speeds as this has been previously shown to affect the accuracy[72].

Once the measurement of spatiotemporal variables has been established with the GPS devices, the next step should be to investigate the effects of inter and intrasubject differences in running kinematics on the acceleration profile captured with the GPS. The mounting site of the GPS device is on the posterior aspect of the upper trunk and is potentially influenced by the segments preceding the trunk in the kinetic chain (pelvis, thigh, shank and foot). In addition, peak acceleration is a variable already outputted by most GPS manufacturers' software[63,64], and it is a commonly used variable to infer running kinematics in running-based studies with IMUs mounted on other anatomical sites[61,62]. Therefore, establishing which segments and surrounding joints have the largest effect on the acceleration profile would provide insight into whether the peak accelerations of the GPS-based IMU can identify differences/changes in running kinematics.

Directly measuring joint kinematics during running with IMUs is particularly difficult outside of the laboratory environment. The implementation of deep learning algorithms within the

data processing procedures of IMU data has shown great potential to overcome previous issues within regression-based methods[39,57]. Direct measurement of running kinematics could benefit practitioners wanting a detailed analysis of an athlete's biomechanics, such as those rehabilitating from an injury and analysing the effect of training interventions to increase performance. If this is achievable with GPS devices, it would provide regular field-based analysis of running kinematics and create the basis for further applied biomechanical research studies concerning sports performance and injury. Subsequently, an investigation into the predictive capabilities of artificial neural networks (ANN) to estimate running kinematics, utilising data from GPS devices, is needed.

Lastly, the methods employed to capture biomechanical variables must be reproducible for practitioners working with GPS devices to ensure ecological validity. Sports science and medical practitioners typically do not have experience in data processing techniques such as data mining, signal processing and coding. Similarly, there are time constraints when working in a sporting environment with many athletes, requiring data processing procedures to be concise and time efficient. For these reasons, the methods should be either simple or use commercially available software to process data.

1.2. Aim:

The main aim of this thesis was to investigate the capabilities of a GPS-based IMU to measure the running biomechanical variables that can be used within the context of athlete monitoring frameworks.

Following this, three main objectives of the research have been defined:

1 To develop a method of identifying key gait events during foot contact to calculate spatiotemporal variables of running gait with a GPS-based IMU (Chapter 3).
2 To investigate the relationship between running kinematics and the acceleration profile of the GPS-based IMU (Chapter 4).
3 To investigate the potential of predicting running kinematics using the GPS-based IMU, running speed and anthropometric data (Chapter 5).

1.3. Predicted Outcomes:

Considering the previous research using IMUs to measure biomechanical variables, as mentioned in section 1.1, the following predicted outcomes of the thesis are:

- The GPS-based IMU can measure spatiotemporal variables of running, but the accuracy is speed-dependent.
- Peak accelerations captured by the GPS-based IMU are related to running kinematics, with the joints/segments closest to the trunk having the largest effect.
- ANNs containing data from GPS-based IMU, running speed and anthropometric measurements will be able to estimate running kinematics.

1.4. Scope and Boundaries:

This thesis investigates the application of a GPS-based IMU to measure biomechanical variables of running on a treadmill with healthy participants. It does not include walking, multidirectional running, overground running, or participants with pathological conditions.

1.5. Ethical Clearance:

The Staffordshire University ethical committee granted ethical clearance for the studies conducted within this thesis, and all participants gave informed written consent before testing (Appendix 1).

1.6. Thesis overview:

In chapter 2 of this thesis, a literature review describes how commonly used IMU variables provide information on either the quantity, rate or quality of locomotion. This chapter provides an overview of previous literature that has employed IMUs to analyse walking and running within the clinical and sports industries. The variables covered within this review are the number of steps, cadence, stride length, speed, distance, stance/flight time, joint kinematics, impact and PlayerLoad^{TM}. The review focuses on the practical and logistical considerations of data collection for each variable by discussing the variations in set-up procedures and how they have been employed in applied research studies.

The first study in this thesis (chapter 3) determined the validity of the GPS-based accelerometer to identify key gait events of foot stance across several running speeds. Previous studies that have used IMUs mounted on the upper trunk to measure spatiotemporal variables during running have had varied accuracy that is speed dependent. Therefore, the methodology developed within this chapter to identify key gait events in the GPS accelerometer data is applied to treadmill running trials conducted at speeds ranging from 10 to 18 km/h. Each trial was captured with a motion capture system, and key gait events of initial foot contact (IFC), midstance (MS) and terminal foot contact (TFC) were identified in the coordinate data from the motion capture system and the vertical acceleration profile of the GPS-based accelerometer. The agreement between the two systems is shown through Bland-Altman plots for the calculation of stance time (s) and timings between IFC – MS and MS – TFC (s).

Following this, chapter 4 aimed to determine the effects of running kinematics over several speeds on the peak upper trunk segmental accelerations during foot contact captured with the GPS-based accelerometer. Observing differences/changes in peak segmental accelerations has been previously employed within running-based studies to analyse the kinematic alterations within an individual's running style. The surrounding joints/segments of the segment to which the accelerometer is attached will influence the magnitude of the peak accelerations, and changes in running kinematics will alter the intersegmental transfer of force throughout the kinetic chain. The positioning of the GPS devices on the upper trunk means that the kinematics of the trunk, pelvis, thigh, shank and foot segments will potentially influence the peak accelerations captured. Therefore, this chapter provides insight into the

joint/segment kinematics that have the largest effects on the peak accelerations captured by the GPS-based IMU at key gait events of foot stance. Additionally, the intersegmental relationship between segment velocities throughout the kinetic chain during foot contact is highlighted by determining which segments influence the peak accelerations of the upper trunk.

The last investigation in this thesis (chapter 5) develops a novel method to predict running kinematics from data available to practitioners working with team sports athletes. In recent years, deep learning algorithms such as artificial neural networks (ANN) have shown greater predictive accuracy than linear regression-based models to estimate joint kinematics from IMU data during walking and running as ANNs can analyse non-linear relationships between independent (input) and dependent (output) variables. Therefore, this chapter investigated whether running kinematics can be accurately estimated through an ANN model containing GPS-based accelerometer variables, running speed and anthropometric data. The results of the ANNs show which kinematic variables can be predicted with high levels of accuracy and provide insights into the individual contributions of each input variable within the models.

Chapter 2: The use of inertial measurement units to quantify the quantity, rate and quality of locomotion.

Parts of this chapter was published in the following book:

Needham, R.A., Sinclair, J.K., Lawson, M., Naemi, R. and Chockalingam, N. (2022). 'Gait analysis – kinematics' in Chockalingam, N. (1st) *Technologies and Techniques in Gait Analysis: Past, Present and Future.* Stevenage: Institution of Engineering & Technology, pp: 61-84.

Abstract:

Inertial measurement units (IMU) such as accelerometers, gyroscopes and magnetometers are powerful tools that can provide field-based analysis of quantity, rate and quality of locomotion during walking and running. Several variables derived from IMU data can provide insight into each of these three aspects of locomotion and have been employed extensively in the clinical and sports industries. This review provides an overview of the extent and context in which the current IMU-derived variables quantify these aspects of locomotion. Furthermore, the practical and logistical aspects of data collection for each variable, variations in set-up procedures, and how these are employed in applied research studies were discussed. It was found that the number of steps and cadence (number of steps/min) are the most valid and practical variables to quantify the quantity and rate of locomotion, respectively. Throughout the reviewed literature, stance and swing time are validated variables that offer basic unilateral insight into the quality of locomotion. Analysing the acceleration profiles of body segments can provide a more detailed insight into the quality of locomotion by either using multiple IMUs to directly estimate joint kinematics or analysing the peak accelerations of a single IMU to infer kinematic strategies. Recent advancements in data processing procedures by integrating deep learning algorithms offer the potential to use IMUs more frequently in applied studies to longitudinally monitor the quality of locomotion in both the clinical and sports industries. Furthermore, future research should look to develop methods using single IMU sensor setups to improve the practicality of collecting data in the field.

2.1. Introduction:

Walking and running are the two most commonly used forms of human locomotion and are achieved through the coordinated movement of the lower limbs to propel and support the body over a surface in a sinuous process. This process is referred to as a gait cycle, which contains stance and swing phases. The simplistic distinction between the two forms of locomotion is that walking employs a double limb support at the start and end of the stance phase, so there is a continuity of ground contact throughout, whereas running involves a single leg support stance phase and has periods of where there is no ground contact[70,73] as shown in Figure 2.1[61].

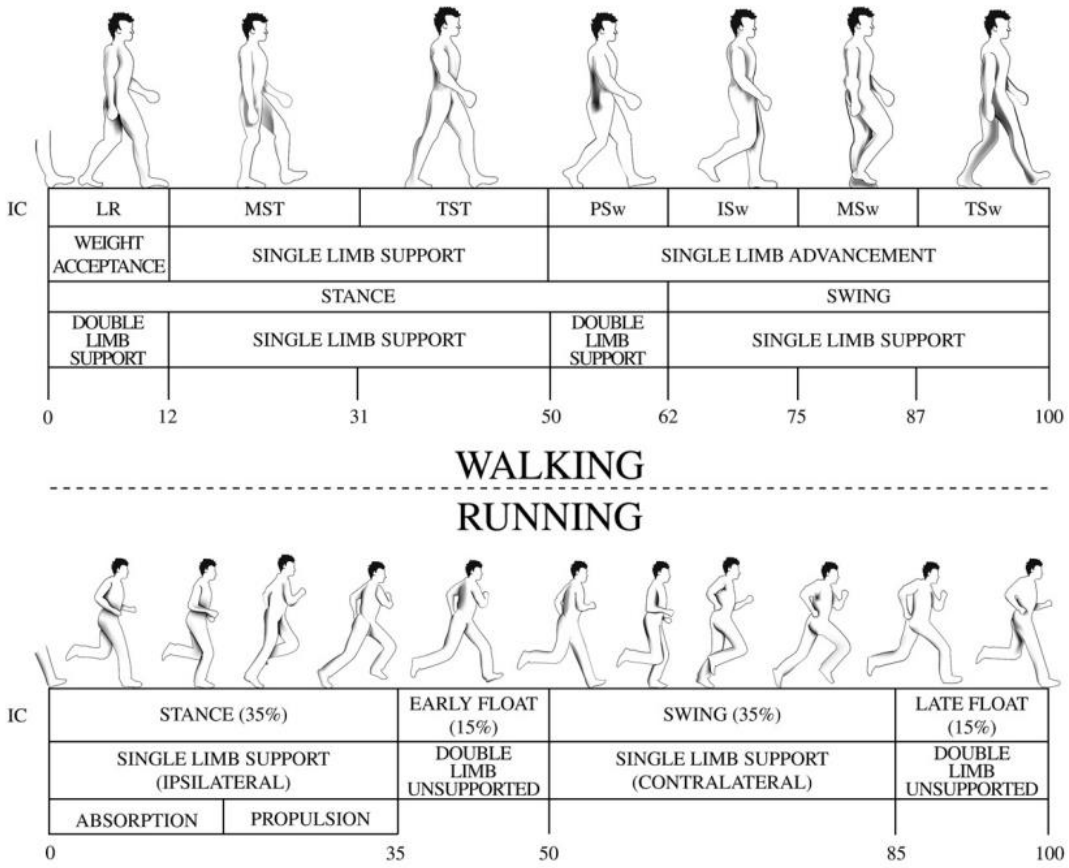

Figure 2.1. Comparison of the phases of the walking and running cycles: Initial Contact (IC), Midstance (MST), Terminal Stance (TST), Preswing (PSw), Initial swing (ISw), Midswing (MSw), and Terminal swing (TSw). Adapted from: Lohman EB, Balan Sackiriyas KS, Swen RW. A comparison of the spatiotemporal parameters, kinematics, and biomechanics between shod, unshod, and minimally supported running as compared to walking. Phys Ther Sport. 2011;12(4):151-163. doi:10.1016/j.ptsp.2011.09.004

The biomechanical evaluation of walking and running offers objective insight into the variance in technique within and between populations of people, leading to it being employed for research purposes in both the clinical[58,74,75] and sports industries[76–78]. The current gold standard to measure the temporal, kinematic and kinetic variables of locomotion utilises optoelectronic motion capture systems that use multiple cameras and force platforms to provide three-dimensional analysis[79,80]. Although some of these systems are used in a variety of environments, these systems are mainly confined to a laboratory and are time-consuming

to set up. Furthermore, they provide analysis for only a brief period and therefore may not accurately reflect a person's natural locomotion in a real-world setting[81]. This has subsequently led to the development of other more practical methods of quantifying locomotion that can be used for longitudinal analysis in the field.

Amongst these methods are inertial measurement units (IMU) as they are lightweight, easily transportable and have low power requirements[82]. IMUs contain either or a combination of the following sensors: accelerometers, gyroscopes and magnetometers. Accelerometers measure the linear acceleration of an object, and gyroscopes measure the rotational acceleration. Together, they can quantify the frequency and intensity of movement in all three planes of motion[28,83]. Magnetometers however, measure the ambulatory position and orientation of an object and are primarily employed within IMUs for azimuth determination and correction of gyroscope drift in the horizontal plane [84,85].

Similar to optical motion analysis systems, IMU sensors are used to quantify locomotion through applying specific algorithms to the IMU data that identify patterns which correspond to gait events, e.g. Initial foot contact and terminal foot contact. This allows for the stance and swing phases of gait to be distinguished and subsequent variables of interest to be calculated (contact time, stride length, peak tibial shock during stance). These algorithms will vary depending on the type of sensor set up used, but there have been several methods validated that have employed either a single IMU sensor[86] or a system of multiple sensors mounted in different anatomical locations[87]. While these methodological processes have been previously debated, the practical use of these variables and the information they are providing the

practitioner on locomotion has yet to be discussed. Norris, Anderson & Kenny (2014)[88] provided some context of application as they separated some commonly used IMU variables into research-orientated and coach-orientated variables. However, they only focused on IMU analysis of running and their method of grouping variables does not provide insight into the aspect of locomotion that is being quantified. A comprehensive overview of these variables could provide practitioners with the knowledge to make the correct choice of IMU sensor set up and to inform them on which variables to measure, depending on the aspect of locomotion intended to be quantified.

Therefore, this review aims to explore how the commonly used IMU variables within walking and running analysis provide information on either the quantity, rate or quality of locomotion. The review focuses on the practical aspects and logistics of data collection for each variable by discussing the variations in set up procedures and how they have been employed in applied research studies.

2.2. Variables related to walking:

2.2.1.1. Number of steps and Cadence:

Counting the number of steps a person makes is one of the simplest forms of analysis, and it is either presented as the total number of steps in any particular time period or as the average number of steps per minute (cadence). Its simplicity lies in the fact that a sensor must only identify the shock or the impact force transmitted to the body during a foot strike, with no requirement to measure the intensity or the temporal characteristics of the foot strike. For

this reason, step counting has been conducted since 1965[89] and was initially measured with a spring-levered pedometer sensor mounted to the hip. However, due to the mechanical design of these pedometers, they have often been found to underestimate the number of steps at lower walking speeds[90,91]. More recently, newer piezoelectric pedometers that are similar to accelerometers have been developed, as they can measure the intensity of force and accurately detect foot strikes at lower speeds[92]. One problem remains, though, because the sensors are uni-axial, the accuracy can become compromised if the sensor is tilted. This is seen with people who are severely overweight or pregnant due to the increase in waist size and wobbling mass of the upper body, which causes misalignment of the sensor and more sensor oscillations[93,94].

As a result, methods using tri-axial accelerometers have been validated when the sensor is mounted at the ankle, thigh and waist[95]. The ability to count steps in all three axes of motion theoretically means that the orientation of the sensor should not affect its accuracy. This has led to the development of step-counting applications for smartphones and other devices using the inbuilt tri-axial accelerometers. Although the validity and reliability of these applications and their algorithms are questionable, especially in real-world conditions[96], further development and research are needed to improve these devices for clinical use.

The total number of steps is a variable that quantifies the quantity of locomotion as more steps are associated with more time a person has spent walking[97]. It is most commonly employed for research purposes within the clinical industry to observe the differences in the amount of physical activity that people with debilitating physical conditions such as

Osteoarthritis[31], Osteoporosis[98], and Multiple Sclerosis[99] undertake. By combining this data with other clinical tests to assess a patient's quality of life, clinicians have been able to set physical output targets in the form of the number of steps per day in intervention programmes[99]. In addition, providing regular feedback to patients on the number of steps undertaken has been a useful motivational tool in intervention programs for overweight hypertensive patients to prevent cardiovascular disease[100]. Aoyagi & Shephard (2011)[101] also proposed that equipping just 5% of the general public with the means to count steps and meet targets could reduce national health care costs by 3.7%, which displays the important value that this variable has in the clinical industry.

On the other hand, Cadence is a variable that quantifies the rate of locomotion as more steps per minute reflects a faster pace of walking and vice versa. It is typically employed similarly to the number of steps within the clinical industry to analyse the rate of the physical output that individuals with debilitating health conditions undertake[31]. However, cadence is also important in the prevention of skeletal diseases caused by bone mineral density loss. Cadences of over 122 ± 10 steps/min corresponded to peak vertical accelerations and peak loading rate values recommended to maintain bone health (>4.9g and 43 BW/s respectively)[102]. Therefore, the regular use of this measure as a proxy measure of peak loading rates is essential for older adults at risk of osteoporosis.

The total number of steps and cadence can provide insight into the quantity and rate of locomotion, however on their own, they do not assess the quality of locomotion. This is

because these variables view the human body as a non-animated mass and cannot differentiate between the motions of the individual limbs or segments of the human body.

2.2.1.2. Stride length, Speed and Distance:

The calculation of average walking speed in the field can be done easily with a stopwatch when the distance covered is known. When the distance is unknown, stride length and number of strides can be used to estimate walking speed[103]. A stride is considered as two consecutive steps on the same limb, and stride length is the distance between these two steps. Multiplying the stride length by the number of strides will give the total distance covered, and dividing the distance over time will give the average walking speed. As previously mentioned, identifying a step with an IMU is simple. However, the calculation of stride length is more complex.

A variety of methods have been developed to measure stride length, yet they all are based initially on identifying foot contact through the protocols previously discussed. Amongst these methods are human gait models, which estimate stride length by measuring the vertical displacement of the centre of mass with an inverted pendulum model[104,105] as illustrated in Figure 2.2[106]. The benefit of this model is that it only requires one triaxial accelerometer placed at the centre of mass to analyse both limbs. Though, this method requires additional anthropometric information, and the calculation procedures are extensive when highly accurate measurement is required[107]. Another approach is the direct integration method, which does not require anthropometric data. This is because it uses an added gyroscope to

measure sensor and limb orientation with respect to the global coordinate system and then integrates the sensor acceleration, from the start and end of the stride, to estimate the stride length[108]. However, for bilateral analysis, an accelerometer and gyroscope need to be attached to each foot, and the accuracy of this method is heavily dependent on the correct identification of sensor orientation.

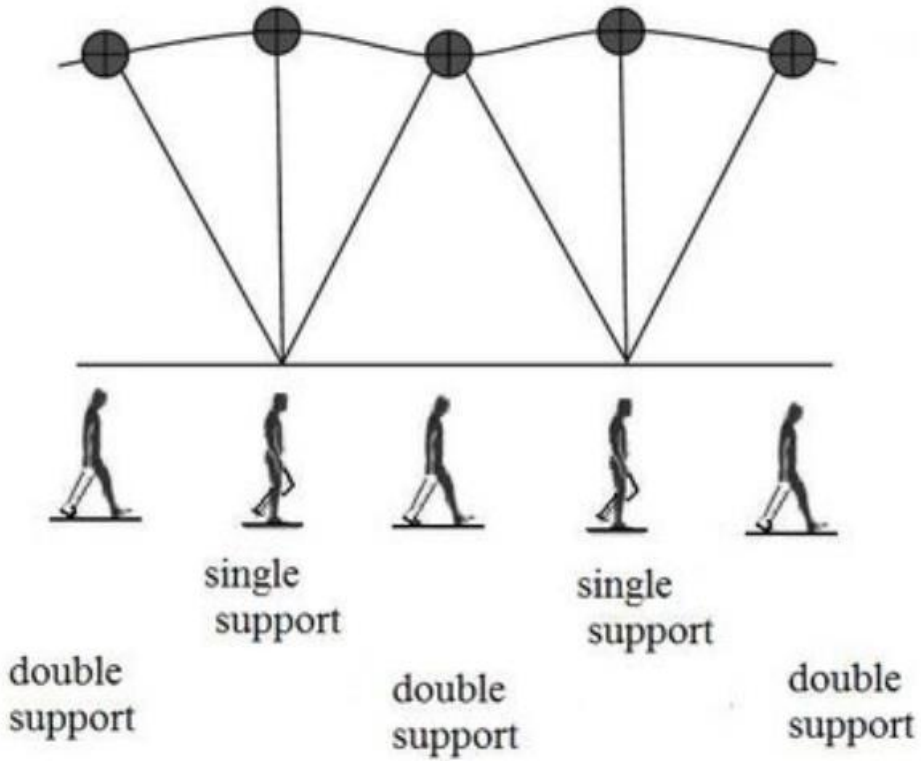

Figure 2.2. Illustration of the inverted pendulum model of walking. Adapted from: Zielinska T, Gao Z, Zurawska M, Zheng Q, Mergner T, Lippi V. Postural balance using a disturbance rejection method. In: 2017 11th International Workshop on Robot Motion and Control (RoMoCo). IEEE; 2017:23-28. doi:10.1109/RoMoCo.2017.8003888

Stride length is a variable that quantifies the quality of locomotion as it provides insight into how a person walks. When combined with the number of steps, the quantity and rate of

locomotion can be quantified through distance and speed, respectively. In theory, using these three variables could appeal to clinical practitioners as they quantify the three aspects of locomotion. In practice, however, this is not the case as the validity of the stride length is only acceptable for people with normal walking gait, and there are large errors when applied to people with pathological conditions[109]. Further research and development are needed before these variables can be used widely for clinical walking gait assessment.

2.2.2. Stance and swing:

Identification of initial foot contact (IFC) and terminal foot contact (TFC) allows for the distinction between the two phases of gait (stance and swing), and subsequently, variables such as stance time and swing time can be calculated. There have been several validated multiple sensor systems that use accelerometers and/or gyroscopes to detect IFC and TFC when mounted at either the foot[110], shank[111] or thigh[112]. For unilateral limb comparison, though, sensors must be placed on each leg, which increases set-up time and cost and requiring data integration procedures. Instead, single sensor systems have also been developed mounted close to the centre of mass, on the pelvis/lumbar spine, to provide unilateral comparisons[35,113]. These methods use linear acceleration peaks within the anterior/posterior axis to detect IFC and TFC and peaks within the medial/lateral axis to identify which foot is in contact with the ground. McCamley et al.[114] also showed that IFC and TFC are identifiable in the vertical axis with enhanced signal processing techniques. Single-sensor methods, therefore, maybe a better option for field-based analysis.

Stance time can be separated into periods of single-limb support and double-limb support by identifying the time between the IFC and TFC of each limb and calculating the difference. It represents the ability of the lower limbs to support the human body during locomotion[115]. Alternatively, swing time, which is the time between TFC and IFC, represents the motor control ability of a person to maintain an evenly balanced walking gait[116]. Stance and swing phase variables are of interest for hemiplegic patients where both neuromuscular and motor control ability is affected. It has been reported that patients who have suffered a stroke spend more time in the double support stance phase, and total swing time is also increased[112,116]. Also, unilateral comparisons have shown that the stance time of the affected limb is less than the unaffected[115]. The analysis of the two phases of gait allows practitioners to assess what degree a person's neuromuscular capability has become impaired and has also been used in the analysis of other pathological conditions that cause large impairments in walking ability, such as Parkinson's disease[117]. However, this is only to a certain extent as they fail to show the effect of only discrete changes in a person's walking gait as seen after an anterior cruciate ligament reconstruction[118].

Similar to stride length, stance time and swing time quantify the quality of locomotion. However, this is achieved only to a basic level, as they view the human body unilaterally regarding the left and right lower limbs and cannot provide insights into the individual motions of the foot, shank and thigh segments within each limb. Usually, the stance and swing time calculation does not require long pre-calibration procedures; hence, they are a more practical option than stride length.

2.2.3. Joint Kinematics:

The analysis of the segmental motions and relationships of the lower limbs during walking can provide insight into the motor control capabilities of the central nervous system. One way of assessing this ability is to observe the relationships of the segments through quantifying joint kinematics[119]. When doing so with IMUs, a multiple-sensor setup is required, which usually involves placing one IMU above and below the joint on the body segments, as shown in Figure 2.3[120]. Sensor fusion algorithms are then used to recreate a biomechanical model of the human body by analysing the linear relationship between the sensor's acceleration profiles. Several methods have been developed to measure joint kinematics using triaxial accelerometers and/or gyroscopes[121–127]. The accuracy of these linear regression-based methods depends on the ability to measure sensor orientation relative to an inertial frame and, therefore, requires lab-based pre-calibration procedures[122]. Some methods have also included magnetometers to reduce gyroscope drift error, which is effective within controlled settings[84]. However, magnetic disturbances are common in buildings, and their inclusion for long-term monitoring is not practical[128].

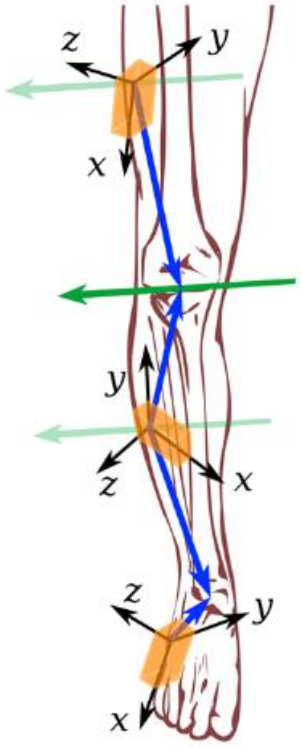

Figure 2.3. Placement of IMU sensors (orange) on the thigh, shank and foot for measurement of knee and ankle joint angles in sensor fusion methods. The green arrows represent the coordinates of the joint axis direction and the blue arrows represent the joint position (blue arrows) in the local coordinate systems. Adapted from: Seel T, Raisch J, Schauer T. IMU-Based Joint Angle Measurement for Gait Analysis. Sensors. 2014;14(4):6891-6909. doi:10.3390/s140406891

In addition, accurate measurement of joint kinematics with the linear regression-based methods relies on the correct positioning of the IMU sensors on the anatomical axis of the segment. Motions of the soft tissue and application methods (in a garment/belt), though, can cause misalignment of the sensors, which significantly reduces accuracy and is a common issue in longitudinal monitoring[55,127]. Integration of deep learning algorithms such as artificial neural networks (ANN) has shown promise in overcoming these issues as they can learn the relationships between input (IMU data) and output (joint kinematics) variables[29,57]. Furthermore, ANNs are not limited to linear relationships and can analyse data when the

normality and/or linearity has become skewed[56]. Therefore, IMU-based methods that utilise ANNs to measure joint kinematics are more robust and are advised in longitudinal monitoring [29,57,58,127].

The development of ANNs within IMU measurement of walking kinematics is only recent, and subsequently, previous applied studies have typically utilised linear regression-based IMU methods. In these studies, the sensor set-up varies depending on the rationale for analysis and which joint and plane/s of motion are relevant. Favre et al.[121] developed a shank and thigh-based IMU set up that measured 3D knee kinematics and could detect subtle differences in individuals who had anterior cruciate ligament reconstruction (ACLR). After one year of rehabilitation, a lower flexion-extension range of motion and higher internal-external range of motion were observed in the ACLR knee compared to the contralateral knee. Conversely, Zijlstra et al.[129] didn't use an above and below joint IMU set up when analysing the differences in the gait of hip arthroplasty patients. A thorax and lower trunk-based IMU setup were used to measure frontal plane pelvic angles and trunk motion, and subsequently, higher peak-to-peak amplitudes in the trunk motion of patients with hip arthroplasty were found compared to healthy controls. These results illustrate the versatility of IMUs to measure and monitor joint kinematics in various pathological conditions, which can be used to assist in the development of surgical and rehabilitation procedures. Considering the development of IMU methods utilising ANNs, there is now scope to employ IMUs further in applied studies to measure pathological walking kinematics.

Measurement of joint kinematics offers the practitioner an in-depth analysis of the quality of locomotion. They quantify quality to a greater extent than other previously mentioned variables as they allow for the differentiation between the motions of individual segments and thus can detect discrete changes in gait that are not observed in stance and swing variables[118]. One disadvantage, though, is that to quantify the quantity and rate of locomotion, other methods of analysis or more IMUs are required. Meanwhile, a single IMU mounted on the pelvis or lumbar spine can determine stance and swing variables, speed, and distance.

2.3. Variables related to running:

2.3.1.1. Number of steps and Cadence:

In theory, the methods to identify foot contact between walking and running are the same. However, the accuracy of the methods employed in walking differs when used for running analysis. When using uni-axial accelerometers, the error increases when the running speed is >10km/h[130]. This is due to an increase in multiplanar motions, and therefore, methods using triaxial accelerometers are needed to accurately detect ground contact during running[130].

Cadence is of interest within applied running research, but it is often expressed as stride frequency or stride rate (cadence divided by 30) in the literature, and there have been several studies that have analysed the effect of manipulating this variable[131,132]. Stride frequency has been shown to influence oxygen consumption, and novice runners have naturally less optimal stride frequencies than experienced runners[131]. Consciously increasing stride frequency has also been linked to reducing the risk of injury as it decreases the tibial acceleration

experienced at the point of ground contact[133]. Including cadence in running analysis could, therefore, be potentially useful for improving running efficiency and reducing injury risk.

The number of steps and cadence still quantify the quantity and rate of locomotion in running as they do in walking. The inclusion of cadence, though, in a controlled setting where the quantity and rate are measured through treadmill-derived distance and speed, as seen so frequently in the literature, shows that cadence can also provide insight into the quality of locomotion. This is to a lesser extent than other variables, as there is no distinction between right and left[131,132].

2.3.1.2. Stride length, Speed and Distance:

As previously mentioned, there is a clear biomechanical distinction between walking and running in that running has periods of no ground contact, referred to as the double float phase[70]. The presence of this phase in running means that the inverted pendulum models used to calculate stride length, distance, and speed in walking cannot be applied directly to running. Instead, running is modelled as a spring-mass system where, during foot contact, the lower limbs (spring) absorb the energy from the upper body (mass) and then release the energy to propel the body upward and forward as illustrated in Figure 2.4[134]. This model is utilised in the direct integration method, proposed by Yang, Mohr & Lee[36], to identify the start and end points of the stride and subsequently calculate stride length, distance and speed. Similar to the walking direct integration methods, this method requires both accelerometer and gyroscope and two mounting sites on either shank for bilateral analysis. Running speed

has also been accurately estimated with accelerometers only through integrating ANNs. This method uses the acceleration profile of the gait cycle at known speeds during a controlled calibration run and then uses the same profile during an uncontrolled run to estimate the speed[135]. The benefit of this method is that it can provide bilateral analysis through a single trunk-mounted accelerometer[136]. Still, several pre-calibration runs are needed to accurately estimate a range of running speeds, which is not convenient when working with multiple athletes.

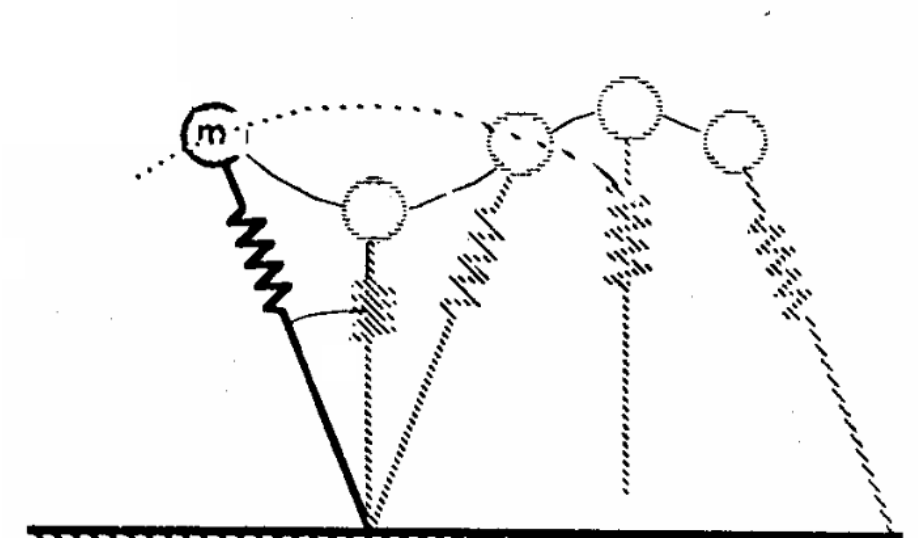

Figure 2.4. Illustration of the spring-mass system whereby the lower limbs are the springs support and propel the upper body mass (m). Adapted from: Blickhan R. The spring-mass model for running and hopping. J Biomech. 1989;22(11-12):1217-1227. doi:10.1016/0021-9290(89)90224-8

One consideration unique to running speed estimation is that accelerated running differs biomechanically from steady-state running as the body leans forward[70,137]. As a result, models that have been validated for steady-state running speed have difficulties when applied to accelerated running, such as sprinting. Parrington et al.[138] tested whether a direct integration method could accurately measure peak velocity and average 10m split time during a 100m

sprint. However, unlike previous methods that used a direct integration model, the authors used a centre of mass-mounted IMU containing an accelerometer and gyroscope. Despite the strong correlations of average 10m split velocities from 10-100m and peak velocity, the model had large errors and poor correlation in the first acceleration phase from 0-10m. Future research should focus on accounting for the differences in running kinematics during the separate phases of accelerated running.

The analysis of stride length during running is potentially useful in preventing and treating running-related injuries. Heiderscheit et al.[139] found that increasing stride frequency and decreasing stride length resulted in less mechanical energy absorbed at the hip and knee joints, possibly reducing the risk of injury. Despite this, the application of IMU-derived stride length, speed and distance in running research is lacking. Similar to walking analysis, these three variables can quantify all three aspects of locomotion with a single sensor, but further research is needed into how a practitioner can use these variables to help improve running performance.

2.3.2. Stance and Swing:

The double float phase is characterised within research studies as flight time[140]. Its inclusion within the gait cycle, along with an increased speed of locomotion, decreases the time spent in stance from 62% for walking to 31% for moderate running and 22% for sprinting[141]. Similar to walking, the measurement of this phase, stance, and swing time requires the identification of IFC and TFC. Due to the increased movement of soft tissues during running, there is more

noise within the IMU signal, and thus, identifying IFC and TFC can be difficult at higher speeds[38]. In addition, the mounting site is important in ensuring signal noise is reduced, and there have been methods validated either mounting IMUs on the tibia[68,86,142] or an IMU at the centre of mass[140,143,144]. Accelerometers and gyroscopes have been validated in these mounting sites for low to moderate running speeds, but gyroscopes perform better at speeds greater than 5.7m/s[38].

The stance phase during running also differs from walking in that the anatomical location of IFC is determined by individual running technique and running speed, which can vary between the heel, midfoot or forefoot. The type of IFC can be identified within the pattern of the accelerometer data by the timing and intensity of the accelerometer peaks throughout the foot contact[140]. Also, it has been suggested that in 'heel strikers', the intensity of the first vertical acceleration peak during the foot contact corresponds to the maximum loading endured, and the intensity of the second vertical acceleration peak corresponds to the maximum thrust produced[143]. This added information from the accelerometer data during the stance phase allows extra insight into the running performance and can be used by track and field coaches to analyse their athletes' force production capabilities during running. There is a correlation between shorter stance times and a faster sprinting performance[145] which is due to a greater application of force during foot contact[146]. Additionally, stance time can be used as a proxy measure of fatigue, as this increases during repeated sprint running[47]. As outline previously, there is a popular focus within training programs to increase force production during ground contact, and measuring the level of fatigue is beneficial in understanding an

athlete's physical condition; therefore, measuring foot stance time can be employed to measure these.

Swing time has also been suggested to be an indicator of running performance. Naturally, swing time decreases as speed increases, but unlike stance time, there is no correlation between swing time and sprinting performance[146]. Instead, swing time has been linked to running economy in long-distance running as athletes who employ foot stride kinematics that increases swing times and minimise stance time have a greater running economy[46]. This indicates that analysing swing time could also be used by track and field coaches with long-distance athletes. The level of the athlete needs to be considered, though, as this correlation does not appear to be consistent with elite-level runners, where non-biomechanical factors have a greater effect on running economy[147].

The association that stance and swing time in running have with other variables such as force production, fatigue and running economy shows that, like with walking, these variables quantify the quality of locomotion. Although they are typically employed within a sports performance context, they could also be used in a clinical setting with people returning to recreational running after injury. Similar to walking, they only offer a basic level of analysis into the quality of locomotion and further variables are required to gain a more in-depth assessment of a person's running biomechanics.

2.3.3. Impact and shock attenuation:

During running, impact forces of 2.5 – 8 times body weight are experienced at the point of foot contact with the ground[148]. Direct measurement of these impact forces needs to be at the point of contact, which is difficult for IMUs due to their size. Instead, many studies use IMUs mounted close to the point of contact on the shank as a proxy measure of impact forces in field-based studies[149]. The first acceleration peak from an accelerometer is used to represent the impact force, and it is referred to as 'shock'. The attenuation of the shock by the body can be analysed by calculating the difference between the peak accelerations of two segments in the kinetic chain. Typically, the shank and head are the chosen mounting sites, as this allows for insight into the force transfer through the major segments of the body[61]. However, placement on L5, close to the COM, has also been employed as a common mounting site to focus on the shock attenuation properties of the lower limbs[150].

The human body is a series of linked segments, with each segment containing its own relative mass, and thus, it does not respond to applied force the same as a single mass particle. Therefore, IMU accelerations only represent the accelerations of the segment to which the IMU is attached, and the intensity of this is not always directly proportional to the intensity of the impact force[60]. This is because of the role effective mass has on segmental acceleration. The effective mass represents the portion of the whole-body mass that is accelerated during impact[151]. It has been demonstrated that effective mass has a dominant effect on segmental acceleration over impact force, and it is possible for segment acceleration to increase when impact forces decrease if effective mass also decreases[60]. Factors that can affect the effective mass are segment geometry, joint stiffness, segment deformation, segment masses and

segment moments of inertia. Therefore, they should be considered when drawing conclusions regarding impact forces from segmental accelerations.

The analysis of shank peak acceleration and shock attenuation during running has frequently been used in the study of running-related injuries[62,71,152]. Injury is believed to occur during running when the accumulation of mechanical forces experienced by the soft tissue or bone exceeds the rate of their repairing and remodelling processes[153]. So therefore, analysing the intensity of the applied force to the body and/or how this force is attenuated throughout the segments within the kinetic chain can provide insights into the injury risk associated with certain conditions/running styles. It has been shown that, when running on harder surfaces, the body regulates the higher ground reaction forces by subconsciously increasing the effective mass, and therefore, there is no difference between tibial acceleration and running surface[154]. The same shock attenuation strategies are seen when running in shoes with different cushioning properties[155]. Though, tibial acceleration increases when the motions of the lower limbs are restricted, as seen in motion-control shoes, which have much firmer cushioning properties[156]. Likewise, shock attenuating strategies have been shown to change when the ability to self-regulate the effective mass becomes impaired under fatigue. How they change depends on the individual athlete's neuromuscular qualities and methods of inducing fatigue[61,62,152].

When measuring peak tibial acceleration alone, the rate of locomotion is quantified as the size of the peak is respective to the speed of locomotion[149]. When the running speed is known, however, measuring the change in peak tibial accelerations can quantify the quality of

locomotion and give an indirect insight into the running kinematics of a person due to the role of a person's effective mass on these peaks. This can also be extended to measuring the attenuation of shock throughout the body or individual segments if multiple IMUs are placed further up the kinetic chain, thus giving further insight into the quality of locomotion.

2.3.4. Joint Kinematics:

The analysis of joint kinematics should, in theory, be the same in running as it is in walking, as joint motion is typically analysed over the entire gait cycle, and the influence of the double float phase does not alter this. The problem is though, as the speed of locomotion increases, so does the multi-planar segmental motion, which causes large errors in methods that employ sensor fusion algorithms as described previously[122]. Additionally, deep learning algorithms have been shown to decrease these errors, but like walking analysis, these methods have only been developed recently[39,157]. As a result, previous applied studies of running haven't employed models to directly estimate joint kinematics and have instead opted for an indirect method by analysing the acceleration patterns of the individual segments to infer kinematic strategies [32,87,158].

The main area of interest in the literature on measuring segmental acceleration patterns during running has come from the changes with fatigue. Strohrmann et al.[87] conducted a comprehensive investigation using 12 IMUs positioned around the body. It was found that fatigue decreased heel lift (maximum deflection of the shank regarding the angle between the shank and vertical) and increased trunk forward leaning (average upper trunk sensor pitch

angle against vertical) independent of running surface or training level. These findings were similar to an earlier pilot study that found foot acceleration during the swing phase to decrease with fatigue[32] and thus shows that the level of fatigue is measurable with the acceleration profile of a single segment.

Considering the advancements of methods that employ deep learning algorithms to measure joint angles directly with IMU data, there is potential to combine this with shock attenuation analysis to provide greater insights into the effective mass/impact force paradigm under fatigue. The additional knowledge of the joint angle and the peak segmental acceleration at the point of impact will allow for impact force estimation if the relationship between the joint angle and the segment effective mass is assumed to be linear[60]. Future applied studies could employ these new techniques to understand further the kinematic and kinetic alterations during running under fatigue.

As with walking, analysis of joint angles through measuring segmental kinematics during running quantifies the quality of locomotion to a detailed level. Again, though, this analysis needs to be combined with measurements of quantity and rate of locomotion to understand the reason for changes. In addition, including deep learning algorithms can potentially offer more accurate measurements of joint angles with IMUs, but how these can employed within applied studies is yet to be explored.

2.3.5. PlayerLoad™:

One method of analysing locomotion that is popular in the sports industry is to measure the sum of linear accelerations of the body during a training session or game. This is due to the inclusion of accelerometers in the GPS tracking devices by manufacturers that sporting teams employ to track the physical output of their players. It is proposed that including an IMU can provide insight into the total applied force or 'mechanical load' placed on the body during exercise[64]. This variable is referred to as 'PlayerLoad™', and the simplicity of the calculation means there is no distinction between its application in analysing walking or running. The normal mounting site of the GPS device is in a special vest that places it between the scapular and the thoracic spinal region, as shown in Figure 2.5. This is significant as the extra distance from the centre of mass causes an overestimation of whole-body acceleration[64,159], which shows that PlayerLoad™ represents the motions of the trunk segment and does not directly measure the applied force on the body as initially thought.

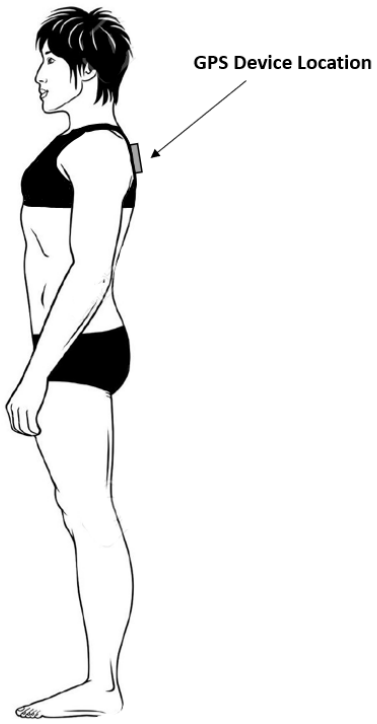

Figure 2.5. Illustration of the GPS devices (grey) positioning between the scapula on the thoracic spinal region within a specially designed vest.

Nevertheless, PlayerLoad™ has been shown to correlate with physical activity level and is employed within team sports to compare the physical demands between training and competition and in longitudinal physical load monitoring[5,160,161]. Caution should be used, though, with the findings in these studies as PlayerLoad™ only has moderate to high reliability in sport-specific locomotion and large variances between individuals[162]. This is because of the influence an individual's running kinematics has on trunk segmental acceleration, and Cormack et al.[163] suggested that PlayerLoad™ can be used to identify fatigue. However, they analysed the changes in contributions from the individual planes of motion to the overall PlayerLoad™ score rather than the sum alone. These findings are similar to previous research that has identified changes with fatigue with analysis of other body segments' accelerations[87].

Therefore, there is potentially useful insight gained from analysing the motions of the trunk segment in greater detail, but future research is needed to understand the mechanisms behind the relationship between the accelerations captured with the GPS-based IMU and running kinematics.

In the literature, PlayerLoad™ is employed as a variable to quantify the quantity and rate (when analysed as average PlayerLoad™ per minute) of locomotion[164–166]. This is incorrect, however, and modifications need to be made to the PlayerLoad™ equation to remove the overestimation error to quantify these two aspects of locomotion accurately. Instead, it can be argued that PlayerLoad™ quantifies the quality of locomotion but only when the accelerations in the individual axis are analysed. It is difficult to compare it to other variables that quantify quality, though, as the level of detail that can be gained into whole body quality of locomotion from measuring the accelerations of the trunk is yet to be explored in-depth.

2.4. Conclusion:

IMUs can accurately quantify the quantity, rate and quality of locomotion without the assistance of other technology. The number of steps is the simplest and easiest form of measuring the quantity of locomotion, and methods using a tri-axial accelerometer are the most accurate for counting steps in walking and running. Likewise, concerning the rate of locomotion, analysing the number of steps per minute (cadence) is the most practical method. Analysing the peak accelerations of the shank can also be employed to measure the rate of locomotion accurately, given its relationship with running speed. The quality of locomotion

can be analysed at two levels. The basic level views the human body in terms of left and right sides and can be characterised during walking and running by measuring stance and swing times with a single COM-mounted gyroscope. For a detailed view, the motions of the individual segments within the body must be analysed and utilising IMUs positioned on the main body segments can infer changes in walking/running kinematics. Furthermore, including ANNs with IMU data has improved the accuracy of directly measuring joint kinematics with IMUs and offers the ability to measure the discrete characteristics in an individual's quality of locomotion. The three aspects of locomotion can also be measured with stride length and stride length-derived speed and distance. However, their methods have lengthy set-up procedures, and their accuracy is limited, thus making these variables impractical for practitioners.

There has been a substantial amount of research showing that there is valuable information to be gained by quantifying all three aspects of locomotion that can be used within the clinical industry to help prevent and rehabilitate people with pathological conditions. A similar impact is seen within the sporting industry using variables which measure the quality of locomotion to enhance physical performance. However, more insight into the practical use of employing this type of analysis could be gained in both industries if sensor setup procedures and error reduction techniques were improved. Utilising single IMU sensor set-ups is preferable when there are time constraints, and integrating deep learning algorithms has shown great potential in overcoming common errors with IMU data collection. In relation to the clinical industry, developing algorithms that use smartphone-based IMUs is a potential avenue to gain more frequent analysis of locomotion. The same can be said for the development of algorithms that

use the data from the IMU contained within GPS tracking devices, as they are already well established and heavily used within the sports industry. The more time patients and athletes spend under observation will give the practitioner a clearer picture of their locomotion ability, improving the practitioner's capacity to detect abnormalities correctly and monitor intervention programmes.

Chapter 3: The validity of a commonly used athlete tracking device to measure foot stance time parameters during running.

This chapter is currently under review in the journal of applied biomechanics and the abstract was presented at the following conference:

Lawson, M., Naemi, R., Needham, R. A., & Chockalingam, N. (2021). The Validity of GPS-Based Accelerometer to Measure Foot Stance Characteristics During Running. *XXVIII Congress of The International Society of Biomechanics.* Stockholm, Sweden.

Abstract:

The overall aim of this study was to determine the validity of the GPS-based accelerometer to identify key gait events across several running speeds. Thirteen male experienced runners ran on a treadmill for 40 seconds at 9 different speeds ranging from 10-18 km/h at 1 km/h increments. Participants wore a GPS device containing an embedded high frequency tri-axial accelerometer and were recorded by an 18-camera motion capture system. Initial foot contact (IFC), midstance (MS) and terminal foot contact (TFC) were identified in the motion capture system and accelerometer and subsequent temporal measures: stance time and time between IFC, MS and TFC were calculated. Bland-Altman plots with 95% limits of agreement, Hedges g effect sizes and permutation t-test (P value = 0.05) were employed to assess the level of agreement between the two systems and to understand the magnitude of the differences observed across each running speed. Results showed lowest mean differences and highest agreement between the two systems for running speeds 15 km/h (Mean difference: -0.01 s; 95% limits of agreement: -0.05 to 0.04 s) and 16 km/h (0.01 s; -0.04 to 0.06 s) for stance time. There was a GPS-based accelerometer underestimation of stance time at lower running speeds, however there were reasonable limits of agreement at 12 km/h (-0.02 s; -0.06 to 0.01 s) and 14 km/h (-0.01 s; -0.05 to 0.02 s). This study showed valid estimations of stance time measures with the GPS based accelerometer at speeds of 12 km/h, 14 km/h, 15 km/h and 16 km/h. The results of this study can provide sports science and medical practitioners with a practical method of measuring spatiotemporal variables of running, which can be used to gain insight into the physical condition of their athletes.

3.1. Introduction:

In team sports, understanding the physical condition of athletes is an integral component for medical and sports science practitioners to appropriately manage training workloads to maximise performance whilst minimising injury risk. It is inevitable that athletes will experience fatigue in the training process however, the accumulation of fatigue due to inadequate recovery can negatively affect performance and increase injury risk [167,168]. Low-frequency fatigue (LFF) is one of the most common types of fatigue in team sports due to the repetitive high-intensity, moderate-to-high-force actions of training and match play [169]. LFF affects the body at the peripheral level as it reduces the force production capabilities of the skeletal musculature [170]. Inhibitions of the neuromuscular system can last up to 72 hours post-exercise [171]. Therefore, strategies must be employed to assess and monitor an athlete's physical condition to ensure that the correct workload prescription is applied.

There has been a wealth of research assessing the neuromuscular fatigue status of team sports players to gain insight into a player's response to workload[18–25]. Several testing methodologies have been utilised, including blood taxonomy [20,21], jump tests [18,19], muscle strength tests [22,23] and repeated sprint testing [24,25]. Albeit these methods are effective, team sports have large squads of players, and these tests are time-consuming and thus impractical for frequent daily use. In preseason, athletes can have multiple training sessions per day[172], and during the competitive season, there can be several games in a week[173]. Consequently, a valid method of assessing an athlete's physical condition is needed, which can be used frequently with large numbers of athletes.

Global positioning systems (GPS) devices are commonly employed within team sports to track an athlete's workload through derivatives of speed and distance, as they can track athletes in any outdoor environment over several hours and require minimal set-up time. Most of the common manufacturers also include high-frequency accelerometers within their devices, which can provide a different type of analysis. When attached to a body segment, accelerometers capture the micromovements of human movement during locomotion. They have been previously employed in running studies to measure foot stance time characteristics [142,144]. Neuromuscular fatigue [47], running economy [46] and running style [48,174] have all been shown to influence an athlete's foot stance times during running, which suggests that this measure could be used to assess an athlete's physical condition. In addition, identifying the key gait events during the gait cycle (initial foot contact, midstance and terminal foot contact) provides the basis for the calculation of other spatiotemporal variables of running (swing time, flight time and step frequency) and further analysis into the impact and propulsion subphases of stance [48,143].

The GPS-based accelerometer is mounted in a specially designed vest, positioning the device around the posterior aspect of the thoracic region of the spine. The mounting site of the accelerometer is an important variable in attaining accurate measurement of gait event timings[68], and consequently, previously validated methods at other sites cannot be applied directly. It was previously found that a commercial device containing an accelerometer attached to the anterior aspect of the thoracic spine, close to the sternum via a chest strap, underestimated stance time during running, but this error was speed dependent and decreased as speed increased[72,174]. Despite this, both authors recommended the use of their

devices for field-based analysis of running stance times as there was good reliability. Therefore, whether the GPS-based accelerometer can accurately determine key gait events across multiple subjects at different running speeds is yet to be determined.

The overall aim of this study was to determine the validity of the GPS-based accelerometer to identify key gait events across several running speeds. Establishing this will provide sports science and medical practitioners with a practical method of measuring running stance characteristics, which can be used to calculate spatiotemporal variables and gain insight into the physical condition of their athletes.

3.2. Material and methods:

3.2.1. Experimental setup:

Thirteen male experienced runners (age: 27 ± 3.7 years, height: 1.81 ± 0.06 m, mass: 82.7 ± 6.2 Kg) ran on a treadmill with 1-degree inclination for 40 seconds repeated at 9 different speeds ranging from 10-18 km/h at 1 km/h increments. Each participant completed 1 trial at each speed and was given a maximum amount of rest between each trial to reduce fatigue accumulation. Each trial began with the treadmill speed set at 10km/h, the participant used the handrails to enter the treadmill and was instructed to run naturally whilst an assistant set the appropriate running speed. After 40 seconds of running, the participant then used the handrails to exit the treadmill whilst the treadmill was returned to 10km/h by the assistant. Participants wore an appropriately sized standard issue vest housing a GPS device (STATSports Apex, Northern Ireland, UK) containing an embedded high-frequency tri-axial accelerometer

and were provided with standardized running shoes (Puma Anzarun). An eighteen-camera motion capture system (VICON, Oxford, UK) recorded the coordinate data of 54 infrared markers (14mm) attached to the participants with double-sided adhesive sticky tape. Ethical clearance for this testing procedure was granted by the Staffordshire University ethical committee and all participants gave informed written consent prior to testing.

3.2.2. Motion capture data acquisition:

A modified Istituto Ortopedico Rizzoli (IOR) marker set with an additional five clusters attached to the left thigh, right thigh, left shank, right shank and the posterior aspect of the GPS device (Figure 3.1) was employed [175–177]. The recording frequency of the eighteen optical cameras (VICON MXT40, Oxford, UK) was set at 100 Hz. The global coordinate system defined the X-axis as anterior-posterior progression (positive in the forward direction), the Y-axis as medio-lateral progression (positive in the left direction) and the Z-axis as the vertical progression (positive in the upward direction). The coordinate data was then transferred from the Vicon Nexus software to Visual 3D (C-Motion Inc, MD, USA) and filtered (4th order Butterworth, 10 Hz cut-off frequency) [178]. Initial foot contact (IFC) was determined as the frame of minimal vertical displacement of the calcaneal or 1st metatarsal (which ever occurred first) foot markers[144]. Terminal foot contact (TFC) was defined as the initial movement upward in vertical displacement of the 1st metatarsal foot marker[144]. Midstance (MS) was determined as the lowest point of centre of mass displacement between IFC and TFC[179].

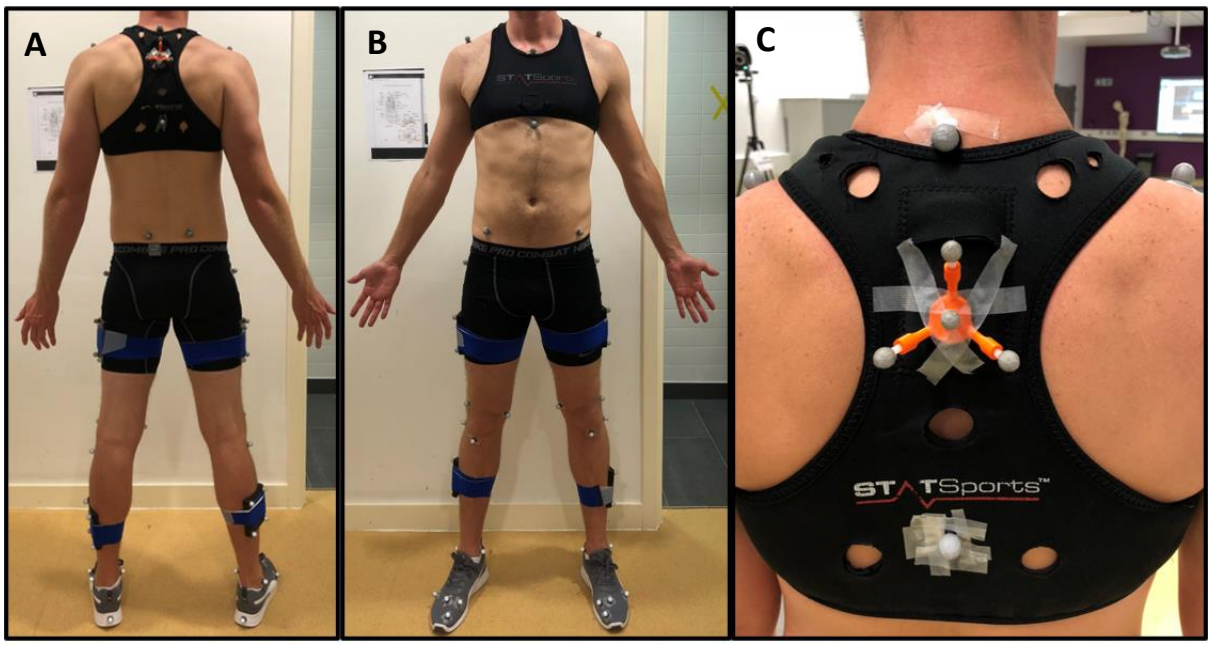

Figure 3.1. Modified IOR marker set up A) Anterior view B) Posterior view C) Cluster attached to the GPS device.

3.2.3. Accelerometer data acquisition:

The GPS device containing a tri-axial accelerometer was positioned around the posterior aspect of the thoracic region of the spine (T2) in a standard issue vest per manufacturer recommendations. The frequency of the accelerometer was set at 100 Hz. The device was orientated vertically, which corresponds the Z-axis to anterior-posterior acceleration (positive in the forward direction), the X-axis to medio-lateral acceleration (positive in the left direction), and the Y-axis to vertical acceleration (positive in the upward direction). Raw accelerometer data was transferred from the STATSports Apex software to Visual 3D (C-Motion Inc, MD, USA). A zero cross-over method of the vertical acceleration profile was used to determine IFC (negative to positive) and TFC (positive to negative) (Figure 3.2)[68]. MS was determined as the second acceleration peak in the vertical acceleration profile following IFC (Figure 3.2) [143].

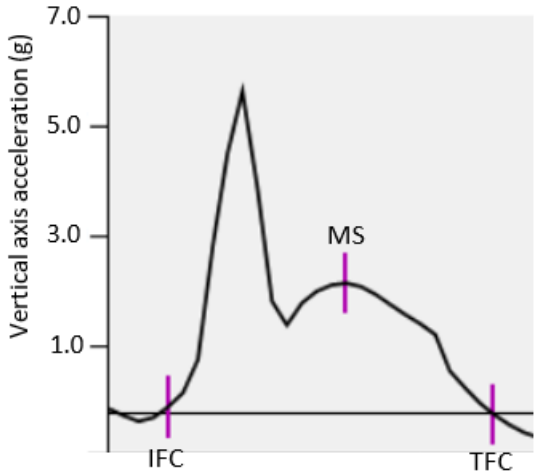

Figure 3.2. GPS-based accelerometer vertical acceleration profile displaying the method for identifying IFC, MS and TFC.

3.2.4. Data synchronisation:

To synchronise the motion capture data and accelerometer data, participants were instructed to stand still while the GPS device was 'tapped' in a downward vertical direction. This was performed before each running trial the participant completed. During the data analysis process in Visual 3D (C-Motion Inc, MD, USA) the following protocol was used to determine the timing of the tap and line up two data sets. In the motion capture data, the cluster marker attached to the GPS device was used to determine the tap as the timing of the first frame when the GPS device progressed negatively in the vertical axis. In the accelerometer data, the timing of the first frame when there was a significant negative acceleration in the vertical axis was determined as the tap.

3.2.5. Data analysis:

Analysis of the foot contacts within each trial was conducted 20 seconds after the synchronisation tap to ensure the participants were in a normal running pattern and were at the correct speed following the treadmill ramp period. The timings of IFC, MS and TFC were determined in both systems for 10 consecutive foot contacts within each trial. The time between IFC and TFC was defined as foot stance time. Stance time and time between IFC, MS and TFC were compared between the motion capture system and accelerometer across each running speed.

3.2.6. Statistical analysis:

The agreement between the motion capture system and the accelerometer was examined for all temporal variables across each speed with Bland-Altman plots including 95% limit of agreement intervals (LOA). Mean differences, Hedges g effect sizes for small sample size and permutation t-tests (p value = 0.05*)* were calculated to understand the magnitude of the difference between the two systems and determine if it was significant. Statistical analysis was conducted using SPSS software version-22 (IBM Corporation, Armonk, NY).

3.3. Results:

Stance time was significantly different ($p < 0.05$) with large to very large effect sizes (ES) between the two systems for speed conditions: 10 km/h (ES: -1.44), 11 km/h (ES: -1.32), 12 km/h (ES: -1.24), 13 km/h (ES: -0.87), 14 km/h (ES: -0.88), 17 km/h (ES: 0.88) and 18 km/h (ES:

1.02). There was a non-significant ($p > 0.05$) difference with small effect sizes for speeds 15 km/h (ES: -0.26) and 16 km/h (ES: 0.40) (Table 3.1).

Table 3.1. Validity of average stance time and average time between IFC, MS and TFC measured with the GPS-based accelerometer (GPS-ACC) compared to the motion capture system (MCS).

Speed	Variable	MCS (s)	GPS-ACC (s)	Difference (s)	Lower 95% LOA	Upper 95% LOA	Hedges g	p Value
10 km/h	Stance time (s)	0.29	0.26	-0.03	-0.09	0.02	-1.44	0.00
	IFC-MS time (s)	0.11	0.12	0.00	-0.05	0.05	0.09	0.81
	MS-TFC time (s)	0.18	0.14	-0.04	-0.06	-0.02	-2.82	0.00
11 km/h	Stance time (s)	0.28	0.25	-0.03	-0.07	0.01	-1.32	0.00
	IFC-MS time (s)	0.11	0.11	0.00	-0.04	0.05	0.18	0.64
	MS-TFC time (s)	0.17	0.14	-0.03	-0.05	-0.01	-2.43	0.00
12 km/h	Stance time (s)	0.26	0.24	-0.02	-0.06	0.01	-1.24	0.00
	IFC-MS time (s)	0.10	0.11	0.00	-0.03	0.03	0.15	0.69
	MS-TFC time (s)	0.16	0.13	-0.02	-0.05	0.00	-1.70	0.00
13 km/h	Stance time (s)	0.26	0.23	-0.02	-0.08	0.04	-0.87	0.03
	IFC-MS time (s)	0.10	0.11	0.00	-0.05	0.05	0.12	0.75
	MS-TFC time (s)	0.15	0.13	-0.02	-0.06	0.01	-1.52	0.00
14 km/h	Stance time (s)	0.24	0.23	-0.01	-0.05	0.02	-0.88	0.03
	IFC-MS time (s)	0.10	0.10	0.01	-0.02	0.04	0.39	0.30
	MS-TFC time (s)	0.14	0.12	-0.02	-0.05	0.01	-1.37	0.00
15 km/h	Stance time (s)	0.23	0.23	-0.01	-0.05	0.04	-0.26	0.50
	IFC-MS time (s)	0.10	0.10	0.01	-0.03	0.04	0.63	0.10
	MS-TFC time (s)	0.14	0.12	-0.01	-0.06	0.03	-0.71	0.07
16 km/h	Stance time (s)	0.22	0.23	0.01	-0.04	0.06	0.40	0.30
	IFC-MS time (s)	0.09	0.10	0.01	-0.02	0.03	0.61	0.12
	MS-TFC time (s)	0.13	0.13	0.00	-0.06	0.06	0.09	0.81
17 km/h	Stance time (s)	0.21	0.23	0.02	-0.04	0.08	0.88	0.03
	IFC-MS time (s)	0.09	0.10	0.01	-0.03	0.04	0.65	0.10
	MS-TFC time (s)	0.12	0.13	0.01	-0.06	0.08	0.40	0.33
18 km/h	Stance time (s)	0.20	0.23	0.02	-0.04	0.08	1.02	0.01
	IFC-MS time (s)	0.08	0.09	0.01	-0.02	0.04	0.89	0.03
	MS-TFC time (s)	0.12	0.13	0.01	-0.05	0.08	0.48	0.23

*LOA = limits of agreement

Bland-Altman plots show an underestimation of stance time in the GPS-based accelerometer for speed conditions: 10 km/h (Mean difference: -0.03 s; LOA: -0.09 to 0.02 s), 11 km/h (Mean difference: -0.03 s; LOA: -0.07 to 0.01 s), 12 km/h (Mean difference: -0.02 s; LOA: -0.06 to 0.01 s), 13 km/h (Mean difference: -0.02 s; LOA: -0.08 to 0.04 s), 14 km/h (Mean difference: -0.01 s; LOA: -0.05 to 0.02 s) (Figure 3.3a). The errors in these speeds are attributed to the time between MS and TFC (Table 3.1, Figure 3.3b). An overestimation of stance time occurs at speed conditions: 17 km/h (Mean difference: 0.02 s; LOA: -0.04 to 0.06 s) and 18 km/h (Mean difference: 0.02 s; LOA: -0.04 to 0.08 s) (Figure 3.3a). Both the time between IFC and MS, and the time between MS and TFC contribute to the error in these speeds (Table 3.1, Figure 3.3b).

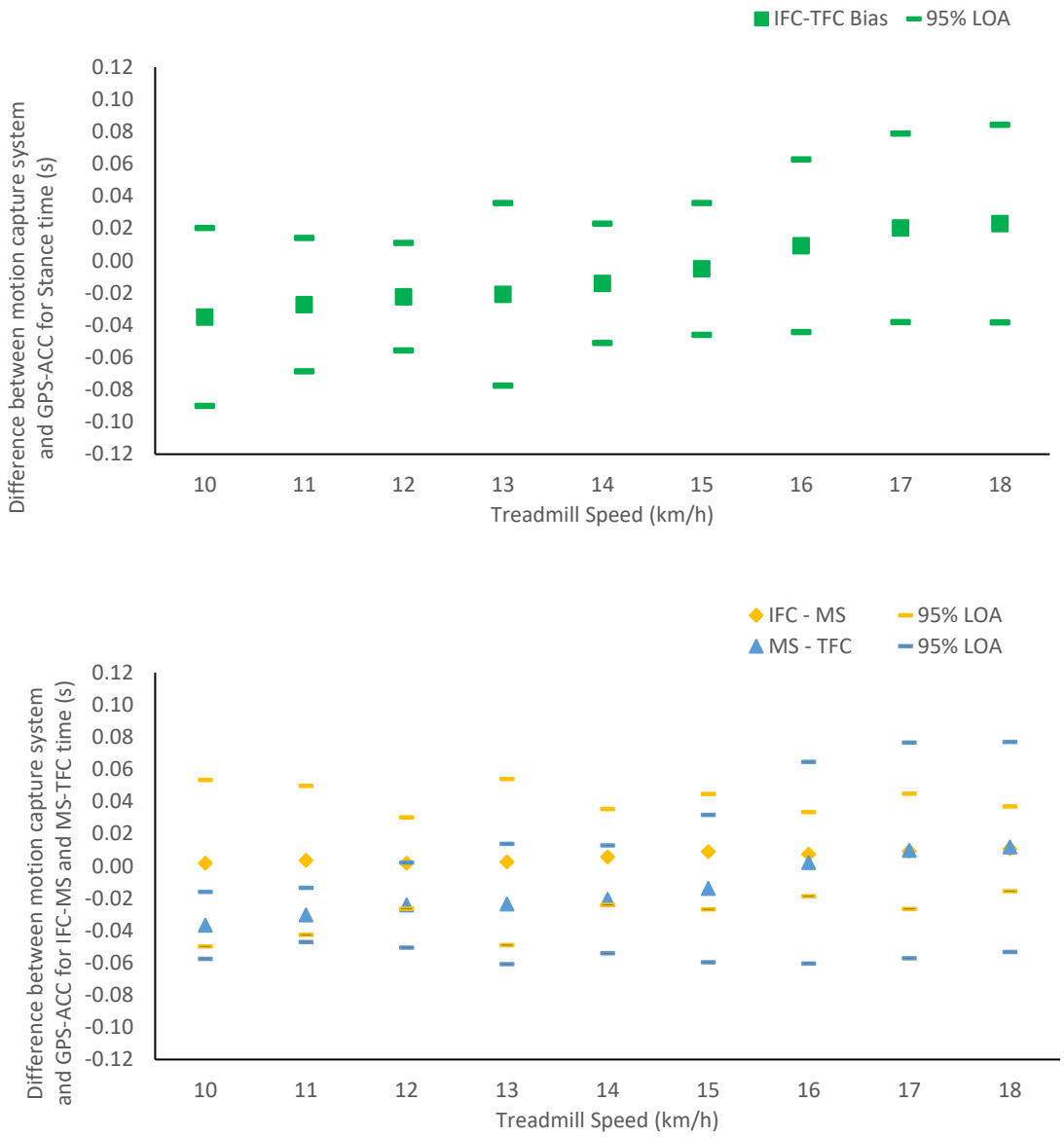

Figure 3.3. Bland-Altman plots of the difference between the motion capture system and GPS-based accelerometer in timings between a) Stance time, b) IFC and TFC, MS and TFC. LOA= limits of agreement.

Figure 3.4 shows the stance time individual means for each participant for the motion capture system and GPS-based accelerometer. There are inter-participant variances in all speed conditions which are larger at 10 km/h, 11 km/h, 13 km/h, 17 km/h and 18 km/h.

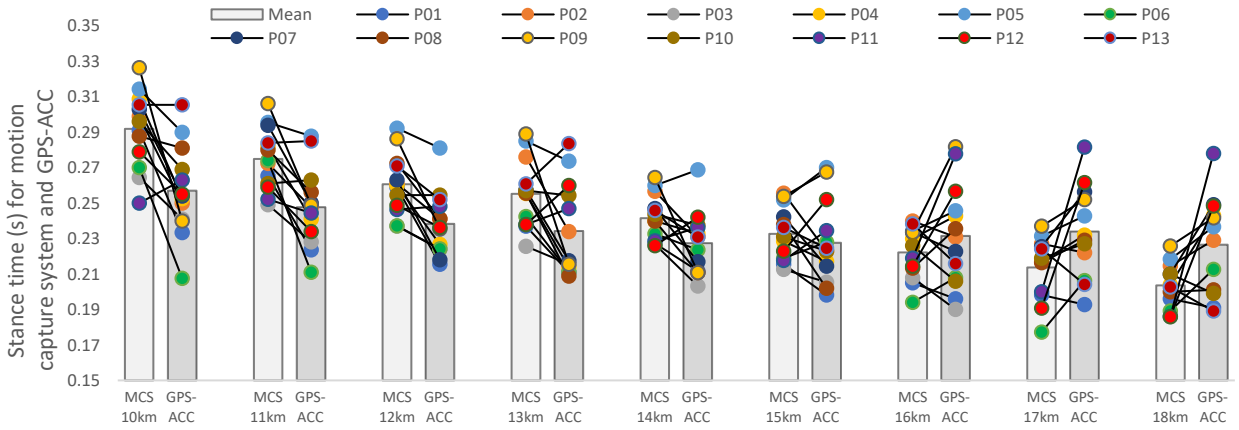

Figure 3.4. Differences between the motion capture system (MCS) and GPS-based accelerometer (GPS-ACC) in timings between Stance time for individual participants per speed trial.

3.4. Discussion:

Previous investigations of accelerometers mounted on the anterior aspect of the upper trunk, with a chest strap, found underestimations of stance time at running speeds around 10-12 km/h that decreased as the speed increased[72]. The present study observed similar results, as the error decreased from 10 – 15 km/h, despite the accelerometer being positioned on the posterior aspect of the upper trunk and within a vest. Furthermore, analysis of the subphases shows that the error present in the lower running speeds is due to a shorter MS-TFC subphase, and this caused the stance time to be underestimated. It has been suggested that the underestimation at lower running speeds is due to greater vertical oscillations present at the centre of mass compared to higher running speeds [72], which may have led to TFC being more difficult to distinguish in the accelerometer's vertical acceleration profile.

Conversely, when running speed was >16 km/h an overestimation of stance time was present which was due to errors in identifying key gait events in both subphases of stance. As running

speed increases, there is greater forward inclination and multiplanar displacement of the trunk segment[180,181]. The present study employed a uniaxial method of determining IFC and TFC with the vertical axis acceleration profile. As the trunk becomes more inclined, the sensor orientation becomes maligned from the global vertical axis, and an increase in multiplanar displacement can cause added noise within the acceleration profile. Subsequently, this can reduce the accuracy of the uniaxial zero-cross over method at higher running speeds. A method that integrates all accelerometer axis profiles when running at speeds >16 km/h may reduce this error[66]. Additionally, as running speed increases, foot contact time decreases, which can exaggerate the magnitude of the size of the errors.

Hedges g effect sizes indicated that stance time had a small, non-significant difference between the two systems at 15 km/h and 16 km/h with reasonable limits of agreement. 12 and 14 km/h had significant differences with large effect sizes but also had reasonable limits of agreement, which suggests that although there is an underestimation of stance time with the accelerometer at these speeds, they are still acceptable speeds to conduct accurate field-based measurement of stance time. 13 km/h is the outlier in these results and can be due to the small sample size of the participants employed in this study and may improve with an increased sample size.

Analysis of the individual participants provides further insight into the determinants of the differences between the two systems that group means mask. The transfer from an underestimation to an overestimation of stance time does not occur at the same speed for all participants. For example, in participants 5 and 12, an overestimation occurs at 13 and 14

km/h, respectively and increases as speed increases. In contrast, in participants 1 and 13, an overestimation does not occur independent of the running speed. Differences in lower-limb kinematics between participants due to running style have been previously shown to influence the acceleration profile of the trunk segment [182]. Lower-limb kinematics were not characterised in the present study. However, these individual trends within the results suggest that individual running style may be a determinant of the accelerometer's accuracy in measuring stance time. Further investigation into the influence of different running styles and their relationship to running speed is needed to confirm this.

The zero-cross over method employed with the present study is relatively simple when compared to other accelerometer-based methods of measuring stance time [140] as it is uniaxial and requires a limited data processing procedure. The rationale for this is to provide sport science practitioners working with GPS-based accelerometer data with an accessible method of calculating spatiotemporal variables with the data that is already being collected to measure an athlete's workload. By establishing the key gait events during foot stance, the GPS-based accelerometer can calculate variables such as stance/swing/flight time, step frequency and the timings of the subphases of foot stance[48,143]. These variables will allow for the characterisation of an athlete's spatiotemporal running profile, which can be used to group athletes for further investigations into their relation to sports performance and injury occurrence[48]. Additionally, the associated errors highlighted with the different running speeds provide insight into the appropriate speed thresholds that practitioners can confidently employ spatiotemporal analysis and utilise these variables as a proxy measure to monitor an athlete's physical condition.

3.5. Conclusion:

The present study has shown valid estimations of the accelerometers contained within the GPS devices to measure foot stance characteristics at speeds of 12 km/h, 14 km/h, 15 km/h and 16 km/h and, therefore, providing sports science and medicine practitioners with a simple method of conducting spatiotemporal analysis in the field. The prevalence of this study will allow for the measurement of spatiotemporal variables within the team sports setting. Application of these variables will allow for the characterisation of running styles within a cohort of athletes and provide the basis for further investigations into how these variables can provide insights into an athlete's physical condition.

Chapter 4: The effects of running kinematics, on the peak upper trunk GPS measured accelerations during foot contact at different running speeds.

This chapter was published in the following journal:

Lawson, M., Naemi, R., Needham, R. A., & Chockalingam, N. (2023). The Effects of Running Kinematics on Peak Upper Trunk GPS-Measured Accelerations during Foot Contact at Different Running Speeds. *Applied Sciences*, 14(1), 63.

Abstract:

The overall aim of this study was to determine the effects of running kinematics, on the peak upper trunk segmental accelerations captured with an accelerometer embedded in a commonly used GPS device. Thirteen male participants (age: 27 ± 3.7 years, height: 1.81 ± 0.06 m, mass: 82.7 ± 6.2 Kg) with extensive running experience completed a single trial of treadmill running (1-degree inclination) for 40 seconds at 9 different speeds ranging from 10 -18 km/h at 1 km/h increments. 3D peak upper trunk acceleration values were captured via a GPS device containing a tri-axial accelerometer. Participants running kinematics were calculated from the coordinate data captured by an 18-camera motion capture system. A series of generalized linear mixed models were employed to determine the effects of the kinematic variables on the accelerometer acceleration peaks across the key gait phases of foot contact. Results showed that running kinematics had significant effects on peak accelerometer-measured accelerations in all axes ($p < 0.05$). Overall, peak segment velocities had a larger effect than joint/segment kinematics on resultant (F values = 720.9 / 54.2), vertical (F values = 149.8 / 48.1) and medial-lateral (F values = 55.4 / 33.4) peak accelerometer accelerations. The largest effect on peak accelerometer accelerations was observed during the impact subphase of foot contact at the adduction/abduction velocity of the shank (F value = 129.2, coefficient = -0.03) and anterior/posterior velocity of the pelvis (F value = 58.9, coefficient = 0.01). Axis dependant effects of running kinematics were also observed, specifically at the trunk segment in the vertical and anterior-posterior peak accelerometer accelerations. This study showed the intersegmental relationship between joint/segment kinematics, segment velocities and the resulting peak accelerations of the upper trunk during running over several speeds. These findings provide insights into the lower body's GRF attenuation capacity and its contribution to trunk stability whilst running.

4.1. Introduction:

Accelerometers are often employed in the field to analyse an athlete's running style as they are low-cost, lightweight and have low power requirements [183]. Estimating joint angles is possible with multiple accelerometer set-ups by placing sensors on the relative segments above and/or below the joint [39,157,184,185]. However, they require extensive set-up and data processing procedures to overcome errors associated with longitudinal analysis, such as sensor misalignment[127]. As a result, measuring the acceleration profile of a single segment and inferring changes in kinematics has often been a methodology employed in running related studies that have analysed a participant's running style over longer periods [71,186–189].

During foot contact, ground reaction forces are transmitted upwards through the kinetic chain, causing the individual segments to accelerate[60]. The accelerations and subsequent velocities of each segment depend on the force transferred by the previous segment and the kinematic and anthropometric profiles of the segments[60]. Observing differences/changes in peak segmental accelerations has been previously employed within running-based studies to analyse the kinematic alterations within an individual's running style[71,190,191]. Suboptimal running kinematics can cause excessive soft tissue and bone stress during running, leading to injury[192] or reduced performance[49]. It is essential for sports science and medicine practitioners to ensure their athletes remain healthy and perform at a high level. Therefore, insights into an athlete's running kinematics will be beneficial to manage training load appropriately or to measure progress during an athlete's injury rehabilitation.

Employing a single accelerometer with minimal set-up and data processing procedures to analyse running style is favourable when analysing in the field with more than one athlete. Global positioning (GPS) devices are used with team sports athletes to monitor their training load by analysing derivatives of distance and speed during training and match play[66]. These devices also contain an embedded tri-axial accelerometer, and most manufacturers' software calculates peak acceleration instances during a training session[193], offering a potentially convenient method to analyse an athlete's running style from already available data. When analysing these peak accelerations, it is important to consider the mounting site of the accelerometer. The surrounding joints/segments of the segment to which the accelerometer is attached will influence the magnitude of the peak accelerations, and changes in running kinematics will alter the intersegmental transfer of force throughout the kinetic chain[191]. This has been previously shown at the shank, where peak accelerometer accelerations have increased when the position of the shank becomes more anteriorly rotated due to increased knee flexion[186]. The GPS devices, however, are positioned in a vest on the posterior aspect of the upper trunk. Therefore, the acceleration peaks captured by the accelerometer will potentially be influenced by the kinematics of the trunk, pelvis, thigh, shank and foot segments.

There has been a limited amount of research that has analysed the effects of running kinematics on the acceleration profile of the trunk. Lindsay, Yaggie & McGregor (2014) investigated the contributions of the lower limb kinematics on the root mean square acceleration (overall magnitude of acceleration over the whole gait cycle) of an accelerometer placed on the lower trunk close to the centre of mass. Sagittal plane kinematics of the hip,

knee and ankle at initial foot contact, midstance and terminal foot contact were significantly correlated to the acceleration profile of the lower trunk[182]. Due to its size and anatomical structure, the trunk contains two segments: lower (lumbar spine) and upper (upper thoracic)[194], and the acceleration profiles of these two segments differ during running[181]. It has been previously suggested that the positioning of the GPS-based accelerometer device on the upper trunk was inappropriate for detecting changes in lower limb kinematics when analysing the overall magnitude of acceleration during running due to noise caused within the acceleration profile by upper-limb movement[64]. However, the experimental setup in that study [64] did not allow for lower limb kinematics to be captured, so it remains unclear whether there is a relationship between running kinematics and the acceleration profile of the upper trunk. Furthermore, analysing the peak acceleration of the upper trunk during foot contact, instead of the overall magnitude of acceleration, may provide a more sensitive measure to differences in running kinematics as utilised in other settings.

Naturally, there will be inter-subject variation in running kinematics within a population of athletes. A simple method of inducing intra-subject changes is to alter the running speed[195,196]. As running speed increases, ground reaction forces and segment velocities increase and as a result, compensatory mechanisms of the musculoskeletal system are employed to attain stability of the trunk segments[197]. To gain a comprehensive insight into the intersegmental relationship between the lower body and trunk, analysis must be conducted over several different running speeds.

Therefore, this study aimed to determine the effects of running kinematics, over several speeds, on the peak upper trunk segmental accelerations during foot contact captured with an accelerometer embedded in a commonly used GPS device by achieving the following objectives: (1) determine which joint/segments have the largest effect on the peak upper trunk accelerations at initial foot contact (IFC), midstance (MS) and terminal foot contact (TFC); (2)Highlight the intersegmental relationship between segment velocities throughout the kinetic chain during foot contact by determining which segments influence the peak accelerations of the upper trunk.

Understanding which running kinematics have the greatest effect on the accelerometer data will allow sports science and medicine practitioners to use GPS-based accelerometer data to measure an athlete's running style in the field. We hypothesize that there will be a significant relationship between running kinematics and the peak accelerations captured by the GPS-embedded accelerometer.

4.2. Methodology:

4.2.1. Experimental set-up:

Thirteen male participants (age: 27 ± 3.7 years, height: 1.81 ± 0.06 m, mass: 82.7 ± 6.2 Kg) with extensive running experience were recruited for this study. Participants completed a single trial of treadmill running (1-degree inclination) for 40 seconds at 9 different speeds starting at 10 km/h and proceeding to 18 km/h at 1 km/h increments. Maximum rest time was allowed between sets to ensure minimal fatigue accumulation. Participants were provided

with standardised running shoes (Puma Anzarun) and wore an appropriately sized standard issue vest containing a GPS device (Statsports Apex, Northern Ireland, UK) which contained an embedded high-frequency tri-axial accelerometer. Each trial was captured by an 18-camera motion capture system (Vicon, Oxford, UK). Ethical clearance for this testing procedure was granted by the Staffordshire University ethical committee and all participants gave informed written consent prior to testing.

4.2.2. Data Processing:

Eighteen optical cameras (VICON MXT40, Oxford, UK) recorded the coordinate data of fifty-four infrared markers (14mm) attached to the participants at a frequency of 100 Hz. A modified Istituto Ortopedico Rizzoli (IOR) marker set with five additional clusters attached to the left thigh, right thigh, left shank, right shank and the posterior aspect of the GPS device[175–177] was employed to calculate kinematic variables. The global coordinate system defined the X-axis to represent anterior-posterior movement (positively oriented forward), the Y-axis for medial-lateral movement (positively oriented to the left), and the Z-axis for vertical movement (positively oriented upward). The coordinate data was then transferred from the Vicon Nexus software to Visual 3D (C-Motion Inc, MD, USA) and filtered (4th order Butterworth, 10 Hz cut-off frequency).

The tri-axial accelerometer embedded within the GPS device was mounted around the posterior aspect of the thoracic spine (T2) housed vertically within a standard issue vest. The orientation of the device aligned the Y-axis to vertical (VT) acceleration (positive in the upward

direction), the X-axis to medial-lateral (ML) acceleration (positive in the left direction), and the Z-axis to anterior-posterior (AP) acceleration (positive in the forward direction). Time-series data of the accelerometer was recorded at 100 Hz. Raw accelerometer data was transferred from the STATSports Apex software to Visual 3D (C-Motion Inc, MD, USA).

To synchronise the data between the optical motion capture system and accelerometer, an assistant 'tapped' the GPS device in a downward vertical direction at the beginning of each trial. The frame of the tap was identified in both data sets. Ten consecutive gait cycles were selected for analysis following a 20-second ramp period to allow for participants to reach the target running speed.

4.2.3. Running kinematic variables:

A total of 160 kinematics variables were calculated, during key gait events of foot stance, to provide a comprehensive insight into the intersegmental relationship between joint/segment angles and subsequent segment velocities throughout the stance phase. A kinematic method[144,198] (Chapter 3) was employed to determine IFC, MS and TFC. Three-dimensional joint/segment angles were calculated for the thorax, trunk, pelvis, hip, thigh, knee, shank, ankle and foot at IFC, MS and TFC. Additionally, three-dimensional peak segment velocities were calculated for the thorax, trunk, pelvis, thigh, shank and foot during the two subphases of foot stance (IFC - MS and MS – TFC). Averages of each variable were calculated across the ten gait cycles.

4.2.4. Accelerometer variables:

Peak accelerometer accelerations during foot stance were calculated by initially identifying the time events of IFC and TFC within the accelerometer data (Chapter 3). Within each instance of foot stance, the peak acceleration values for each axis and resultant (RES) acceleration were identified. The averages of the peak acceleration values were calculated across the ten cycles for each axis and the resultant acceleration.

4.2.5. Statistical Analysis:

Generalised linear mixed model (GLMM) analysis was selected as the appropriate method of establishing the effects of the running kinematics (fixed effects) on peak accelerometer accelerations (dependent variables) due to the study design containing multiple measures per subject. GLMM's are regression models that allow for autocorrelation and are therefore preferred when observations are not independent and contain repeated measures[199,200]. The data structure of the fixed effect and dependent variables was continuous, so a linear model with an identity link function was employed (Eq. 4.1).

$$f(x) = x \qquad \textit{(Eq. 4.1)}$$

Where *f* is the function, and *x* represents the variable values.

A series of GLMM's were conducted due to the number of fixed effects and dependent variables. Fixed effect variables were separated into two categories, and the running speed was defined as the repeated measure. Category 1 contained the joint/segment three-dimensional kinematics at IFC, MS and TFC. Category 2 contained the peak segmental

velocities between IFC-MS and MS-TFC. Preliminary GLMM analysis was conducted on the individual joint/segment kinematics, separately for category 1 and 2 variables against each dependant variable, to filter out non-significant variables (p value > 0.05).

The remaining Category 1 and 2 fixed effect variables were then further analysed by GLMM against each dependent variable. A type III F-test was used to determine the magnitude of the effect of each fixed effect variable (F value), whether it was direct or inverse (fixed effects coefficient) and if it was significant (p value < 0.05). Averages and standard deviations of all F values were calculated to separate the significant fixed effect variables into groups of small effect: F value < average – (0.5*standard deviation), medium effect: F value > average – (0.5*standard deviation) and < average + (0.5*standard deviation) and large effect: F value > average + (0.5*standard deviation). Mean difference (g) between the actual and predicted peak accelerometer accelerations with 95% limits of agreement (LOA) were also calculated from the GLMMs to assess accuracy of each model. In addition, residual effect estimates were calculated to understand the residual effect of running speed on the GLMMs. Statistical analysis was conducted using SPSS software (IBM Corporation, Armonk, NY).

4.3. Results:

GLMMs for category 1 and 2 fixed effect variables showed a significant relationship for all dependent variables (p < 0.05, Table 4.1). Model summaries of the category 1 fixed effects GLMMs to estimate the peak accelerations were RES (Mean difference: -0.01 g; LOA: -0.43 g, 0.42 g; F value: 54.18; p < 0.05), VT (Mean difference: -0.01 g; LOA: -0.49 g, 0.47 g; F value:

48.06; p < 0.05), AP (Mean difference: 0.00 g; LOA: -0.16 g, 0.17 g; F value: 56.43; p < 0.05) and ML (Mean difference: -0.01 g; LOA: -0.20 g, 0.18 g; F value: 33.41; p < 0.05). Model summaries of the category 2 fixed effects GLMMs to estimate the peak accelerations were RES (Mean difference: 0.00 g; LOA: -0.42 g, 0.43 g; F value: 720.83; p < 0.05), VT (Mean difference: -0.01 g; LOA: -0.61 g, 0.64 g; F value: 149.79; p < 0.05), AP (Mean difference: 0.00 g; LOA: -0.21 g, 0.21 g; F value: 53.93; p < 0.05) and ML (Mean difference: 0.00 g; LOA: -0.17 g, 0.17 g; F value: 55.38; p < 0.05). Significant residual effects of running speed were observed on peak RES, VT and ML accelerations for category 1 fixed effect variables (p < 0.05, Table 4.2). However, running speed had significant residual effects on all peak accelerations for category 2 fixed effect variables (p < 0.05, Table 4.3).

Table 4.1. GLMM summary of category 1 and 2 fixed effects variables for each dependent variable.

	Peak RES Acceleration		Peak VT Acceleration		Peak AP Acceleration		Peak ML Acceleration	
GLMM	F value	Significance	F value	Significance	F value	Significance	F value	Significance
Category 1	54.18	0.00*	48.07	0.00*	56.43	0.00*	33.41	0.00*
Category 2	720.89	0.00*	149.79	0.00*	53.92	0.00*	55.38	0.00*

**Significance is < 0.05,* RES = Resultant, VT = Vertical, AP = Anterior/posterior, ML = Medial-Lateral

Table 4.2. The residual effect of running speed on peak accelerations of the GPS-embedded accelerometer for category 1 fixed effect variables.

	Peak RES Acceleration		Peak VT Acceleration		Peak AP Acceleration		Peak ML Acceleration	
Speed	Estimate	Significance	Estimate	Significance	Estimate	Significance	Estimate	Significance
10 km/h	0.08	0.04*	0.12	0.04*	0.01	0.14	0.01	0.10
11 km/h	0.03	0.10	0.03	0.17	0.01	0.28	0.02	0.04*
12 km/h	0.08	0.03*	0.08	0.04*	0.01	0.10	0.01	0.08
13 km/h	0.04	0.09	0.04	0.20	0.03	0.11	0.01	0.10
14 km/h	0.01	0.22	0.04	0.13	0.01	0.10	0.01	0.06
15 km/h	0.04	0.12	0.04	0.16	0.00	0.45	0.00	0.40
16 km/h	0.04	0.10	0.09	0.09	0.01	0.20	0.01	0.09
17 km/h	0.09	0.05	0.07	0.09	0.01	0.28	0.00	0.52
18 km/h	0.11	0.06	0.11	0.06	0.01	0.20	0.04	0.04*

**Significance is < 0.05,* RES = Resultant, VT = Vertical, AP = Anterior/posterior, ML = Medial-Lateral

Table 4.3. The residual effect of running speed on peak accelerations of the GPS-embedded accelerometer for category 2 fixed effect variables.

	Peak RES Acceleration		Peak VT Acceleration		Peak AP Acceleration		Peak ML Acceleration	
Speed	Estimate	Significance	Estimate	Significance	Estimate	Significance	Estimate	Significance
10 km/h	0.09	0.04*	0.12	0.02*	0.02	0.07	0.00	0.21
11 km/h	0.06	0.04*	0.00	0.82	0.01	0.07	0.01	0.02*
12 km/h	0.02	0.16	0.05	0.07	0.01	0.04*	0.00	0.19
13 km/h	0.19	0.03*	0.18	0.04*	0.02	0.07	0.00	0.20
14 km/h	0.01	0.23	0.05	0.08	0.01	0.07	0.01	0.04*
15 km/h	0.01	0.26	0.16	0.05	0.01	0.08	0.01	0.06
16 km/h	0.05	0.14	0.14	0.10	0.02	0.09	0.01	0.04*
17 km/h	0.09	0.06	0.16	0.05	0.02	0.14	0.01	0.06
18 km/h	0.10	0.06	0.28	0.12	0.01	0.25	0.03	0.05

**Significance is < 0.05,* RES = Resultant, VT = Vertical, AP = Anterior/posterior, ML = Medial-Lateral

F-test results showed significant effects ($p < 0.05$) of category 1 fixed effect variables on the peak accelerations in the upper trunk-mounted accelerometer, which varied between axes and were dependent on the phase during contact. For peak RES accelerations, the thorax (IFC), pelvis (MS), hip (IFC & MS), knee (IFC & TFC), shank (TFC) and ankle (MS) had significant ($p < 0.05$) F values ranging from 5.4 – 26.4 (Figure 4.1). For peak VT accelerations, the thorax (IFC & TFC), pelvis (IFC, MS & TFC), hip (IFC), knee (TFC) and ankle (MS) had significant ($p < 0.05$) F values ranging from 4.2 – 18.2 (Figure 4.2). For peak AP accelerations, the thorax (MS), pelvis (IFC), ankle (MS), and foot (TFC) had significant ($p < 0.05$) F values ranging from 4.3 – 10.9 (Figure 4.3). Lastly, for peak ML accelerations, the thorax (MS), pelvis (IFC), ankle (MS) and foot (TFC) all had significant ($p < 0.05$) F values ranging from 4.2 – 5.3 (Figure 4.4).

Category 2 fixed effect variables had significant effects in both subphases of foot contact (IFC-MS & MS-TFC) and the largest range in F values (4.2 – 129.2). For RES, VT and AP peak accelerations, the thorax, pelvis and thigh significantly affected both subphases ($p < 0.05$, Figures 4.1-4.3). The shank had a significant effect in both subphases for RES but only in IFC-

MS for VT and ML acceleration peaks ($p < 0.05$, Figures 4.1,4.2 & 4.4). The foot also had a significant effect in AP during MS-TFC and during both subphases for ML acceleration peaks ($p < 0.05$, Figures 4.3 & 4.4). In addition, the pelvis and thigh significantly affected ML acceleration peak during MS-TFC ($p < 0.05$, Figure 4.4).

The reader is encouraged to take notice of the coefficients (+/-) in figures 4.1-4.4 to understand whether the effects of the kinematics were direct or inverse. In addition, all the F-test results from the GLMMs can be found in Appendices 2, 3, and 4.

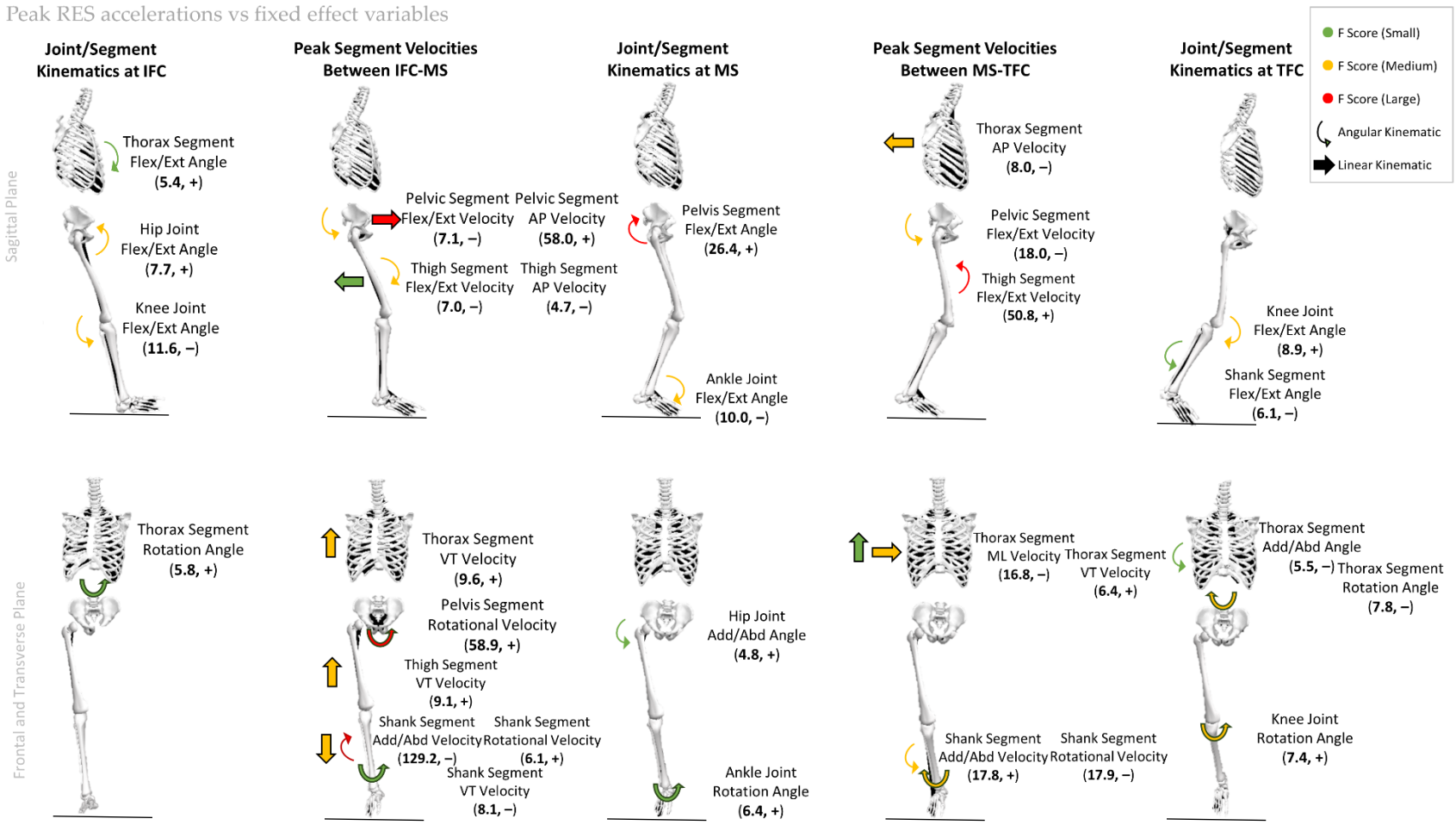

Figure 4.1. Category 1 & 2 variables with a significant effect ($p < 0.05$) on the peak RES accelerations of the GPS-based accelerometer at each key gait phase. F value and fixed effects coefficient (+ = direct, - = inverse) are displayed within the brackets of each variable. The direction of the arrows represents the motion of the joint/segment that has a significant effect at each key gait phase.

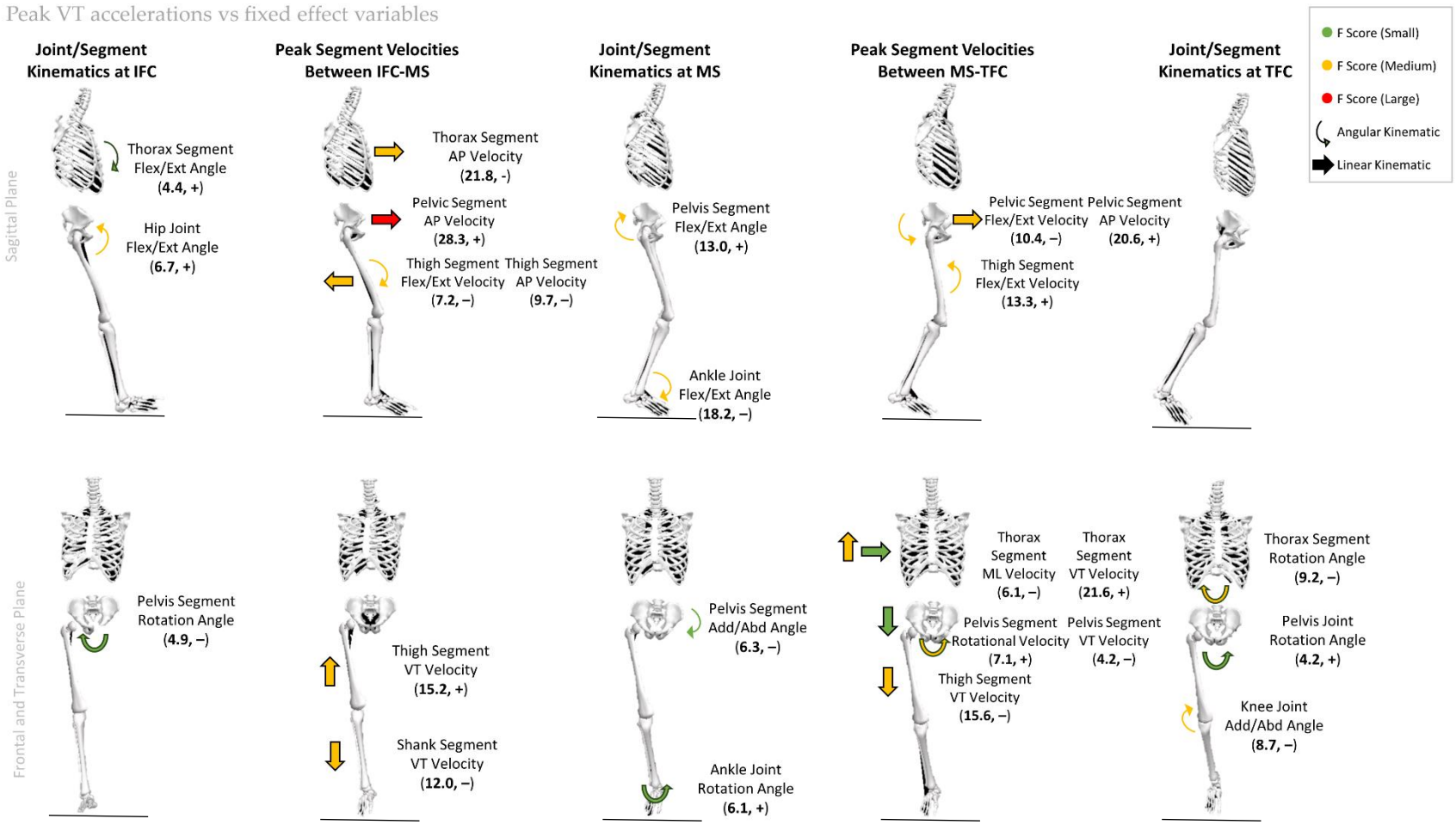

Figure 4.2. Category 1 & 2 variables with a significant effect ($p < 0.05$) on the peak VT accelerations of the GPS-based accelerometer at each key gait phase. F value and fixed effects coefficient (+ = direct, - = inverse) are displayed within the brackets of each variable. The direction of the arrows represents the motion of the joint/segment that has a significant effect at each key gait phase.

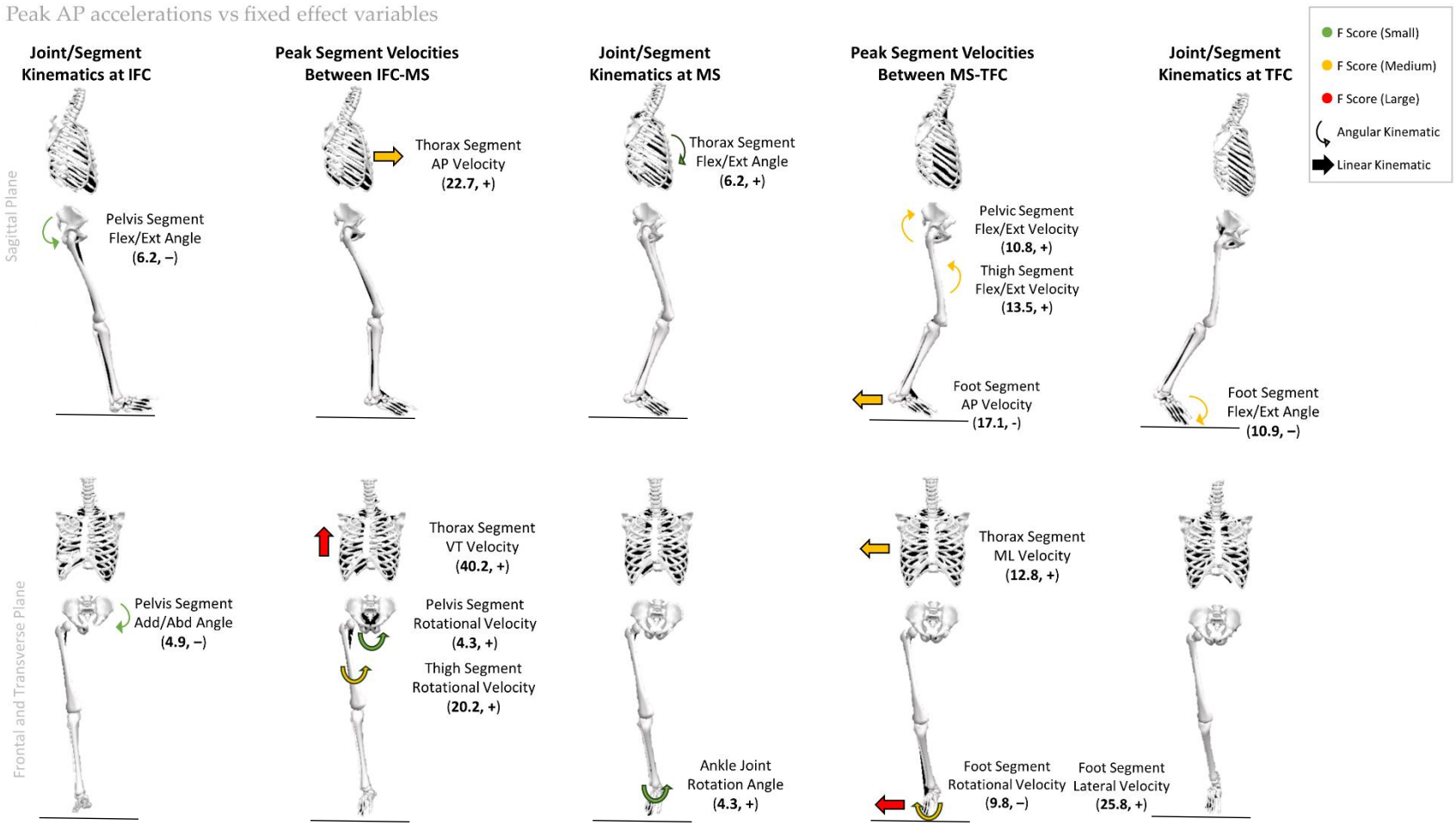

Figure 4.3. Category 1 & 2 variables with a significant effect ($p < 0.05$) on the peak AP accelerations of the GPS-based accelerometer at each key gait phase. F value and fixed effects coefficient (+ = direct, - = inverse) are displayed within the brackets of each variable. The direction of the arrows represents the motion of the joint/segment that has a significant effect at each key gait phase.

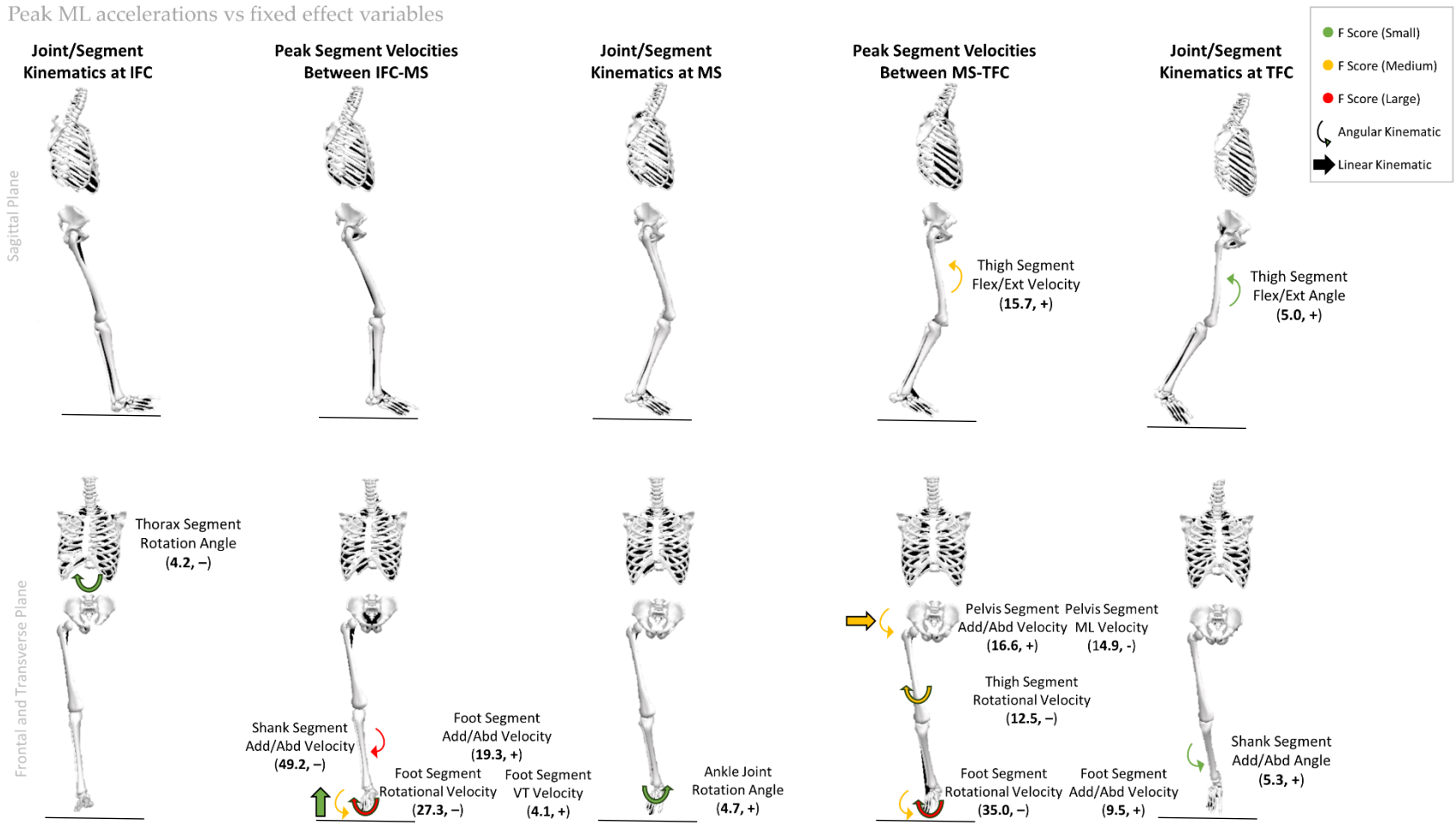

Figure 4.4. Category 1 & 2 variables with a significant effect ($p < 0.05$) on the peak ML accelerations of the GPS-based accelerometer at each key gait phase. F value and fixed effects coefficient (+ = direct, - = inverse) are displayed within the brackets of each variable. The direction of the arrows represents the motion of the joint/segment that has a significant effect at each key gait phase.

4.4. Discussion:

The present study aimed to determine the effects of running kinematics during foot contact on the peak upper trunk accelerations captured by an accelerometer embedded within a commonly used GPS tracking device. Variables of running kinematics were separated into two categories: joint/segment kinematics at IFC, MS and TFC, and peak segment velocities between IFC-MS and MS-TFC. Analysing these variables independently, through GLMMs, allowed for insights into which joint/segments have the largest effect on the peak upper trunk accelerations, which key gait event this occurs and the effect of the subsequent peak velocities of the bodily segments during the impact (IFC-MS) and propulsion (MS-TFC) subphases of foot contact.

GLMM summaries showed that category 2 fixed effect variables (peak segment velocities) had a larger effect (F value) than the category 1 fixed effect variables (joint/segment kinematics) on the RES, VT and ML accelerometer peak accelerations (Table 4.1). In addition, running speed had a greater residual effect on the category 2 fixed variables (Table 4.2). To our knowledge, these comparisons have not been previously reported however, they substantiate the relationships described by Derrick (2004) on the determinants of bodily segmental accelerations when exposed to impact forces during running. These findings validate the value of including segment velocities in future studies can lead to a better understanding of the intersegmental relationship during running instead of focusing on joint kinematics alone, as seen in previous studies[182,186,201].

It has previously been well documented that increased joint stiffness and stability around the lower limb segments result in less GRF being attenuated and more force transferring up the kinetic chain, leading to greater impact and propulsion forces during running[182,202,203]. Our results support findings from Lindsay et al. (2014) as decreased knee flexion at IFC increases the shank segment's stability, reducing the shank's peak linear and angular velocities during the impact subphase (IFC-MS) and causing greater peak accelerometer accelerations (Figure 4.1). The shank segment had the largest effect on peak RES (F value = 129.2, Figure 4.1) and ML (F value = 49.2, Figure 4.4) accelerometer accelerations of all peak segment velocities, thus displaying its important role in the transfer of GRF throughout the kinetic chain.

Additionally, during MS, the role of the ankle is apparent as there is a medium-sized effect of decreased ankle flexion resulting in larger RES (F value = 10.0, Figure 4.1) and VT (F value = 18.2, Figure 4.2) peak accelerations, suggesting that larger acceleration peaks are related to reduced decoupling of the ankle joint. Increased joint stiffness can increase propulsion force capabilities during stance[203], resulting in larger peak segment velocities. This is shown in the propulsion subphase (MS-TFC) as increased peak angular (flexion) velocity of the thigh has a large to medium-sized effect on the peak accelerometer accelerations in all axes (Figures 4.1-4.4). Furthermore, large to medium-sized effects were observed for foot segment linear (posterior and medial) and angular (internal rotation) peak velocities on the AP and ML peak accelerometer accelerations (Figures 4.3 & 4.4). These findings differ from previous investigations[182] as the ankle flexion angle was associated with TFC and they did not analyse segmental velocities, possibly due to the different accelerometer mounting sites.

The proximal joints and segments of the trunk were shown in our results also to influence the peak accelerometer accelerations. During impact (IFC-MS), the second largest effect on peak RES accelerometer accelerations was observed at the pelvis segment (F value = 58.0, Figure 4.1). Increased hip flexion at IFC, which also supports previous findings[182], reduces the effective mass of pelvis segment[60], causing increased linear (anterior) and angular (internal rotation) peak velocities during impact (IFC-MS) (Figure 4.1). This results in increased flexion of the pelvis at MS due to the pelvis decoupling to support the deceleration of the trunk segment post-impact as it supports trunk stability. During propulsion (MS-TFC), there are medium-sized effects of pelvis angular (extension and internal rotation) and linear (anterior) peak velocities, which contribute to larger RES and VT peak accelerometer accelerations (Figures 4.1 & 4.2). Conversely, reduced extension peak velocities (increased flexion) at the pelvis contributed to larger AP peak accelerometer accelerations, and greater frontal plane peak velocities at the pelvis resulted in larger ML peak accelerometer accelerations (Figures 4.3 & 4.4). This indicates that insights can be gained into pelvis extension and stability properties of athletes by analysing the differences between VT, AP and ML peak accelerometer accelerations.

Furthermore, similar differences between the peak accelerometer accelerations were also observed regarding the thorax segment velocities. Reduced peak linear (anterior) velocity during impact and increased peak linear (vertical) velocity during propulsion of the thorax resulted in larger VT peak accelerometer accelerations (Figure 4.2). Whereas increased linear (vertical and anterior) peak velocity during impact and increased linear (lateral) peak velocity of the thorax resulted in larger AP peak accelerometer accelerations (Figure 4.3). As force is

transferred from the pelvis to the trunk, the surrounding musculature is activated to maintain stability and influences the subsequent displacement of the trunk segment[197]. Therefore, our results suggest that analysing the differences between the VT and AP peak accelerometer accelerations may provide insights into these mechanisms.

Findings from this study show that GRF attenuation properties of the surrounding joints to the shank segment and the kinematics of the pelvis in maintaining trunk stability, specifically at MS, have the largest effects on the peak accelerometer accelerations. The practical applications of these findings are that peak accelerometer accelerations could be valuable in analysing an athlete's rehabilitation from an ACL reconstruction, as this has been shown to affect knee extension during running[52]. Alternatively, observing the differences between the axis of peak accelerometer accelerations throughout an athlete's training session may be used to provide insight into the level of neuromuscular fatigue specifically affecting the stability of pelvis/trunk segments[87,163]. The relationships found in this study also show that peak accelerations can be used to identify differences/changes in running styles between athletes and further add to the characterisation of running styles within a cohort of athletes with the GPS-based IMU, as proposed in chapter 3.

Direct comparisons of our results to those of Lindsey et al. (2014) were not possible due to the differences in statistical analysis between studies. The present study utilised GLMMs as repeated measures were present, whereas Lindsey et al. (2014) employed a stepwise regression analysis. Similar findings were observed though, regarding the significant effects of the hip and knee flexion/extension angle on the RES acceleration profile at IFC (Figure 4.1).

Lindsey at al. (2014) mounted their accelerometer on the lower trunk. Therefore, it can be suggested that hip and knee kinematics at IFC affect both the lower and upper trunk acceleration profiles.

In addition, our results refute previous suggestions[64] that the mounting site of the accelerometer on the upper trunk is unacceptable for observing changes in lower limb running kinematics. The limitations of the present study are that the findings only apply to straight-line running, as the trials were conducted on a treadmill. It is suggested that practitioners utilise the coordinate data from the GPS devices to ensure instances of straight-line running are selected when applying the current findings to field-based running style analysis[204]. Treadmill running was selected in the study design to control the running speed and to induce intra-subject variations in running kinematics by altering the speed between each trail. As a result, GRF was not captured due to the absence of an embedded force platform. Considering the residual effects of running speed observed, especially in the category 2 fixed effect variables, understanding the associated changes in joint/segment kinetics with each running speed and how that differed across a wider variety of running styles would have provided a more comprehensive insight into the effect of different running styles on the GPS based accelerometer accelerations. The outcome of this study was favourable, considering the significant associations found with relatively small participants. In the future, having a bigger sample size would allow for further verifications of the outcome of this study.

4.5. Conclusion:

In summary, GLMMs within this study have demonstrated the intersegmental relationship between joint/segment kinematics, segment velocities and the resulting peak accelerations of the upper trunk during running over several speeds. Specifically, peak shank and pelvis velocities during impact (IFC-MS) had the largest effect on the RES upper trunk peak accelerations captured by the accelerometer contained within the GPS device. Furthermore, differences in pelvis and thorax peak velocities affected the peak accelerometer accelerations in the individual axes (VT, AP and ML). The findings of this study provide rationale for including analysis of peak accelerations captured from the GPS-based accelerometer within a framework to characterise an athlete's running style in the field. The strengths of the relationships found between running kinematics and the peak accelerations highlight the potential value of employing these variables within applied research studies to investigate their relationships with lower body GRF attenuation and trunk stability mechanisms.

Chapter 5: Can Machine Learning Predict Running Kinematics Based on Upper Trunk GPS-Based IMU Acceleration? A Novel Method of Conducting Biomechanical Analysis in the Field Using Artificial Neural Networks.

This chapter was published in the following journal:

Lawson, M., Naemi, R., Needham, R. A., & Chockalingam, N. (2024). Can Machine Learning Predict Running Kinematics Based on Upper Trunk GPS-Based IMU Acceleration? A Novel Method of Conducting Biomechanical Analysis in the Field Using Artificial Neural Networks. *Applied Sciences*, 14(5),1750.

Abstract

This study aimed to investigate whether running kinematics can be accurately estimated through an artificial neural network (ANN) model containing GPS-based accelerometer variables, running speed and anthropometric data. Thirteen male participants with extensive running experience completed treadmill running trials at several speeds. Participants wore a GPS device containing a tri-axial accelerometer and running kinematics were captured by an 18-camera motion capture system for each trial. Multiple multilayer perceptron neural networks model was constructed to estimate participant's 3D running kinematics with the following input variables: 3D peak accelerometer acceleration during foot stance (g), stance time (s), running speed (km/h), participant height (cm), leg length (cm) and mass (kg). Pearson's correlation coefficient (r), root mean squared error (RMSE), and relative root mean squared error (rRMSE) showed ANN models provide accurate estimations of joint/segment angles (mean rRMSE = 13.0 ± 4.3%) and peak segment velocities (mean rRMSE = 22.1 ± 14.7%) at key gait phases across foot stance. Highest accuracies were achieved for flexion/extension angles of the thorax, pelvis and hip, and peak thigh flexion/extension and vertical velocities (rRMSE < 10%). The current findings provide sports science and medical practitioners, working with this data, a method of conducting field-based analysis of running kinematics.

5.1. Introduction:

In recent years, there has been an exploration of using inertial measurement units (IMUs) to estimate joint kinematics during walking and running[29,57,58,127,185,205]. Conducting biomechanical analysis in the field with IMUs allows sports science and medical practitioners to capture an individual's locomotion characteristics more frequently and with a reduced cost/set-up time than lab-based analysis[183]. IMUs such as accelerometers have been extensively employed to analyse the acceleration profile of bodily segments to infer the potential differences between individuals or changes in an individual's walking/running kinematics[110,142,182]. However, with advances in data processing procedures, it is now possible to accurately estimate joint kinematics with IMUs[29,57,58,127,205].

Conventional models utilising IMUs to estimate joint kinematics have been previously employed within the health industry to analyse patients' walking kinematics. Analysis of patients rehabilitating from hip arthroplasty[129] and knee ligament reconstruction[121] have been used to inform the long-term effects of and effectiveness on patients' functionality post-surgery. These earlier models mount IMUs on the proximal/distal segments to the relevant joint and measure the IMU sensor orientation relative to the inertial frame[30]. Lab-based pre-calibration is required to ensure accurate sensor-sensor alignment to the anatomical axes and measurement of segment geometry so that a joint orientation matrix can be calculated (similar to stereophotogrammetry)[30]. The IMUs are utilised to reconstruct a biomechanical model of the human body, and the linear relationships between the sensor acceleration profiles are used to estimate the joint kinematics[125–127].

Integration of accelerometer, gyroscope and magnetometer data with sensor fusion algorithms have shown root mean squared error (RMSE) of <3.6° when estimating 3D lower limb joint angles in the laboratory[40]. Nevertheless, concerns with using IMUs to measure segmental orientation have been previously stated when applying these systems in the field[30]. Magnetometers are employed to reduce drift errors that can occur in the gyroscope's angular velocity data by 'resetting' the sensor orientation, but magnetic disturbances in the field can affect the magnetometer's reference coordinates and thus not recommended for field base use[30,54]. Additionally, soft tissue motion can lead to the misalignment of the IMU sensors[55], which is inevitable when conducting longitudinal analysis and greatly reduces the accuracy of models that rely on the linear relationship between two aligned sensors[127]. As a result, there is a lack of research that has successfully implemented these methods in the field over longer periods of time[206]. Recent developments in advanced data processing procedures have overcome previous regression-based problems with sensor misalignment and have subsequently renewed the possibility of conducting field-based predictions of joint kinematics with IMUs[127].

Deep learning algorithms such as artificial neural networks (ANN) allow for greater predictive accuracy than linear regression-based models when non-linear relationships between independent (input) and dependent (output) variables are present[56]. ANNs consist of interconnected units (neurons) separated into three layers: input, hidden and output. Each layer contains several neurons, which are connected and appropriately weighted depending on the strength of the connection between neurons[56,207]. Each ANN consists of training and testing modules whereby in the training module, the model learns the relationship between

variables and appropriately "weights" each connection depending on the fitting of the data structure[56]. The testing module then tests the algorithm to analyse how accurately the model predicted the output variable.

Several classes of ANNs have been employed within studies that have attempted to predict biomechanical variables during locomotion. Amongst these classes, the multilayer perceptron (MLP) networks have performed well when predicting joint kinematics during walking[29,57,58]. MLP networks are considered a simpler form of ANNs that are easy to train and often employed as the baseline ANN to compare newer models against[57]. MLPs have shown a relative root mean squared error (rRMSE) of <9% for lower limb kinematics during walking[58], although this error has increased to ~34% when analysing knee moments during running-based tasks[185]. As a result, more complex ANNs (convolutional neural networks) have been developed, integrating musculoskeletal simulations into the training module to improve accuracy[39,157]. However, these models' pre-calibration procedures are extensive and require access to a biomechanics laboratory. In principle, though, the increased accuracy of including musculoskeletal simulations highlights the value of utilising additional biomechanical input variables in ANNs to predict joint kinematics when compared to IMU data alone.

Previous investigations utilising IMUs and ANNs to predict joint kinematics have typically stemmed from a clinical background[29,205], and its application within sports has not been explored. With team sports athletes, IMUs contained within global positioning systems (GPS) are commonly used to monitor athletes' workload along with GPS-derived variables such as distance and running speed[64,66]. As the GPS devices are mounted at approximately the

posterior aspect of the upper thoracic spine, the IMUs capture the acceleration profile of the upper trunk segment. Previous research (Chapter 3 & 4) has shown that characteristics of foot stance can be accurately identified within the accelerometer data and that an individual's running kinematics significantly influences the acceleration peaks. Additionally, athlete anthropometrics[208], stance time[209] and running speed[195,196] have also been shown to have a relationship with an athlete's running kinematics. These variables are accessible to practitioners working with team sports athletes as anthropometric measurements are routinely collected during skinfold body composition assessments[210], and running speed can be accurately measured with coordinate data derived from GPS devices[211]. Considering this, including these variables in addition to IMU data could potentially increase the accuracy of ANNs in predicting running kinematics.

The capacity to utilise IMUs within GPS devices to conduct field-based biomechanical analysis of their athletes offers sports science and medical practitioners a convenient and valuable tool to track an athlete's progression during injury rehabilitation. Including accurate estimations of an individual's running kinematics would add to the level of detail the GPS-based IMU can offer when conducting biomechanical analysis in the field. Therefore, the present study aims to investigate whether running kinematics can be accurately estimated through an ANN model containing GPS-based accelerometer variables, running speed and anthropometric data. This study intends to explore the predictive capabilities of data that is easily accessible to sports science and medical practitioners working with team sports athletes to conduct comprehensive biomechanical analysis in the field.

5.2. Methodology:

The present study used data and findings from a previous study (chapter 4) to train a series of ANNs to predict kinematic variables (section 5.2.3) that had been identified to influence the acceleration profile of the GPS-based accelerometer. Additional input variables, such as anthropometric, stance time characteristics and running speed (section 5.2.2), were added to the dataset to strengthen the ANN's predictive capabilities.

5.2.1. Experimental Set-Up:

Thirteen experienced male runners (age: 27 ± 3.7 years, height: 1.81 ± 0.06 m, mass: 82.7 ± 6.2 Kg) completed nine trials of treadmill running (1-degree inclination) for 40 seconds at speeds starting at 10 km/h and increasing at 1 km/h increments to 18 km/h. Treadmill running trials were captured by an 18-camera motion capture system (Vicon, Oxford, UK). Each participant wore a standard-issue vest containing a GPS device (Statsports Apex, Northern Ireland, UK) with an embedded high-frequency tri-axial accelerometer and was provided with standardised running shoes (Puma Anzarun). The Staffordshire University ethical committee granted ethical clearance for this testing procedure, and all participants gave informed written consent before testing.

The standard issue vest positioned the GPS device around the thoracic spine's posterior aspect, and the embedded tri-axial accelerometer sampling frequency was set to 100 Hz. Fifty-four infrared markers (14mm) were attached to the participants that corresponded to the modified Istituto Ortopedico Rizzoli (IOR) marker set with five additional clusters attached to

the left thigh, right thigh, left shank, right shank and the posterior aspect of the GPS device[175–177]. Eighteen optical cameras (VICON MXT40, Oxford, UK) recorded the coordinate data of the infrared markers at 100 Hz. Raw accelerometer and marker coordinate data were transferred from the respective software (STATSport APEX and Vicon Nexus) to Visual 3D (C-Motion Inc, MD, USA). Synchronisation of accelerometer and motion capture data was conducted by an assistant 'tapping' the GPS device at the beginning of each running trial. The frame of the tap was established in each data set, and then ten consecutive gait cycles were selected for analysis following a 20-second ramp period.

5.2.2. Input variables:

Accelerometer variables consisting of stance time characteristics and peak accelerations during foot stance were selected as the accelerometer input variables. Instances of initial foot contact (IFC), midstance (MS) and terminal foot contact (TFC) were identified in the vertical acceleration profile (Chapter 3), and the subsequent timings (s) between these events were calculated (stance time, IFC-MS time, MS-TFC time). The vertical (VT), anterior/posterior (AP), medial/lateral (ML) and resultant (RES) peak accelerations (g) during foot stance were then calculated by identifying the largest value in each axis during this time frame. Averages of each accelerometer variable were calculated across the ten gait cycles.

Participant height (cm), body mass (kg) and leg length (cm) (distance from the anterior superior iliac spine to the medial malleolus) were recorded prior to testing and included as the anthropometric input variables[208]. Running speed was derived from the treadmill speed within each trial.

5.2.3. Output Variables:

A previous investigation (Chapter 4) highlighted joint/segment kinematics that had significant relationships with the peak accelerations of the GPS-based accelerometer at specific timings during foot stance. Therefore, these findings provided the basis for selecting the output variables that the present study would utilise as output variables within a series of ANNs. Joint/segment angles at IFC, MS and TFC, and peak segment velocities during the impact (IFC-MS) and propulsion (MS-TFC) subphases were calculated for all bodily joints/segments. However, the following subsections (5.2.3.1, 5.2.3.2) describe the kinematics that were included as output variables. The averages of the output variables were calculated over the ten gait cycles for each trial.

5.2.3.1. Joint/Segment angles:

- Thorax flexion/extension and internal/external rotation angles at IFC.
- Pelvis flexion/extension and adduction/abduction angles at IFC.
- Hip flexion/extension angle at IFC.
- Knee flexion/extension angle at IFC.
- Thorax flexion/extension angle at MS.
- Pelvis flexion/extension angle at MS.
- Ankle flexion/extension and internal/external rotation angles at MS.
- Thigh flexion/extension angle at TFC.
- Shank adduction/abduction angle at TFC.
- Foot flexion/extension angle at TFC.

5.2.3.2. Peak segmental velocities:

- Thorax vertical and horizontal linear velocities during impact.
- Pelvis horizontal linear velocity during impact.
- Pelvis internal/external angular velocity during impact.
- Thigh vertical linear velocity during impact.
- Thigh internal/external angular velocity during impact.
- Shank adduction/abduction angular velocity during impact.
- Foot adduction/abduction and internal/external velocities during impact.
- Thorax vertical and lateral linear velocities during propulsion.
- Pelvis horizontal and lateral linear velocities during propulsion.
- Pelvis flexion/extension, adduction/abduction and internal/external angular velocities during propulsion.
- Thigh vertical linear velocity during propulsion.
- Thigh flexion/extension and internal/external angular velocities during propulsion.
- Shank adduction/abduction and internal/external angular velocities during propulsion.
- Foot horizontal and lateral linear velocities during propulsion.
- Foot internal/external angular velocity during propulsion.

5.2.4. ANN model:

The MLP class of ANNs was chosen as the deep learning algorithm to test the predictive capabilities of the input variables using the IBM SPSS Modeler software version-22 (IBM Corp.,

Armonk, N.Y., USA). The model contained a feedforward architecture and was set to default, using a single hidden layer and automatically selecting the most appropriate number of hidden layer units (minimum = 1, maximum = 50). The dataset was partitioned randomly into ~70% testing sample and ~30% training sample depending on the relative number of cases. Activation link functions selected were the hyperbolic tangent (Eq. 5.1) for the hidden layers and the identity function (Eq. 5.2) for the output layer due to the presence of scale-dependent variables.

$$\gamma(c) = tanh(c) = (e^{c} - e^{-c})/(e^{c} + e^{-c}) \quad \textit{(Eq. 5.1)}$$

Where $\gamma(c)$ is the link function, $tanh(c)$ is the hyperbolic tangent and e^{c} is the exponential function.

$$\gamma(c) = c \quad \textit{(Eq. 5.2)}$$

Where γ is the function, and c represents the variable values.

49 ANNs were produced, and each output variable was tested separately. Each ANN consisted of all input variables except for the peak accelerometer accelerations. The axis of peak accelerometer accelerations chosen depended on the output variable that had previously displayed a relationship with that input variable (Chapter 4). Therefore, each ANN contained either the RES, VT, AP or ML peak accelerometer accelerations.

5.2.5. Statistical Analysis:

Descriptive statistics of the ANN were conducted to provide insight into the average sample size percentages of the training and testing modules and the average number of units within the hidden layer. The Root Mean Squared Error (RMSE) and relative Root Mean Squared Error (rRMSE) for each ANN were calculated and used to assess the accuracy of each model in the training and testing modules. Pearson's correlation coefficient (r) was used to measure the agreement between ANN estimated output variables, categorised as weak ($r \leq 0.35$), moderate ($0.35 < r \leq 0.67$), strong ($0.67 < r \leq 0.90$) and excellent (≥ 0.90)[185]. Sensitivity analysis of the input variables was performed to determine the individual importance of the predictors in determining the neural network. All statistical analysis was performed using SPSS software version 22 (IBM Corporation, Armonk, NY).

5.3. Results:

The average dataset partitions utilised within the ANNs were 72.8% ± 4.1% (training) and 27.2% ± 4.1% (testing) with 4.1 ± 1.5 hidden units. Model summaries showed, on average, the accuracies of the ANNs to estimate the output variables were greater for joint/segment angles (testing rRMSE = 13.0% ± 4.3%, r = 0.95 ± 0.03) than peak segment velocities (testing rRMSE = 22.1% ± 14.7%, r = 0.91 ± 0.07) (Table 5.1). Mean correlation coefficients showed excellent estimations of both groups of output variables ($r > 0.90$) (Table 5.1).

Table 5.1. Mean accuracy (RMSE, root-mean squared error; rRMSE, relative root-mean squared error; *r*, Pearson's correlation coefficient) of the estimated outcome variables by groups.

Output Variable Group	Training		Testing		
	RMSE	rRMSE (%)	RMSE	rRMSE (%)	*r*
Joint/Segment Angles (°)	3.33 ± 2.88	8.8 ± 7.4	1.86 ± 0.65	13.0 ± 4.3	0.95 ± 0.03
Peak Segment Velocities (m/s)	5.35 ± 4.28	14.1 ± 11.5	3.83 ± 3.14	22.1 ± 14.7	0.91 ± 0.07
All Variables	4.52 ± 3.87	12.0 ± 10.3	3.03 ± 2.62	18.4 ± 12.4	0.93 ± 0.06

Joint angle estimations had the smallest range in rRMSE (4.1% - 20.5%), with thorax flexion/extension angle during MS being the most accurate (RMSE = 0.65°; rRMSE = 4.1%; *r* = 0.98) (Table 5.2). However, estimations of the thigh flexion/extension peak angular velocity during propulsion (MS-TFC) had the greatest accuracy of all output variables (RMSE = 0.24 m/s; rRMSE = 2.2%; *r* = 0.9) (Table 5.3), which performed better when the RES accelerometer peak acceleration was included over the AP. There were four joint angles (Hip flexion/extension at IFC; Thorax flexion/extension at IFC; Pelvis flexion/extension at IFC; Pelvis flexion/extension at MS) and two peak segment velocities (Thigh flexion/extension during propulsion; Thigh vertical during propulsion) that had rRMSE of < 10%.

Table 5.2. Individual accuracy (RMSE, root-mean squared error; rRMSE, relative root-mean squared error; *r*, Pearson's correlation coefficient) of the estimated joint/segment angles during testing.

Accelerometer Peak Accel Axis	Output Variable			RMSE (°)	rRMSE (%)	*r*
	Body Joint/Segment	Plane of Motion	Gait Phase			
RES	HIP	Flexion/Extension	IFC	2.26	9.9%	0.96
	KNEE	Flexion/Extension	IFC	2.47	19.3%	0.83
	THORAX	Flexion/Extension	IFC	0.93	7.6%	0.98
	THORAX	Internal/External Rotation	IFC	1.86	15.0%	0.92
	ANKLE	Flexion/Extension	MS	2.19	12.2%	0.96
	PELVIS	Flexion/Extension	MS	1.56	9.2%	0.96
ML	THORAX	Internal/External Rotation	IFC	1.46	11.6%	0.95
	ANKLE	Internal/External Rotation	MS	1.17	12.6%	0.95
	SHANK	Adduction/Abduction	TFC	2.47	10.9%	0.96
	THIGH	Flexion/Extension	TFC	3.27	15.8%	0.97
VT	HIP	Flexion/Extension	IFC	1.70	10.0%	0.97
	THORAX	Flexion/Extension	IFC	1.58	19.5%	0.94
	ANKLE	Flexion/Extension	MS	1.79	13.6%	0.96
	PELVIS	Flexion/Extension	MS	1.08	11.5%	0.98
	ANKLE	Internal/External Rotation	MS	1.87	15.4%	0.96
AP	PELVIS	Adduction/Abduction	IFC	2.10	12.7%	0.94
	PELVIS	Flexion/Extension	IFC	1.82	9.6%	0.95
	THORAX	Flexion/Extension	MS	0.65	4.1%	0.98
	ANKLE	Internal/External Rotation	MS	2.15	19.0%	0.93
	FOOT	Flexion/Extension	TFC	2.91	20.5%	0.92

Table 5.3. Individual accuracy (RMSE, root-mean squared error; rRMSE, relative root-mean squared error; *r*, Pearson's correlation coefficient) of the estimated peak segment velocities during testing.

Accelerometer Peak Accel Axis	Output Variable			RMSE (m/s)	rRMSE (%)	*r*
	Body Segment	Plane of Motion	Gait Phase			
RES	SHANK	Adduction/Abduction	IFC-MS	1.88	12.2%	0.97
	PELVIS	Internal/External Rotation	IFC-MS	3.09	15.5%	0.91
	PELVIS	Anterior/Posterior	IFC-MS	1.32	10.8%	0.94
	SHANK	Adduction/Abduction	MS-TFC	4.93	44.9%	0.69
	PELVIS	Flexion/Extension	MS-TFC	2.99	20.7%	0.88
	THIGH	Flexion/Extension	MS-TFC	0.24	2.2%	0.99
	SHANK	Internal/External Rotation	MS-TFC	5.30	28.8%	0.91
	THORAX	Medial/Lateral	MS-TFC	2.43	15.6%	0.96
ML	FOOT	Adduction/Abduction	IFC-MS	5.29	29.3%	0.87
	SHANK	Adduction/Abduction	IFC-MS	2.57	13.5%	0.96
	FOOT	Internal/External Rotation	IFC-MS	2.89	18.4%	0.92
	PELVIS	Adduction/Abduction	MS-TFC	3.20	28.0%	0.89
	THIGH	Flexion/Extension	MS-TFC	0.61	5.3%	0.99
	FOOT	Internal/External Rotation	MS-TFC	10.07	31.0%	0.88
	THIGH	Internal/External Rotation	MS-TFC	6.30	27.0%	0.91
	PELVIS	Medial/Lateral	MS-TFC	6.73	19.8%	0.93
VT	PELVIS	Anterior/Posterior	IFC-MS	4.83	28.1%	0.87
	THORAX	Anterior/Posterior	IFC-MS	6.26	47.8%	0.85
	THIGH	Vertical	IFC-MS	5.71	27.2%	0.91
	THIGH	Flexion/Extension	MS-TFC	0.71	5.7%	0.98
	PELVIS	Anterior/Posterior	MS-TFC	2.75	17.4%	0.92
	THIGH	Vertical	MS-TFC	1.34	9.3%	0.91
	THORAX	Vertical	MS-TFC	2.76	18.0%	0.93
AP	THIGH	Internal/External Rotation	IFC-MS	2.06	13.2%	0.98
	THORAX	Anterior/Posterior	IFC-MS	4.88	48.5%	0.80
	THORAX	Vertical	IFC-MS	15.06	65.0%	0.82
	THIGH	Flexion/Extension	MS-TFC	0.52	4.4%	0.99
	FOOT	Anterior/Posterior	MS-TFC	3.18	20.4%	0.91
	FOOT	Medial/Lateral	MS-TFC	1.22	12.9%	0.95

Sensitivity analysis of the input variables showed that participant height (cm) had the highest average relative importance across estimations of joint angles (mean = 75% ± 25%) and was the most important variable in 7 ANNs (figure 5.1). Whereas participants right leg length (cm) had the highest average relative importance across estimations of peak segment velocities (mean = 63% ± 29%) and was the most important in 8 ANNs (figure 5.2). Peak

accelerometer accelerations were ranked 4th (joint angles) and 7th (peak segment velocities) in average relative importance (figures 5.1 & 5.2).

Estimation of joint/segment angles

Output variable	Speed	ACC Peak	Height	Mass	LLegLength	RLegLength	StanceTime	IFC-MSTime	MS-TFCTime
1	44%	63%	73%	44%	100%	43%	24%	75%	37%
2	18%	65%	100%	49%	75%	74%	34%	79%	23%
3	32%	65%	100%	91%	27%	10%	43%	72%	75%
4	20%	16%	100%	82%	39%	35%	19%	41%	17%
5	29%	8%	74%	80%	65%	100%	35%	45%	48%
6	28%	29%	100%	38%	37%	25%	34%	29%	21%
7	19%	11%	100%	46%	46%	61%	15%	31%	22%
8	30%	58%	51%	100%	65%	80%	42%	91%	69%
9	24%	53%	100%	43%	25%	70%	8%	30%	5%
10	87%	41%	75%	31%	88%	100%	30%	66%	56%
11	43%	46%	61%	35%	100%	50%	37%	32%	41%
12	38%	61%	93%	91%	34%	57%	65%	100%	58%
13	46%	57%	25%	100%	95%	43%	19%	70%	40%
14	49%	100%	89%	56%	61%	31%	38%	36%	12%
15	36%	84%	60%	80%	84%	98%	13%	100%	72%
16	19%	54%	42%	54%	58%	100%	23%	65%	24%
17	27%	50%	100%	42%	57%	19%	21%	19%	25%
18	25%	100%	43%	23%	26%	23%	23%	29%	26%
19	36%	100%	76%	58%	42%	18%	32%	51%	68%
20	73%	96%	39%	100%	50%	54%	71%	74%	27%
Mean	**36%**	**58%**	**75%**	**62%**	**59%**	**55%**	**31%**	**57%**	**38%**
STDEV	**18%**	**28%**	**25%**	**26%**	**25%**	**30%**	**16%**	**26%**	**21%**

Key: Output Variable Number) Accelerometer Peak Accel Axis-Body Segment-Plane of motion-Gait phase.

1) RES-HIP-Flex/Ext-IFC; 2) RES-KNEE-Flex/Ext-IFC; 3) RES-THORAX-Flex/Ext-IFC; 4) RES-THORAX-Int/Ext Rot-IFC; 5) RES-ANKLE-Flex/Ext-MS; 6) RES-PELVIS-Flex/Ext-MS; 7) ML-THORAX-Int/Ext Rot-IFC; 8) ML-ANKLE-Int/Ext Rot-MS; 9) ML-SHANK-Add/Abd-TFC; 10) ML-THIGH-Flex/Ext-TFC; 11) VT-HIP-Flex/Ext-IFC; 12) VT-THORAX-Flex/Ext-IFC; 13) VT-ANKLE-Flex/Ext-MS; 14) VT-PELVIS-Flex/Ext-MS; 15) VT-ANKLE-Int/Ext Rot-MS; 16) AP-PELVIS-Add/Abd-IFC; 17) AP-PELVIS-Flex/Ext-IFC; 18) AP-THORAX-Flex/Ext-MS; 19) AP-ANKLE-Int/Ext Rot-MS; 20) AP-FOOT-Flex/Ext-TFC

Figure 5.1. Matrix of relative importance for the input variables in the estimation of joint/segment angles. Speed = running speed (km/h); ACC peak = accelerometer peak acceleration (g); Height = participant height (cm); Mass = participant mass (kg); LLegLength = participant left leg length (cm); RLegLength = participant right leg length (cm); StanceTime = accelerometer derived stance time (s); IFC-MSTime = accelerometer derived time between IFC and MS; MS-TFCTime = accelerometer derived time between MS and TFC; STDEV = Standard deviation.

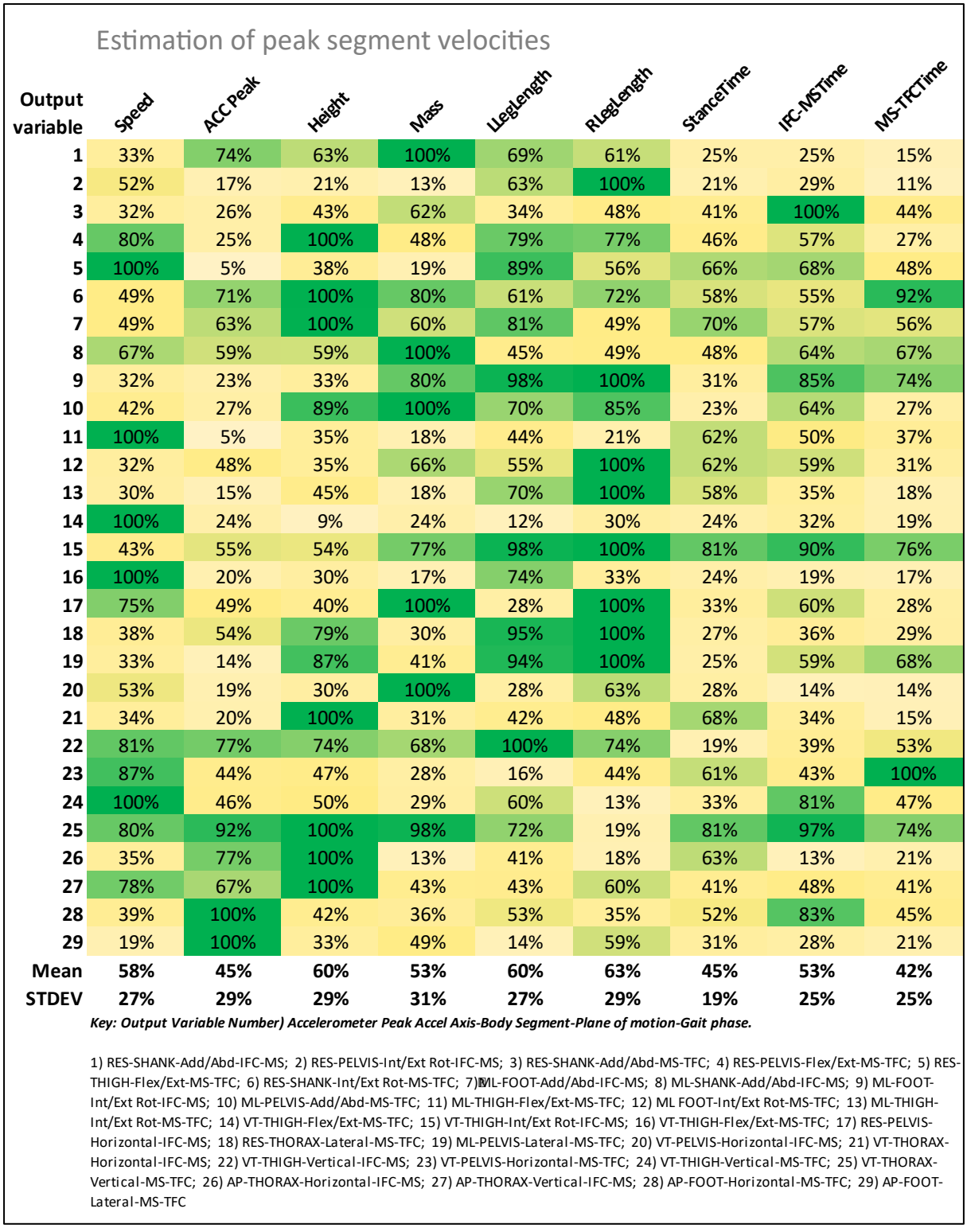

Output variable	Speed	ACC Peak	Height	Mass	LLegLength	RLegLength	StanceTime	IFC-MSTime	MS-TFCTime
1	33%	74%	63%	100%	69%	61%	25%	25%	15%
2	52%	17%	21%	13%	63%	100%	21%	29%	11%
3	32%	26%	43%	62%	34%	48%	41%	100%	44%
4	80%	25%	100%	48%	79%	77%	46%	57%	27%
5	100%	5%	38%	19%	89%	56%	66%	68%	48%
6	49%	71%	100%	80%	61%	72%	58%	55%	92%
7	49%	63%	100%	60%	81%	49%	70%	57%	56%
8	67%	59%	59%	100%	45%	49%	48%	64%	67%
9	32%	23%	33%	80%	98%	100%	31%	85%	74%
10	42%	27%	89%	100%	70%	85%	23%	64%	27%
11	100%	5%	35%	18%	44%	21%	62%	50%	37%
12	32%	48%	35%	66%	55%	100%	62%	59%	31%
13	30%	15%	45%	18%	70%	100%	58%	35%	18%
14	100%	24%	9%	24%	12%	30%	24%	32%	19%
15	43%	55%	54%	77%	98%	100%	81%	90%	76%
16	100%	20%	30%	17%	74%	33%	24%	19%	17%
17	75%	49%	40%	100%	28%	100%	33%	60%	28%
18	38%	54%	79%	30%	95%	100%	27%	36%	29%
19	33%	14%	87%	41%	94%	100%	25%	59%	68%
20	53%	19%	30%	100%	28%	63%	28%	14%	14%
21	34%	20%	100%	31%	42%	48%	68%	34%	15%
22	81%	77%	74%	68%	100%	74%	19%	39%	53%
23	87%	44%	47%	28%	16%	44%	61%	43%	100%
24	100%	46%	50%	29%	60%	13%	33%	81%	47%
25	80%	92%	100%	98%	72%	19%	81%	97%	74%
26	35%	77%	100%	13%	41%	18%	63%	13%	21%
27	78%	67%	100%	43%	43%	60%	41%	48%	41%
28	39%	100%	42%	36%	53%	35%	52%	83%	45%
29	19%	100%	33%	49%	14%	59%	31%	28%	21%
Mean	**58%**	**45%**	**60%**	**53%**	**60%**	**63%**	**45%**	**53%**	**42%**
STDEV	**27%**	**29%**	**29%**	**31%**	**27%**	**29%**	**19%**	**25%**	**25%**

Key: Output Variable Number) Accelerometer Peak Accel Axis-Body Segment-Plane of motion-Gait phase.

1) RES-SHANK-Add/Abd-IFC-MS; 2) RES-PELVIS-Int/Ext Rot-IFC-MS; 3) RES-SHANK-Add/Abd-MS-TFC; 4) RES-PELVIS-Flex/Ext-MS-TFC; 5) RES-THIGH-Flex/Ext-MS-TFC; 6) RES-SHANK-Int/Ext Rot-MS-TFC; 7) ML-FOOT-Add/Abd-IFC-MS; 8) ML-SHANK-Add/Abd-IFC-MS; 9) ML-FOOT-Int/Ext Rot-IFC-MS; 10) ML-PELVIS-Add/Abd-MS-TFC; 11) ML-THIGH-Flex/Ext-MS-TFC; 12) ML FOOT-Int/Ext Rot-MS-TFC; 13) ML-THIGH-Int/Ext Rot-MS-TFC; 14) VT-THIGH-Flex/Ext-MS-TFC; 15) VT-THIGH-Int/Ext Rot-IFC-MS; 16) VT-THIGH-Flex/Ext-MS-TFC; 17) RES-PELVIS-Horizontal-IFC-MS; 18) RES-THORAX-Lateral-MS-TFC; 19) ML-PELVIS-Lateral-MS-TFC; 20) VT-PELVIS-Horizontal-IFC-MS; 21) VT-THORAX-Horizontal-IFC-MS; 22) VT-THIGH-Vertical-IFC-MS; 23) VT-PELVIS-Horizontal-MS-TFC; 24) VT-THIGH-Vertical-MS-TFC; 25) VT-THORAX-Vertical-MS-TFC; 26) AP-THORAX-Horizontal-IFC-MS; 27) AP-THORAX-Vertical-IFC-MS; 28) AP-FOOT-Horizontal-MS-TFC; 29) AP-FOOT-Lateral-MS-TFC

Figure 5.2. Matrix of relative importance for the input variables in the estimation of peak segment velocities. Speed = running speed (km/h); ACC peak = accelerometer peak acceleration (g); Height = participant height (cm); Mass = participant mass (kg); LLegLength = participant left leg length (cm); RLegLength = participant right leg length (cm); StanceTime = accelerometer derived stance time (s); IFC-MSTime = accelerometer derived time between IFC and MS; MS-TFCTime = accelerometer derived time between MS and TFC; STDEV = Standard deviation.

5.4. Discussion:

This study aimed to determine the predictive capabilities of ANNs containing GPS-based accelerometer, running speed and anthropometric data to estimate running kinematics. The study's results provide insights into the application of deep learning algorithms with data that is easily accessible to sports science and medical practitioners working with team sports athletes to conduct analyses of running kinematics in the field.

Correlation coefficients of the estimated vs actual output variables ranged from strong to excellent across all output variables, showing the model's performance was highly accurate. Overall, estimations of joint/segment angles (mean rRMSE = 13.0 ± 4.3%) were better than peak segment velocities (mean rRMSE = 22.1 ± 14.7%). Previous research (Chapter 4) found that peak segment velocities had a greater effect on GPS-accelerometer peak accelerations than joint/segment angles in linear regression-based analysis. Conversely, in the current study, better accuracy was observed in predicting joint/segment angles than peak segment velocities, indicating a stronger relationship between the input variables and joint/segment angles. Including added input variables (running speed, stance times, anthropometrics) or the capability of ANNs to utilise non-linear relationships may be responsible for this finding.

Sensitivity analysis of the input variables highlighted that the GPS-accelerometer-derived variables were, on average, not the most important variables in both joint/segment and peak segment velocities estimations (Figures 5.1 & 5.2). The performance of each ANN must be considered, as the accelerometer peak acceleration had the highest relative importance in

estimating thorax flexion/extension at MS, which was the most accurate estimation of all joint/segment angles. Despite this, the value of including anthropometric data in the ANNs has become evident in the current study. The highest mean relative importance for joint/segment angles were participant height (75 ± 25 %) and mass (62 ± 26 %), and for peak segment velocities, leg length (right = 63 ± 29 %; left = 60 ± 27 %) and height (60 ± 29 %) were highest. Anthropometric data has been previously employed within pre-calibration procedures of conventional neural networks to improve the accuracy of estimating joint kinematics[57], and our results show that anthropometric data can also aid multilayer perceptron ANNs instead of relying on IMU data alone.

The five joint/segment angles that had the highest accuracy during testing were thorax flexion/extension at IFC (RMSE = 0.93°; rRMSE = 7.6%; *r* = 0.98) and MS (RMSE = 0.65°; rRMSE = 4.1%; *r* = 0.98), pelvis flexion/extension at IFC (RMSE = 1.82°; rRMSE = 9.6%; *r* = 0.95) and MS (RMSE = 1.56°; rRMSE = 9.2%; *r* = 0.96), and hip flexion/extension at IFC (RMSE = 2.26°; rRMSE = 9.9%; *r* = 0.96). Previous investigations have typically only analysed lower limb kinematics and found hip flexion/extension RMSE values of 5.1 – 5.6° and knee flexion/extension RMSE values of 4.8 – 6.5° during running[39,157]. The present study differed from previous investigations as estimations of joint/segment angles at specific gait events were estimated rather than the continuous joint angle over the whole gait cycle and the type of ANN used. Nevertheless, our results showed that the RMSE values of knee flexion/extension at IFC were 2.47°. It can be suggested that MLP ANNs could achieve similar or greater accuracy in estimating hip and knee sagittal joint angles than previous methods. Accurate estimations of peak thigh flexion/extension and vertical velocities during propulsion

were also observed (rRMSE ≤ 9.3%) however, there are no previous studies to compare these results against.

Analysing the sagittal plane kinematics of athletes in the field can provide sports science and medical practitioners with useful insight into their athletes' physical condition and running performance. Trunk flexion/extension angle has been shown to increase when localised muscular fatigue is present[87,212]. Additionally, more experienced runners typically have less trunk flexion and reduced peak hip flexion during foot contact, resulting in increased performance[49] and reduced injury risk[213]. Segment velocities can also be used to characterise performance, as thigh flexion/extension angular velocity is a determining factor during sprint running[214]. Our results showed that all these variables can be accurately estimated with ANNs, thus providing practitioners with a method to quantify variables related to running performance and monitoring fatigue in the field.

The findings of this study can also be used in relation to sports injury analysis. Accurate estimations of knee flexion/extension angle were found, which could be employed regarding anterior cruciate ligament (ACL) injuries. Athletes who have undergone ACL reconstruction can have limited knee extension during running for up to one year post-surgery[52]. Therefore, monitoring this variable during rehabilitation can provide insights into an athlete's progress. It has also been suggested that athletes with limited knee flexion during running, jumping and cutting tasks have a greater risk of suffering non-contact ACL injuries[53], which is prevalent among female athletes[215]. However, it must be stated that the current study only analysed the prediction capabilities during straight line steady state running. Whether the same accuracies

in running kinematic estimation can be achieved in jumping and multidirectional tasks remains unclear. Yet, the present study offers the potential for practitioners to accurately measure sagittal plane kinematics that are of interest in hip and knee injuries.

Furthermore, the methodology employed within this study utilised commercially available software (IBM SPSS Modeler software version-22) to compute the MLP ANNs. Using this software does not require knowledge or experience in building and training ANNs. Most sports science and medicine university degrees teach the use of SPSS software during their research methods modules. Thus, the methodology used within the present study is reproducible to those sports science and medical practitioners who have undergone a university degree and can be introduced into their daily practices.

The limitations of the present study are that output variables were specific to gait events. Analysing joint/segment angles and velocities over the whole gait cycle would provide a more comprehensive insight into the predictive capacity of ANNs to predict running kinematics with data from GPS devices and anthropometric measurements. Additionally, MLPs are a simple form of ANNs, and greater accuracy may be achieved with more complex classes of ANNs[57].

5.5. Conclusion:

The present study explored the predictive capabilities of using ANNs with GPS-based accelerometer data, treadmill-derived running speed and anthropometric measurements to estimate running kinematics. Accurate estimations of joint/segment angles and peak segment

velocities were achieved, with the highest estimation accuracy for flexion/extension angles of the thorax, pelvis and hip, and peak thigh flexion/extension and vertical velocities. Our findings provide sports science and medical practitioners, working with this data, a method of conducting field-based analysis of running kinematics.

Chapter 6: Discussion

6.1. Motive:

The motivation for this thesis was to provide sports science and medical practitioners working with GPS devices with a set of methods to conduct biomechanical analysis of their athletes in the field from the IMU data collected by these devices. Current approaches to predict injury risk perform poorly with the standard variables outputted from GPS devices[12], and there is a need for additional variables to enhance the level of insight into the physical condition of athletes within athlete monitoring frameworks. Utilising additional assessments to understand an athlete's response to the training load theoretically could provide this insight. Yet, conventional methods such as maximal performance testing[18,19,22] and blood taxonomy[20,21], contain barriers (equipment costs, athlete motivation etc.) that prevent frequent use within practice. Incorporating biomechanical analysis with GPS devices could overcome these barriers as they can capture an athlete's movement strategies conveniently in the field without the need for additional equipment. Furthermore, biomechanical variables have been previously employed to measure fatigue[47,87,163], aid in assessing injury risk[53,213] and used to track an athlete's progress during injury rehabilitation[121,129]. Therefore, displaying the potential value of utilising biomechanical analysis as a measure of response.

6.2. Overview of IMU-derived biomechanical variables (Chapter 2):

To understand which biomechanical variables can provide insights into an individual's physical condition, I conducted an overview of literature encompassing the practical and logistical applications of IMUs to analyse locomotion in clinical and sporting settings (Chapter 2). This process revealed that IMU-derived variables quantified either the quantity, rate or quality of

locomotion. The number of steps and cadence (number of steps per minute) can accurately measure the quantity and rate of locomotion[31,95,130]. The quality of locomotion can be analysed at a basic level by measuring stance and swing times[35,140], as they allow for analysis of the left and right limbs. For a detailed view, as seen in running analyses, the acceleration profiles of the individual segments within the body must be captured, which can be used to infer changes/differences in body kinematics[142,150]. The accuracy of each variable depended on the data processing procedures, the type of IMU employed and the mounting site of the IMU. Stride length, distance and speed could also quantify all three aspects of locomotion, but they had varied accuracies and required long set-up and data processing procedures[36,138]. Similarly, IMU measurement of joint angles had complications in longitudinal use due to errors associated with sensor misalignment[55]. However, introducing machine learning algorithms has been shown to reduce these errors[39,57], but these developments are only recent, and there is a lack of applied research studies in this area. Lastly, in relation to this thesis, methods employing a single IMU sensor are favourable within the sporting environment as there is a reduced set-up time, and they are less likely to interfere with performance than using multiple IMUs.

The outcomes of this review provided direction into which variables can potentially be accurately measured with the GPS-based IMU and those that can provide insights into an individual's physical condition. The GPS devices already capture the distance and speed of locomotion with the coordinate data; therefore, IMU-derived variables of quantity and rate were not required. Variables characterising the quality of locomotion, though, could provide this added insight.

Spatiotemporal variables such as stance and swing time are correlated to biomechanical predictors of running performance[145,147] and are influenced by fatigue[47]. Analysing peak accelerations of a bodily segment can inform on the changes in running kinematics and are also associated with fatigue[61,152]. Despite the issues with field-based accuracy in linear regression-based models, IMU estimations of joint angles can provide insight into the subtle kinematic differences in an individual's locomotion during injury rehabilitation[121,129]. Considering the long pre-calibration and data processing procedures, IMU-derived stride length was not a variable chosen to be included in this thesis. Instead, stride length can be calculated by including the global positioning data (distance) divided by step count, which emphasises the importance of detecting foot contact with GPS devices. Furthermore, by validating the variables mentioned above, grouping athletes' running styles, as proposed in the dual axis framework[48], would be achievable with GPS devices.

Based on the findings of the overview, three key objectives were identified:

1 To develop a method of identifying key gait events during foot contact to calculate spatiotemporal variables of running gait with the GPS-based IMU (Chapter 3).
2 To investigate the relationship between running kinematics and the acceleration profile of the GPS-based IMU (Chapter 4)
3 To investigate the potential of predicting running kinematics using the GPS-based IMU, running speed and anthropometric data (Chapter 5).

6.3. Validation of GPS-derived spatiotemporal variables (Chapter 3):

To calculate spatiotemporal variables (stance and swing time) with IMUs, it is paramount to accurately identify gait events of initial foot contact (IFC) and terminal foot contact (TFC). Additionally, by identifying midstance (MS), the two subphases of foot stance (impact and propulsion) can be characterised[143]. Methodologies have been validated with IMUs mounted at the shank[142], pelvis[143,216] and sternum[72,174] to identify IFC, MS and TFC. However, they cannot be directly applied to the GPS-based IMUs data as the devices are mounted on the posterior aspect of the upper trunk and changes in mounting sites can affect accuracy[68].

In this thesis (Chapter 3), a novel method of identifying IFC, MS and TFC was developed by utilising the vertical acceleration profile of the GPS-based accelerometer. IFC and TFC were identified through a zero cross-over method, and MS was identified as the second peak within the acceleration profile following IFC. The advantage of this method is that it is relatively simple to conduct compared to other methods[140] as it does not require additional filtering of the data post export out of the GPS software and is uniaxial. Comparisons of stance time with those measured by the motion capture system showed GPS-measured underestimations at running speeds of 10 – 15 km/h and overestimations of 16 – 18 km/h, similar to previous validated methods mounting the IMUs on the sternum[72]. The highest agreement between systems was observed at running speeds of 12 km/h, 14 km/h, 15 km/h and 16 km/h. Furthermore, errors in stance time estimations were largely associated with identifying TFC, and the measurement of the IFC-MS time was the most accurate of the two subphases of foot stance.

The zero cross-over method presented within this thesis showed accurate measurements of the characteristics of foot stance with the GPS-based accelerometer, thereby providing a method to calculate spatiotemporal running variables. As a result, sports science and medical practitioners can use GPS devices to categorise their athlete's running styles, as presented in the dual axis framework[48], by measuring stance/flight time, step frequency and stride length (GPS-derived distance ÷ step frequency). Oeveran et al.[48] proposed that these spatiotemporal variables are associated with biomechanical predictors of running performance, and categorising running styles may guide future research regarding training interventions and injury prevalence.

Another important finding in this chapter was apparent when analysing the between-participant variances in stance time estimations. The GPS method showed that the influence of individual running styles may be characterised in the GPS-based accelerometer data. The transfer of an underestimation of stance time to an overestimation did not occur at the same speed for all participants. Differences in running styles can cause this, as it has been previously shown that lower limb kinematics can influence the acceleration profile of the trunk segment[182]. Moreover, this suggests that the GPS-based IMU could provide further insights into the differences in running styles than only analysing spatiotemporal variables.

6.4. The effects of running kinematics on the GPS acceleration profile (Chapter 4):

To understand whether the acceleration profile of the GPS devices is influenced by differences in running kinematics, an investigation was conducted in this thesis (Chapter 4) into the effects

of running kinematics on the peak accelerations captured by the GPS-based accelerometer. Analysing peak accelerations of a body segment with accelerometers has been previously employed to investigate kinematic changes in applied running-based studies[61,62,152,217]. Typically, the accelerometer is placed on the segment above a joint in the lower body and changes in the joint angle will cause changes in peak accelerations during foot contact[142]. Albeit, the upper trunk has not been a mounting site previously employed in this manner and considering the distance from the point of ground contact the GPS is, it was unclear which joints/segments would have the largest effect on the GPS peak accelerations. Lindsey et al.[182] investigated an accelerometer mounted on the lower trunk and found significant effects of lower limb sagittal plane kinematics. However, they analysed the magnitude of the acceleration profile over the whole gait cycle and employed a different mounting site. Considering the above, it was important to conduct a comprehensive investigation into which joints/segments have the largest effects on GPS accelerations.

In order to gain insight into the intersegmental relationship between joint/segment angles and subsequent segment velocities throughout the stance phase, two categories of kinematic variables were included. Category one variables included joint/segment kinematics at IFC, MS and TFC, and category two variables included peak segment velocities during impact (IFC-MS) and propulsion (MS-TFC). A series of generalised linear mixed models were employed to determine the size of the effect of each variable on the resultant (RES), vertical (VT), anterior-posterior (AP) and mediolateral (ML) peak GPS-accelerometer accelerations, if they were significant and whether the relationship was direct or inverse. Multiple speeds per participant were included to observe inter and intra-participant variances in running kinematics.

The outcomes of this investigation showed that the peak segment velocities had a larger effect than the joint/segment kinematics on the RES, VT and AP peak GPS-accelerometer accelerations. More specifically, the velocities of the shank (inverse effect) and pelvis (direct effect) during impact (IFC-MS) had the largest effects of all variables. These findings suggest that the attenuation properties of the surrounding joints to the shank (reduced shank velocity = increased GPS acceleration) and the kinematics of the pelvis to maintain trunk stability (increased pelvis velocity = increased GPS acceleration) are the two characteristics of running style that have the largest effect on the peak RES accelerations of the GPS. Moreover, by analysing differences between peak accelerations in the individual axis of the GPS-accelerometer (VT, AP and ML), insights into the differences/changes in stability properties of the pelvis/trunk segments can be achieved.

The practical applications of this investigation are that practitioners may conveniently analyse the peak accelerations captured with the GPS devices to measure running kinematics indirectly. Most GPS manufacturers' software calculates peak acceleration instances during a training/game session[193], and therefore, does not require any additional data processing. RES peak accelerations could be used to analyse the effect of training interventions employed to improve lower limb stifness[218,219]. Additionally, by analysing the differences between VT, AP and ML peak accelerations during a training/game session, the level of neuromuscular fatigue affecting an athlete's trunk can also be determined[87,163]. As a result, peak accelerations can be included within a framework to categorise athletes' running styles along with spatiotemporal variables as described previously[48].

This investigation also provided valuable information into the strength of the relationships between running kinematics and the acceleration profiles of the GPS-based accelerometer. It has been previously suggested that the device's mounting site was unsuitable for detecting differences in lower limb kinematics[64]. This investigation refuted these claims and showed evidence of a relationship. This finding was pivotal in deciding the next chapter within this thesis as it laid the foundations for investigating whether the GPS devices could be used to estimate running kinematics directly (Chapter 5).

6.5. A novel method for predicting running kinematics (Chapter 5):

The work presented within this thesis led to the development of a number of novel methods to measure biomechanical variables with GPS devices related to analysing the physical condition of athletes. Spatiotemporal variables and peak accelerations offer a method to measure an athlete's running style. Yet, these methods are indirect and do not allow for detailed insight into individual joint/segment kinematics. Direct measurement of joint/segment kinematics is crucial in analysing the progress of an individual's rehabilitation from injury[52,121] and can depict discrete kinematic contributors to performance[49,214]. However, field-based measurement of joint kinematics with IMUs is practically impossible with the conventional linear regression-based methods when applying them to team sports athletes. This is because they require IMUs to be placed above and/or below the joint, and movement of the sensors (which is certain during high-velocity running) during data capture greatly reduces accuracy[127].

Recent developments of including deep learning algorithms, such as artificial neural networks (ANN), in the IMU data processing have shown promise in overcoming sensor misalignment errors[127]. ANN models can detect non-linear relationships between input and output variables[56], and accurate joint kinematics estimation was previously achieved while running with ANNs containing IMU data[39,58]. Considering this and the relationships found previously (Chapter 4) between running kinematics and the GPS accelerometer data, this thesis explored the predictive capabilities of the data collected by the GPS-based IMU to be used within ANNs to estimate running kinematics.

The advantage of ANNs is that they contain a training module whereby the model learns the strength of the relationships between variables and appropriately 'weights' the importance of each input variable[56]. ANNs then test out the input variables' predictive performance in the testing module[56]. To increase the performance of the ANN model developed in this thesis, I decided to include input variables available to sports science practitioners that had previously demonstrated a relationship with running kinematics. Consequently, peak GPS accelerations, stance time[209], running speed[195,196] and athlete anthropometrics[208] were selected as they met these criteria.

The output variables chosen to be estimated were the joint/segment angles and peak segment velocities shown in Chapter 4 to have a significant relationship with the GPS accelerometer data. Model summaries from the testing modules of the ANNs showed the

highest accuracies for predicting sagittal plane kinematics of the thorax, pelvis and hip at IFC and peak thigh velocity during MS-TFC (relative root-mean-squared error < 10%). In addition, sagittal plane knee kinematics at IFC had less error than previous studies[39,58] (root-mean-squared error = 2.47°). Although predictions of these variables were restricted to specific gait events (IFC, MS and TFC) and not over the whole gait cycle, the results showed promising accuracy of the GPS IMU and anthropometric data to predict running kinematics.

As previously mentioned, analysing running kinematics can be of great value to practitioners working with athletes. In particular, the variables that could be accurately predicted i.e. sagittal plane kinematics of the trunk, hip, and thigh, are important when evaluating running performance[49,214]. Furthermore, flexion/extension angles of the hip and knee can be used to assess injury risk[53,213]. Findings from this thesis showed that all these variables can be predicted with ANNs containing GPS and anthropometric data with different levels of accuracy. There may be concerns with the complexity of employing ANNs in the daily practices of sports science and medical practitioners, as it is assumed that experience in coding and data processing is needed. However, the ANNs employed within this thesis were developed in commercially available software (IBM SPSS Modeler software version-22) using the multilayer perceptron class (MLP) of ANNs. Most sports science and medicine university degrees teach the use of SPSS software, and therefore, the methods presented here are reproducible for those practitioners who have undergone a university degree.

As a result, the novel findings of this investigation provide sports science and medical practitioners working with GPS devices and anthropometric data with a practical method of

conducting field-based analysis of running kinematics that can be used to measure the subtle characteristics of an athlete's biomechanics. The high levels of accuracy achieved within this study are notable, considering the previous issues with estimating kinematic data with a single IMU sensor, and the method presented could be instrumental in conducting frequent biomechanical analyses of athletes.

6.6. Concluding remarks:

In this thesis, a series of methods to conduct biomechanical analysis of running was developed with a GPS-based IMU commonly used by team sports athletes. These newly developed data processing and analysis techniques lay the foundations for increasing the biomechanical understanding of athletes in the field concerning sports performance and injury occurrence. Including biomechanical variables within athlete monitoring frameworks can provide insight into the quality of an athlete's locomotion, thereby providing sports science and medical practitioners with a measure of response to training load that can be explored to understand how these variables can assess the physical condition of athletes.

The accuracy of utilising the GPS-based IMU to measure spatiotemporal variables of running, as well as using these devices to measure running kinematics, was demonstrated within this thesis. Applying these variables will enable the characterisation of running styles in a cohort of athletes, which can be used in applied research studies for injury prediction modelling and assessing the effectiveness of training interventions to improve running performance. The impact of this thesis lies within the practicality of the methods developed to measure the

biomechanical variables. The direct measurement of such biomechanical data needs access to comprehensive motion capture equipment that is not feasible in real-world settings, such as athletic performance on the pitch. All variables use the data collected within the GPS-based IMU and do not require additional IMU sensors or motion capture technologies. The only additional data required are anthropometric measurements and running speed when using ANNs to estimate running kinematics, which are easily attainable. Furthermore, the data processing procedures utilised are simple or use commercially available software, thereby presenting to sports science and medical practitioners with reproducible methods that can be conveniently implemented into their daily work.

6.7. Implications for practice:

The work presented in this thesis has utilised the practical experience I have accrued working as a sports science practitioner in professional football over the past 12 years. During this time, several considerations in implementing a successful athlete monitoring framework have become apparent. Assessment of an athlete's physical condition is a complex process. An over-reliance on the measurement of training load (dose) can often lead to shortcomings as an athlete's activity is only captured for a small percentage of their total daily workload and does not take into account activity away from the immediate training environment. Utilising a dose/response model; whereby additional information is utilised to understand an athlete's response to the training program, can provide the contextual insight needed to inform interventions.

As previously mentioned, there can be barriers within the football environment that prevent the frequent use of assessments to measure an athlete's response[16]. Aside from the equipment costs and specialised training needed, in my experience, player/coach buy-in has the biggest influence on gaining accurate and frequent measures of response. Jump and muscle strength testing requires allocated time away from the pitch and maximal effort from the athletes. Likewise, subjective questionnaires count on the honest participation from the athletes and accurate self-assessment. These assumptions are not always met as professional football is a high-pressure and volatile environment where psychological factors can affect the integrity of these assessments. It's from this perspective that conducting biomechanical analysis with GPS devices can add great value. The methods provided in this thesis allow for an athlete's response to training load to be measured whilst they are in their natural training environment with minimal time cost and additional effort from the athletes. It must be stated though, the study designs employed within this thesis were laboratory-based and the application of GPS-based biomechanical variables is yet to be explored in a practical setting. Therefore, it is recommended that they should be initially used in conjunction with other methods of measuring response to understand their sensitivity to assess an athlete's physical condition.

Admittedly, there are other wearable systems that can provide biomechanical analysis which have been designed for use in football. A dual IMU sensor system (Playermaker, London, UK) is an alternative to conventional GPS devices to measure locomotion speed and distance that also provides spatiotemporal biomechanical analysis[220–222]. These devices are mounted on each foot which is a previously validated location to mount IMUs to measure variables such

as stance time[223]. Comparisons between this system and the GPS-based IMU method were not explored within this thesis. However, the influence of sensor placement is important when considering other biomechanical variables. Chapters 4 & 5 showed that the upper trunk mounting site allows for the kinematics of the lower body and trunk to be inferred and estimated with the GPS-based IMU peak accelerations. These relationships may not be present with a foot-mounted IMU as it will be unable to measure the attenuation of force throughout the kinetic chain. Furthermore, differences are present between systems when measuring running speed and distance[221,222], which could deter practitioners from replacing GPS devices with a foot-mounted IMU system. GPS devices have been used by team sports traditionally, so there is a wealth of historical data to which retrospective analysis can be conducted with the methods displayed in this thesis.

There are two considerations before applying the methods developed in this thesis to field-based analysis of an athlete's biomechanics with the GPS-based IMU. Firstly, the methods are explicit to linear steady-state running, so therefore, the running must be in a controlled setting or periods of linear running must be filtered from the training/game session. Secondly, the method developed to measure the spatiotemporal variables is most accurate within running speeds of 12 – 16 km/h, which needs to be considered when conducting this analysis.

The global coordinate data collected by the GPS devices can be employed to separate periods of linear running and between speed thresholds by applying a filter to the raw data[67]. During a football match, approximately 29.7% ± 2.8% of total distance run (10943 ± 935m) is between speeds of 11 and 19 km/h[224] which is dependent on playing position and league standard[225].

Periods of linear steady state running within these speeds may be considerably lower but even 1% would equate to approximately 100m and 70-80 foot strikes that can be analysed. Alternatively, a controlled running drill could be implemented into a warm up/cool down and these instances can be manually separated within the GPS manufacturer's software.

Once the periods of straight-line running have been established, there are several applications of the biomechanical variables in relation to sports performance and injury. Utilising the spatiotemporal variables will allow for the characterisation of running styles between athletes. Particularly, stance/flight time and step frequency/length can provide insight into the running economy and force production capabilities of athletes[46,49–51]. Including the resultant peak accelerations during foot stance can also provide insight into each athlete's lower limb stiffness characteristics, which can be used to further depict differences in running style and/or analyse the effectiveness of training programs to enhance this physical quality[218]. On the other hand, analysing differences between the peak accelerations within the individual axes along with stance time[47] can be used as a proxy measure of neuromuscular fatigue affecting the motions of the trunk, such as the musculature of the pelvis and posterior chain[87].

Moreover, direct estimation of running kinematics can measure the discrete changes in an athlete's running style, which is highly valuable during an athlete's rehabilitation from injury. Practitioners could use this analysis with athletes returning from trunk, pelvis, hip and knee injuries to track progress or with healthy athletes to assess injury risk[53,213]. It could also benefit training interventions focused on modifying trunk posture and hip kinematics to improve

running performance[49]. Lastly, considering the relatively few longitudinal studies capturing athletes' biomechanics in the field, the practicability of the methods displayed in this thesis will enable the identification of new relationships between these biomechanical variables and sporting performance/injury.

6.8. Future directions:

A landmark finding of this thesis was the accuracy of applying deep learning algorithms to estimate discrete characteristics of running kinematics with GPS-based IMU data, running speed and anthropometric measurements. The results showed that sagittal plane kinematics of the trunk, pelvis and hip can be determined with less than 10% error. A recommendation for further investigations would be to increase the sample size of the dataset within the artificial neural networks to improve the capacity of the model to estimate a wider range of kinematic variables. Combining the data from the GPS-based IMU with a marker-less motion capture system may be a viable option, considering the advancements in optical tracking technologies[226].

Another application of this thesis could be to utilise the estimations of running kinematics within further research studies to identify the running styles linked to athletes' injury risk. Capturing the field-based movement profiles of the trunk, pelvis, and hip would allow for the correlation of an athlete's normative ranges with their injury history to attain insight into the characteristics of athletes with high injury risk. A similar methodology could be used to determine the biomechanical predictors of performance and further add to the research in

this area[48]. Additionally, utilising GPS-based IMU biomechanical variables with other measures of response or with other IMU systems (Playermaker™) in these settings, could provide a comparative insight into the advantages gained from regularly conducting biomechanical analysis in team sports. Establishing this will provide practitioners with the guidance on the sensitivity of the GPS-based IMU to determine an athlete's physical condition and define its role within an athlete monitoring framework.

Finally, even though the variables outlined in this thesis were related to straight-line running, this work provides scope for further investigations into quantifying multidirectional movement with the GPS-based IMU. Providing this would allow for insights into the shuffling, cutting and changing direction movement patterns that are so frequent in the activity profiles of team sports athletes.

References:

1. Edgecomb SJ, Norton KI. Comparison of global positioning and computer-based tracking systems for measuring player movement distance during Australian Football. *J Sci Med Sport*. 2006;9(1-2):25-32. doi:10.1016/j.jsams.2006.01.003

2. Willmott AGB, James CA, Bliss A, Leftwich RA, Maxwell NS. A comparison of two global positioning system devices for team-sport running protocols. *J Biomech*. 2019;83:324-328. doi:10.1016/j.jbiomech.2018.11.044

3. Beato M, Coratella G, Stiff A, Iacono A Dello. The Validity and Between-Unit Variability of GNSS Units (STATSports Apex 10 and 18 Hz) for Measuring Distance and Peak Speed in Team Sports. *Front Physiol*. 2018;9. doi:10.3389/fphys.2018.01288

4. Buchheit M, Racinais S, Bilsborough JC, et al. Monitoring fitness, fatigue and running performance during a pre-season training camp in elite football players. *J Sci Med Sport*. 2013;16(6):550-555. doi:10.1016/j.jsams.2012.12.003

5. Ritchie D, Hopkins WG, Buchheit M, Cordy J, Bartlett JD. Quantification of Training and Competition Load Across a Season in an Elite Australian Football Club. *Int J Sports Physiol Perform*. 2016;11(4):474-479. doi:10.1123/ijspp.2015-0294

6. Buchheit M, Lacome M, Cholley Y, Simpson BM. Neuromuscular Responses to Conditioned Soccer Sessions Assessed via GPS-Embedded Accelerometers: Insights Into Tactical Periodization. *Int J Sports Physiol Perform*. 2018;13(5):577-583. doi:10.1123/ijspp.2017-0045

7. Gabbett TJ. GPS Analysis of Elite Women's Field Hockey Training and Competition. *J Strength Cond Res*. 2010;24(5):1321-1324. doi:10.1519/JSC.0b013e3181ceebbb

8. Noblett H, Hudson S, Killey J, Fish M. The Physical and Physiological Match-Play Locomotor Activity Profiles of Elite Domestic Male Field Hockey. *J Sport Sci Med*. Published online June 1, 2023:273-280. doi:10.52082/jssm.2023.273

9. Ekstrand J, Waldén M, Hägglund M. Hamstring injuries have increased by 4% annually in men's professional football, since 2001: a 13-year longitudinal analysis of the UEFA Elite Club injury study. *Br J Sport Med*. 2016;50(12):731-737. http://bjsm.bmj.com/content/50/12/731.short

10. Ekstrand J, Bengtsson H, Waldén M, Davison M, Khan KM, Hägglund M. Hamstring injury rates have increased during recent seasons and now constitute 24% of all injuries in men's professional football: the UEFA Elite Club Injury Study from 2001/02 to 2021/22. *Br J Sports Med*. 2023;57(5):292-298. doi:10.1136/bjsports-2021-105407

11. Bahr R. Risk factors for sports injuries -- a methodological approach. *Br J Sports Med*. 2003;37(5):384-392. doi:10.1136/bjsm.37.5.384

12. Carey DL, Ong K, Whiteley R, Crossley KM, Crow J, Morris ME. Predictive Modelling of Training Loads and Injury in Australian Football. *Int J Comput Sci Sport*. 2018;17(1):49-66. doi:10.2478/ijcss-2018-0002

13. Rossi A, Pappalardo L, Cintia P, Iaia FM, Fernàndez J, Medina D. Effective injury forecasting in soccer with GPS training data and machine learning. Sampaio J, ed. *PLoS One*. 2018;13(7):e0201264. doi:10.1371/journal.pone.0201264

14. Claudino JG, Capanema D de O, de Souza TV, Serrão JC, Machado Pereira AC, Nassis GP. Current Approaches to the Use of Artificial Intelligence for Injury Risk Assessment and Performance Prediction in Team Sports: a Systematic Review. *Sport Med - Open*.

2019;5(1):28. doi:10.1186/s40798-019-0202-3

15. Van Eetvelde H, Mendonça LD, Ley C, Seil R, Tischer T. Machine learning methods in sport injury prediction and prevention: a systematic review. *J Exp Orthop*. 2021;8(1):27. doi:10.1186/s40634-021-00346-x

16. Akenhead R, Nassis GP. Training Load and Player Monitoring in High-Level Football: Current Practice and Perceptions. *Int J Sports Physiol Perform*. 2016;11(5):587-593. doi:10.1123/ijspp.2015-0331

17. Silva JR, Rumpf MC, Hertzog M, et al. Acute and Residual Soccer Match-Related Fatigue: A Systematic Review and Meta-analysis. *Sport Med*. 2018;48(3):539-583. doi:10.1007/s40279-017-0798-8

18. Robineau J, Jouaux T, Lacroix M, Babault N. Neuromuscular Fatigue Induced by a 90-Minute Soccer Game Modeling. *J Strength Cond Res*. 2012;26(2):555-562. doi:10.1519/JSC.0b013e318220dda0

19. Nedelec M, Dupont G. The influence of playing position in soccer on the recovery kinetics of cognitive and physical performance. *J Sports Med Phys Fitness*. 2019;59(11):1812-1819. doi:10.23736/S0022-4707.19.09433-7

20. Silva JR, Ascensão A, Marques F, Seabra A, Rebelo A, Magalhães J. Neuromuscular function, hormonal and redox status and muscle damage of professional soccer players after a high-level competitive match. *Eur J Appl Physiol*. 2013;113(9):2193-2201. doi:10.1007/s00421-013-2633-8

21. Stone KJ, Hughes MG, Stembridge MR, Meyers RW, Newcombe DJ, Oliver JL. The influence of playing surface on physiological and performance responses during and

after soccer simulation. *Eur J Sport Sci*. 2016;16(1):42-49. doi:10.1080/17461391.2014.984768

22. Cohen DD, Zhao B, Okwera B, Matthews MJ, Delextrat A. Angle-Specific Eccentric Hamstring Fatigue After Simulated Soccer. *Int J Sports Physiol Perform*. 2015;10(3):325-331. doi:10.1123/ijspp.2014-0088

23. Delextrat A, Baker J, Cohen DD, Clarke ND. Effect of a simulated soccer match on the functional hamstrings-to-quadriceps ratio in amateur female players. *Scand J Med Sci Sports*. 2013;23(4):478-486. doi:10.1111/j.1600-0838.2011.01415.x

24. Nedelec M, Wisloff U, McCall A, Berthoin S, Dupont G. Recovery after an Intermittent Test. *Int J Sports Med*. 2012;34(06):554-558. doi:10.1055/s-0032-1316364

25. Krustrup P, Zebis M, Jensen JM, Mohr M. Game-induced fatigue patterns in elite female soccer. *J strength Cond Res*. 2010;24(2):437-441. doi:10.1519/JSC.0b013e3181c09b79

26. Stone KJ, Hughes MG, Stembridge MR, Meyers RW, Newcombe DJ, Oliver JL. The influence of playing surface on physiological and performance responses during and after soccer simulation. *Eur J Sport Sci*. 2016;16(1):42-49. doi:10.1080/17461391.2014.984768

27. Naclerio F, Larumbe-Zabala E, Cooper R, Allgrove J, Earnest CP. A Multi-Ingredient Containing Carbohydrate, Proteins L-Glutamine and L-Carnitine Attenuates Fatigue Perception with No Effect on Performance, Muscle Damage or Immunity in Soccer Players. Nater U, ed. *PLoS One*. 2015;10(4):e0125188. doi:10.1371/journal.pone.0125188

28. Mathie MJ, Coster AC, Lovell NH, Celler B. Accelerometry: providing an integrated, practical method for long-term, ambulatory monitoring of human movement. *Physiol Meas*. 2004;25(2):1-20. doi:10.1088/0967-3334/25/2/R01

29. Mundt M, Thomsen W, Witter T, et al. Prediction of lower limb joint angles and moments during gait using artificial neural networks. *Med Biol Eng Comput*. 2020;58(1):211-225. doi:10.1007/s11517-019-02061-3

30. Picerno P. 25 years of lower limb joint kinematics by using inertial and magnetic sensors: A review of methodological approaches. *Gait Posture*. 2017;51:239-246. doi:10.1016/j.gaitpost.2016.11.008

31. Winter CC, Brandes M, Mueller C, et al. Walking ability during daily life in patients with osteoarthritis of the knee or the hip and lumbar spinal stenosis: a cross sectional study. *BMC Musculoskelet Disord*. 2010;11(233):1-7. doi:10.1186/1471-2474-11-233

32. Patterson M, McGrath D, Caulfield B. Using a tri-axial accelerometer to detect technique breakdown due to fatigue in distance runners: A preliminary perspective. In: *Proceedings of the Annual International Conference of the IEEE Engineering in Medicine and Biology Society, EMBS*. ; 2011:6511-6514. doi:10.1109/IEMBS.2011.6091606

33. Gouttebarge V, Wolfard R, Griek N, de Ruiter CJ, Boschman JS, van Dieën JH. Reproducibility and validity of the myotest for measuring step frequency and ground contact time in recreational runners. *J Hum Kinet*. 2015;45:19-26. doi:10.1515/hukin-2015-0003

34. Beets MW, Morgan CF, Banda JA, et al. Convergent validity of pedometer and

accelerometer estimates of moderate-to-vigorous physical activity of youth. *J Phys Act Health*. 2011;8 Suppl 2:S295-305. Accessed June 10, 2016. http://www.ncbi.nlm.nih.gov/pubmed/21918244

35. Bugané F, Benedetti MG, Casadio G, et al. Estimation of spatial-temporal gait parameters in level walking based on a single accelerometer: Validation on normal subjects by standard gait analysis. *Comput Methods Programs Biomed*. 2012;108(1):129-137. doi:10.1016/j.cmpb.2012.02.003

36. Yang S, Mohr C, Li Q. Ambulatory running speed estimation using an inertial sensor. *Gait Posture*. 2011;34(4):462-466. doi:10.1016/j.gaitpost.2011.06.019

37. McGrath D, Greene BR, O'Donovan KJ, Caulfield B. Gyroscope-based assessment of temporal gait parameters during treadmill walking and running. *Sport Eng*. 2012;15(4):207-213. doi:10.1007/s12283-012-0093-8

38. Bergamini E, Picerno P, Pillet H, Natta F, Thoreux P, Camomilla V. Estimation of temporal parameters during sprint running using a trunk-mounted inertial measurement unit. *J Biomech*. 2012;45(6):1123-1126. doi:10.1016/j.jbiomech.2011.12.020

39. Dorschky E, Nitschke M, Martindale CF, van den Bogert AJ, Koelewijn AD, Eskofier BM. CNN-Based Estimation of Sagittal Plane Walking and Running Biomechanics From Measured and Simulated Inertial Sensor Data. *Front Bioeng Biotechnol*. 2020;8. doi:10.3389/fbioe.2020.00604

40. Picerno P, Cereatti A, Cappozzo A. Joint kinematics estimate using wearable inertial and magnetic sensing modules. *Gait Posture*. 2008;28(4):588-595.

doi:10.1016/J.GAITPOST.2008.04.003

41. Lafortune MA, Lake MJ, Hennig EM, Lafortune, M. A., Lake, M. J., & Hennig EM. Differential shock transmission response of the human body to impact severity and lower limb posture. *J Biomech*. 1996;29(12):1531-1537. doi:10.1016/0021-9290(96)00092-9

42. Giandolini M, Horvais N, Rossi J, Millet GY, Samozino P, Morin J. Effect of foot strike pattern on axial and transverse shock severity during downhill trail running. *33rd Int Conf Biomech Sport*. 2015;(January 2016):1-7. doi:10.1016/j.jbiomech.2016.04.001

43. Mercer JA, Vance J, Hreljac A, Hamill J. Relationship between shock attenuation and stride length during running at different velocities. *Eur J Appl Physiol*. 2002;87(4-5):403-408. doi:10.1007/s00421-002-0646-9

44. Lieberman DE, Warrener AG, Wang J, Castillo ER. Effects of stride frequency and foot position at landing on braking force, hip torque, impact peak force and the metabolic cost of running in humans. *J Exp Biol*. 2015;218(21):3406-3414. doi:10.1242/jeb.125500

45. Nummela A, Keränen T, Mikkelsson L. Factors Related to Top Running Speed and Economy. *Int J Sports Med*. 2007;28(8):655-661. doi:10.1055/s-2007-964896

46. Santos-Concejero J, Tam N, Granados C, et al. Stride angle as a novel indicator of running economy in well-trained runners. *J Strength Cond Res*. 2014;28(7):1889-1895.

47. Morin J-B, Jeannin T, Chevallier B, Belli A. Spring-Mass Model Characteristics During Sprint Running: Correlation with Performance and Fatigue-Induced Changes. *Int J Sports Med*. 2006;27(2):158-165. doi:10.1055/s-2005-837569

48. van Oeveren BT, de Ruiter CJ, Beek PJ, van Dieën JH. The biomechanics of running and running styles: a synthesis. *Sport Biomech*. Published online March 4, 2021:1-39. doi:10.1080/14763141.2021.1873411

49. Folland JP, Allen SJ, Black MI, Handsaker JC, Forrester SE. Running Technique is an Important Component of Running Economy and Performance. *Med Sci Sport Exerc*. 2017;49(7):1412-1423. doi:10.1249/MSS.0000000000001245

50. da Rosa RG, Oliveira HB, Gomeñuka NA, et al. Landing-Takeoff Asymmetries Applied to Running Mechanics: A New Perspective for Performance. *Front Physiol*. 2019;10. doi:10.3389/fphys.2019.00415

51. Santos-Concejero J, Granados C, Irazusta J, et al. DIFFERENCES IN GROUND CONTACT TIME EXPLAIN THE LESS EFFICIENT RUNNING ECONOMY IN NORTH AFRICAN RUNNERS. *Biol Sport*. 2013;30(3):181-187. doi:10.5604/20831862.1059170

52. Asaeda M, Deie M, Kono Y, Mikami Y, Kimura H, Adachi N. The relationship between knee muscle strength and knee biomechanics during running at 6 and 12 months after anterior cruciate ligament reconstruction. *Asia-Pacific J Sport Med Arthrosc Rehabil Technol*. 2019;16:14-18. doi:10.1016/j.asmart.2018.11.004

53. Yu B, Garrett WE. Mechanisms of non-contact ACL injuries. *Br J Sports Med*. 2007;41(Supplement 1):i47-i51. doi:10.1136/bjsm.2007.037192

54. Picerno P, Cereatti A, Cappozzo A. A spot check for assessing static orientation consistency of inertial and magnetic sensing units. *Gait Posture*. 2011;33(3):373-378. doi:10.1016/J.GAITPOST.2010.12.006

55. Frick E, Rahmatalla S. Joint Center Estimation Using Single-Frame Optimization: Part

2: Experimentation. *Sensors*. 2018;18(8):2563. doi:10.3390/s18082563

56. Aryadoust V, C. M. Goh C. Predicting Listening Item Difficulty with Language Complexity Measures: A Comparative Data Mining Study. *CaMLA Work Pap*. 2014;2:1-16.

57. Mundt M, Johnson WR, Potthast W, Markert B, Mian A, Alderson J. A Comparison of Three Neural Network Approaches for Estimating Joint Angles and Moments from Inertial Measurement Units. *Sensors*. 2021;21(13):4535. doi:10.3390/s21134535

58. Lim, Kim, Park. Prediction of Lower Limb Kinetics and Kinematics during Walking by a Single IMU on the Lower Back Using Machine Learning. *Sensors*. 2019;20(1):130. doi:10.3390/s20010130

59. Edwards WB, Derrick TR, Hamill J. Musculoskeletal Attenuation of Impact Shock in Response to Knee Angle Manipulation. *J Appl Biomech*. 2012;28(5):502-510. doi:10.1123/jab.28.5.502

60. Derrick TR. The effects of knee contact angle on impact forces and accelerations. *Med Sci Sports Exerc*. 2004;36(5):832-837. doi:10.1249/01.MSS.0000126779.65353.CB

61. García-Pérez JA, Pérez-Soriano P, Llana Belloch S, Lucas-Cuevas AG, Sánchez-Zuriaga D. Effects of treadmill running and fatigue on impact acceleration in distance running. *Sports Biomech*. 2014;13(3):259-266. doi:10.1080/14763141.2014.909527

62. Derrick TR, Dereu D, Mclean SP. Impacts and kinematic adjustments during an exhaustive run. *Med Sci Sport Exerc*. 2002;34(6):998-1002. doi:10.1097/00005768-200206000-00015

63. Wundersitz DW, Gastin PB, Robertson SJ, Netto KJ. Validity of a Trunk-Mounted

Accelerometer to Measure Physical Collisions in Contact Sports. *Int J Sports Physiol Perform*. 2015;10(6):681-686. doi:10.1123/ijspp.2014-0381

64. Barrett S, Midgley A, Lovell R. PlayerLoad™: Reliability, convergent validity, and influence of unit position during treadmill running. *Int J Sports Physiol Perform*. 2014;9(6):945-952. doi:10.1123/ijspp.2013-0418

65. Gaudino P, Gaudino C, Alberti G, Minetti AE. Biomechanics and predicted energetics of sprinting on sand: Hints for soccer training. *J Sci Med Sport*. 2013;16(3):271-275. doi:10.1016/j.jsams.2012.07.003

66. Buchheit M, Gray A, Morin J-BB. Assessing Stride Variables and Vertical Stiffness with GPS-Embedded Accelerometers: Preliminary Insights for the Monitoring of Neuromuscular Fatigue on the Field. *J Sports Sci Med*. 2015;14(4):698-701. Accessed June 10, 2016. http://www.ncbi.nlm.nih.gov/pubmed/26664264

67. Buttfield A. The Development and Application of a Novel Method of Analysing Within-step Accelerations Collected During Australian Rules Football Games. *Comput Sci*. Published online 2016.

68. Heiden T, Burnett A. Determination of heel strike and toe-off in the running stride using an accelerometer: Application to field-based gait studies. In: *ISBS-Conference Proceedings Archive*. Vol 1. ; 2008.

69. Martínez-Mesa J, González-Chica DA, Bastos JL, Bonamigo RR, Duquia RP. Sample size: how many participants do I need in my research? *An Bras Dermatol*. 2014;89(4):609-615. doi:10.1590/abd1806-4841.20143705

70. Novacheck TF. The biomechanics of running. *Gait Posture*. 1998;7(1):77-95.

71. Abt JJP, Sell TTC, Chu Y, Lovalekar M, Burdett RG, Lephart SM. Running kinematics and shock absorption do not change after brief exhaustive running. *J Strength Cond Res*. 2011;25(6):1-7. doi:10.1519/JSC.0b013e3181ddfcf8

72. Backes A, Skejø SD, Gette P, et al. Predicting cumulative load during running using field-based measures. *Scand J Med Sci Sports*. 2020;30(12):2399-2407. doi:10.1111/sms.13796

73. Lohman EB, Balan Sackiriyas KS, Swen RW. A comparison of the spatiotemporal parameters, kinematics, and biomechanics between shod, unshod, and minimally supported running as compared to walking. *Phys Ther Sport*. 2011;12(4):151-163. doi:10.1016/j.ptsp.2011.09.004

74. Knutzen KM, Bates BT, Hamill J. Electrogoniometry of post-surgical knee bracing in running. *Am J Phys Med*. 1983;62(4):172-181.

75. Astephen JL, Deluzio KJ, Caldwell GE, Dunbar MJ. Biomechanical changes at the hip, knee, and ankle joints during gait are associated with knee osteoarthritis severity. *J Orthop Res*. 2008;26(3):332-341. doi:10.1002/jor.20496

76. Preatoni E, Ferrario M, Donà G, Hamill J, Rodano R. Motor variability in sports: a non-linear analysis of race walking. *J Sports Sci*. 2010;28(12):1327-1336.

77. Larson P, Higgins E, Kaminski J, et al. Foot strike patterns of recreational and sub-elite runners in a long-distance road race. *J Sports Sci*. 2011;29(15):1665-1673.

78. Benson L, Clermont C, Watari R, Exley T, Ferber R. Automated Accelerometer-Based Gait Event Detection During Multiple Running Conditions. *Sensors*. 2019;19(7):1483. doi:10.3390/s19071483

79. Baker R. Gait analysis methods in rehabilitation. *J Neuroeng Rehabil*. 2006;3(4):1-10. doi:10.1186/1743-0003-3-4

80. Higginson B. Methods of running gait analysis. *Curr Sports Med Rep*. 2009;8(3):136-141. Accessed June 13, 2016. http://journals.lww.com/acsm-csmr/Abstract/2009/05000/Methods_of_Running_Gait_Analysis.10.aspx

81. Kiani K, Snijders CJ, Gelsema ES. Computerized analysis of daily life motor activity for ambulatory monitoring. *Technol Heal Care*. 1997;5(4):307-318.

82. Fong DT, Chan Y. The Use of Wearable Inertial Motion Sensors in Human Lower Limb Biomechanics Studies: A Systematic Review. *Analysis*. 2010;10(12):11556-11565. doi:10.3390/s101211556

83. Lobo J, Dias J. Relative pose calibration between visual and inertial sensors. *Int J Rob Res*. 2007;26(6):561-575. http://journals.sagepub.com/doi/abs/10.1177/0278364907079276

84. Picerno P, Cereatti A, Cappozzo A. Joint kinematics estimate using wearable inertial and magnetic sensing modules. *Gait Posture*. 2008;28(4):588-595. doi:10.1016/j.gaitpost.2008.04.003

85. Raffin E, Bonnet S, Giraux P. Concurrent validation of a magnetometer-based step counter in various walking surfaces. *Gait Posture*. 2012;35(1):18-22.

86. Purcell B, Channells J, James D, Barrett R. Use of accelerometers for detecting foot-ground contact time during running. In: *BioMEMS and Nanotechnology II*. Vol 6036. International Society for Optics and Photonics; 2006:603615. doi:10.1117/12.638389

87. Strohrmann C, Harms H, Kappeler-setz C, Tröster G. Monitoring Kinematic

ChangesWith Fatigue in Running Using Body-Worn Sensors. *IEEE Trans Inf Technol Biomed*. 2012;16(5):983-990. doi:10.1109/TITB.2012.2201950

88. Norris M, Anderson R, Kenny IC. Method analysis of accelerometers and gyroscopes in running gait: A systematic review. *Proc Inst Mech Eng Part P J Sport Eng Technol*. 2014;228(1):3-15. doi:10.1177/1754337113502472

89. Hatano Y, Tudor-Locke C. Pedometer-assessed physical activity: measurement and motivations. In: *American College of Sports Medicine Annual Meeting, Baltimore, MD*. ; 2001.

90. Crouter SE, Schneider PL, Karabulut M, Bassett DR. Validity of 10 electronic pedometers for measuring steps, distance, and energy cost. *Med Sci Sports Exerc*. 2003;35(8):1455-1460. doi:10.1249/01.MSS.0000078932.61440.A2

91. Schneider PL, Crouter SE, Lukajic O, Bassett JDR. Accuracy and reliability of 10 pedometers for measuring steps over a 400-m walk. *Med Sci Sports Exerc*. 2003;35(10):1779-1784.

92. Lee JA, Williams SM, Brown DD, Laurson KR. Concurrent validation of the Actigraph gt3x+, Polar Active accelerometer, Omron HJ-720 and Yamax Digiwalker SW-701 pedometer step counts in lab-based and free-living settings. *J Sports Sci*. 2015;33(10):991-1000. doi:10.1080/02640414.2014.981848

93. Feito Y, Bassett DJ, Thompson D, Tyo B. Body Mass Index Affects Accelerometer Counts During Walking: 1869. *Med Sci Sport Exerc*. 2009;41(5):156-157. https://journals.lww.com/acsm-msse/Fulltext/2009/05001/Body_Mass_Index_Affects_Accelerometer_Counts.2069.a

spx

94. DiNallo JM, Downs DS, Le Masurier G. Objectively assessing treadmill walking during the second and third pregnancy trimesters. *J Phys Act Health*. 2012;9(1):21-28. Accessed June 10, 2016. http://www.ncbi.nlm.nih.gov/pubmed/22232501

95. Fortune E, Lugade V, Morrow M, Kaufman K. Validity of Using Tri-Axial Accelerometers to Measure Human Movement – Part II: Step Counts at a Wide Range of Gait Velocities. *Med Eng Phys*. 2014;36(6):659-669. doi:10.1016/j.medengphy.2014.02.006

96. Orr K, Howe HS, Omran J, et al. Validity of smartphone pedometer applications Public Health. *BMC Res Notes*. 2015;8(1):1-9. doi:10.1186/s13104-015-1705-8

97. Tudor-Locke C, Bassett DR. How many steps/day are enough? *Sport Med*. 2004;34(1):1-8.

98. Dohrn I-M, Hagströmer M, Hellénius M-L, Ståhle A. Gait Speed, Quality of Life, and Sedentary Time are Associated with Steps per Day in Community-Dwelling Older Adults with Osteoporosis. *J Aging Phys Act*. 2016;24(1):22-31. http://ezproxy.staffs.ac.uk/login?url=http://search.ebscohost.com/login.aspx?direct=true&db=s3h&AN=112457908&site=ehost-live

99. Motl RW, Pilutti LA, Learmonth YC, Goldman MD, Brown T. Clinical Importance of Steps Taken per Day among Persons with Multiple Sclerosis. *PLoS One*. 2013;8(9):e73247. doi:10.1371/journal.pone.0073247

100. Stefani L, Mascherini G, Scacciati I, De Luca A, Maffulli N, Galanti G. Positive effect of the use of accelerometry on lifestyle awareness of overweight hypertensive patients.

Asian J Sports Med. 2013;4(4):241-248. Accessed June 10, 2016. http://www.ncbi.nlm.nih.gov/pubmed/24799998

101. Aoyagi Y, Shephard RJ. A model to estimate the potential for a physical activity-induced reduction in healthcare costs for the elderly, based on pedometer/accelerometer data from the Nakanojo Study. *Sports Med*. 2011;41(9):695-708. doi:10.2165/11590530-000000000-00000

102. Rowlands A V, Schuna JM, Stiles VH, Tudor-Locke C. Cadence, peak vertical acceleration, and peak loading rate during ambulatory activities: implications for activity prescription for bone health. *J Phys Act Health*. 2014;11(7):1291-1294. doi:10.1123/jpah.2012-0402

103. Yang S, Li Q. Inertial sensor-based methods in walking speed estimation: A systematic review. *Sensors*. 2012;12(5):6102-6116.

104. Zijlstra W, Hof AL. Assessment of spatio-temporal gait parameters from trunk accelerations during human walking. *Gait Posture*. 2003;18(2):1-10. http://www.gaitposture.com/article/S0966-6362(02)00190-X/abstract

105. Alvarez D, González RC, López A, Alvarez JC. Comparison of step length estimators from weareable accelerometer devices. In: *Annual International Conference of the IEEE Engineering in Medicine and Biology - Proceedings*. ; 2006:5964-5967. doi:10.1109/IEMBS.2006.259593

106. Zielinska T, Gao Z, Zurawska M, Zheng Q, Mergner T, Lippi V. Postural balance using a disturbance rejection method. In: *2017 11th International Workshop on Robot Motion and Control (RoMoCo)*. IEEE; 2017:23-28. doi:10.1109/RoMoCo.2017.8003888

107. Zijlstra A, Zijlstra W. Trunk-acceleration based assessment of gait parameters in older persons: A comparison of reliability and validity of four inverted pendulum based estimations. *Gait Posture*. 2013;38(4):940-944. http://www.gaitposture.com/article/S0966-6362(13)00212-9/abstract

108. Sabatini A, Martelloni C, Scapellato S. Assessment of walking features from foot inertial sensing. *IEEE Trans Biomed Eng*. 2005;52(3):486-494. Accessed June 13, 2016. http://ieeexplore.ieee.org/xpls/abs_all.jsp?arnumber=1396389

109. Hundza SR, Hook WR, Harris CR, et al. Accurate and reliable gait cycle detection in Parkinson's disease. *IEEE Trans Neural Syst Rehabil Eng*. 2014;22(1):127-137.

110. Boutaayamou M, Schwartz C, Stamatakis J, et al. Development and validation of an accelerometer-based method for quantifying gait events. *Med Eng Phys*. 2015;37(2):226-232. doi:10.1016/j.medengphy.2015.01.001

111. Kotiadis D, Hermens HJ, Veltink PH. Inertial gait phase detection for control of a drop foot stimulator. *Med Eng Phys*. 2010;32(4):287-297.

112. Lau H, Tong K. The reliability of using accelerometer and gyroscope for gait event identification on persons with dropped foot. *Gait Posture*. 2008;27(2):248-257. doi:10.1016/j.gaitpost.2007.03.018

113. Little C, Lee JB, James DA, Davison K. An evaluation of inertial sensor technology in the discrimination of human gait. *J Sports Sci*. 2013;31(12):1312-1318. doi:10.1080/02640414.2013.779739

114. McCamley J, Donati M, Grimpampi E, Mazzà C. An enhanced estimate of initial contact and final contact instants of time using lower trunk inertial sensor data. *Gait*

Posture. 2012;36(2):316-318. doi:10.1016/j.gaitpost.2012.02.019

115. Gaviria M, D'Angeli M, Chavet P, Pelissier J, Peruchon E, Rabischong P. Plantar dynamics of hemiplegic gait: a methodological approach. *Gait Posture*. 1996;4(4):297-305. doi:10.1016/0966-6362(95)01055-6

116. von Schroeder HP, Coutts RD, Lyden PD, Nickel VL. Gait parameters following stroke: a practical assessment. *J Rehabil Res Dev*. 1995;32(1):25. https://search.proquest.com/openview/969ff0af55320599c1a5513c36d3a264/1?pq-origsite=gscholar&cbl=48772

117. Salarian A, Russmann H, Vingerhoets FJG, et al. Gait assessment in Parkinson's disease: toward an ambulatory system for long-term monitoring. *IEEE Trans Biomed Eng*. 2004;51(8):1434-1443.

118. Patterson MR, Delahunt E, Sweeney KT, Caulfield B. An Ambulatory Method of Identifying Anterior Cruciate Ligament Reconstructed Gait Patterns. *Sensors*. 2014;14(1):887-899. doi:10.3390/s140100887

119. Dejnabadi H, Jolles BM, Aminian K. A New Approach for Quantitative Analysis of Inter-Joint Coordination During Gait. *IEEE Trans Biomed Eng*. 2008;55(2):755-764. doi:10.1109/TBME.2007.901034

120. Seel T, Raisch J, Schauer T. IMU-Based Joint Angle Measurement for Gait Analysis. *Sensors*. 2014;14(4):6891-6909. doi:10.3390/s140406891

121. Favre J, Luthi F, Jolles BM, Siegrist O, Najafi B, Aminian K. A new ambulatory system for comparative evaluation of the three-dimensional knee kinematics, applied to anterior cruciate ligament injuries. *Knee Surgery, Sport Traumatol Arthrosc*.

2006;14(7):592-604. doi:10.1007/s00167-005-0023-4

122. Cooper G, Sheret I, McMillian L, et al. Inertial sensor-based knee flexion/extension angle estimation. *J Biomech*. 2009;42(16):2678-2685. doi:10.1016/j.jbiomech.2009.08.004

123. Liu K, Liu T, Shibata K, Inoue Y, Zheng R. Novel approach to ambulatory assessment of human segmental orientation on a wearable sensor system. *J Biomech*. 2009;42(16):2747-2752. doi:10.1016/j.jbiomech.2009.08.008

124. Takeda R, Tadano S, Todoh M, Morikawa M, Nakayasu M, Yoshinari S. Gait analysis using gravitational acceleration measured by wearable sensors. *J Biomech*. 2009;42(3):223-233. doi:10.1016/j.jbiomech.2008.10.027

125. Willemsen ATM, van Alsté JA, Boom HBK. Real-time gait assessment utilizing a new way of accelerometry. *J Biomech*. 1990;23(8):859-863. doi:10.1016/0021-9290(90)90033-Y

126. Dejnabadi H, Jolles BM, Aminian K. A new approach to accurate measurement of uniaxial joint angles based on a combination of accelerometers and gyroscopes. *IEEE Trans Biomed Eng*. 2005;52(8):1478-1484. doi:10.1109/TBME.2005.851475

127. Zimmermann T, Taetz B, Bleser G. IMU-to-Segment Assignment and Orientation Alignment for the Lower Body Using Deep Learning. *Sensors*. 2018;18(1):302. doi:10.3390/s18010302

128. de Vries WHK, Veeger HEJ, Baten CTM, van der Helm FCT. Magnetic distortion in motion labs, implications for validating inertial magnetic sensors. *Gait Posture*. 2009;29(4):535-541. doi:10.1016/j.gaitpost.2008.12.004

129. Zijlstra A, Goosen JHM, Verheyen CCPM, Zijlstra W. A body-fixed-sensor based analysis of compensatory trunk movements during unconstrained walking. *Gait Posture*. 2008;27(1):164-167. doi:10.1016/j.gaitpost.2007.02.010

130. Rowlands A V, Stone MR, Eston RG. Influence of speed and step frequency during walking and running on motion sensor output. *Med Sci Sport Exerc*. 2007;39(4):716-727. https://s3.amazonaws.com/academia.edu.documents/40130263/Influence_of_Speed_and_Step_Frequency_du20151118-30238-f4b25f.pdf?AWSAccessKeyId=AKIAIWOWYYGZ2Y53UL3A&Expires=1521552613&Signature=x3LGUP0AWCFXNROgdppLwLl1VBQ%253D&response-content-disposition=inline%25

131. de Ruiter CJ, Verdijk PWL, Werker W, Zuidema MJ, de Haan A. Stride frequency in relation to oxygen consumption in experienced and novice runners. *Eur J Sport Sci*. 2014;14(3):251-258. doi:10.1080/17461391.2013.783627

132. de Ruiter CJ, van Daal S, van Dieën JH. Individual optimal step frequency during outdoor running. *Eur J Sport Sci*. 2020;20(2):182-190. doi:10.1080/17461391.2019.1626911

133. Clarke TE, Cooper LB, Hamill CL, Clark DE. The effect of varied stride rate upon shank deceleration in running. *J Sports Sci*. 1985;3(1):41-49.

134. Blickhan R. The spring-mass model for running and hopping. *J Biomech*. 1989;22(11-12):1217-1227. doi:10.1016/0021-9290(89)90224-8

135. Herren R, Sparti A, Aminian K, Schutz Y. The prediction of speed and incline in

outdoor running in humans using accelerometry. *Med Sci Sports Exerc*. 1999;31(7):1053-1059.

136. Song Y, Shin S, Kim S, Lee D, Lee KH. Speed Estimation From a Tri-axial Accelerometer Using Neural Networks. In: *2007 29th Annual International Conference of the IEEE Engineering in Medicine and Biology Society*. ; 2007:3224-3227. doi:10.1109/IEMBS.2007.4353016

137. Kugler F, Janshen L. Body position determines propulsive forces in accelerated running. *J Biomech*. 2010;43(2):343-348.

138. Parrington L, Phillips E, Wong A, Finch M, Wain E, MacMahon C. Validation of inertial measurement units for tracking 100m sprint data. In: *ISBS-Conference Proceedings Archive*. Vol 34. ; 2016.

139. Heiderscheit BC, Chumanov ES, Michalski MP, Wille CM, Ryan MB. Effects of Step Rate Manipulation on Joint Mechanics during Running. *Med Sci Sport Exerc*. 2011;43(2):296-302. doi:10.1249/MSS.0b013e3181ebedf4.Effects

140. Wixted AJ, Billing DC, James DA. Validation of trunk mounted inertial sensors for analysing running biomechanics under field conditions, using synchronously collected foot contact data. *Sport Eng*. 2010;12(4):207-212. doi:10.1007/s12283-010-0043-2

141. Mann RA, Hagy J. Biomechanics of walking, running, and sprinting. *Am J Sports Med*. 1980;8(5):345-350.

142. Sinclair J, Hobbs SJ, Protheroe L, Edmundson CJ, Greenhalgh A. Determination of gait events using an externally mounted shank accelerometer. *J Appl Biomech*. 2013;29(1):118-122. doi:2011-0260 [pii]

143. Auvinet B, Gloria E, Renault G, Barrey E. Runner's stride analysis: Comparison of kinematic and kinetic analyses under field conditions. *Sci Sport*. 2002;17(2):92-94. doi:10.1016/S0765-1597(02)00122-3

144. Lee JB, Mellifont RB, Burkett BJ. The use of a single inertial sensor to identify stride, step, and stance durations of running gait. *J Sci Med Sport*. 2010;13(2):270-273. doi:10.1016/j.jsams.2009.01.005

145. Farley CT, Ferris DP. Biomechanics Of Walking and Running: Center Of Mass Movements To Muscle Action. *Exerc Sport Sci Rev*. 1998;26(1):253-285. https://journals.lww.com/acsm-essr/Citation/1998/00260/10_Biomechanics_of_Walking_and_Running__Center_of.12.aspx

146. Weyand PG, Sternlight DB, Bellizzi MJ, Wright S. Faster top running speeds are achieved with greater ground forces not more rapid leg movements. *J Appl Physiol*. 2000;89(5):1991-1999. https://www.physiology.org/doi/full/10.1152/jappl.2000.89.5.1991

147. Santos-Concejero J, Oliván J, Maté-Muñoz JL, et al. Gait-cycle characteristics and running economy in elite Eritrean and European runners. *Int J Sports Physiol Perform*. 2015;10(3):381-387.

148. Jahn WT. Visco-elastic orthotics: Sorbothane II. *J Orthop Sport Phys Ther*. 1983;4(3):174-175. https://www.jospt.org/doi/pdf/10.2519/jospt.1983.4.3.174?code=jospt-site

149. Charry E, Hu W, Umer M, Ronchi A, Taylor S. Study on estimation of peak Ground

Reaction Forces using tibial accelerations in running. *Proc 2013 IEEE 8th Int Conf Intell Sensors, Sens Networks Inf Process Sens Futur ISSNIP 2013*. 2013;1:288-293. doi:10.1109/ISSNIP.2013.6529804

150. Bigelow EMR, Elvin NG, Elvin AA, Arnoczky SP. Peak Impact accelerations during track and treadmill running. *J Appl Biomech*. 2013;29(5):638-644. doi:2012-0046 [pii]

151. Denoth J. Load on the locomotor system and modelling [in] Biomechanics of Running Shoes. In: Nigg BM, ed. *Biomechanics of Running Shoes*. Human Kinetics Publishers; 1986:63-116. https://contentstore.cla.co.uk/secure/link?id=96a3aa7b-9f5f-e611-80c6-005056af4099

152. Clansey AC, Hanlon M, Wallace ES, Lake MJ. Effects of fatigue on running mechanics associated with tibial stress fracture risk. *Med Sci Sports Exerc*. 2012;44(10):1917-1923. doi:10.1249/MSS.0b013e318259480d

153. Harrast MA, Colonno D. Stress fractures in runners. *Clin Sports Med*. 2010;29(3):399-416. http://www.sportsmed.theclinics.com/article/S0278-5919(10)00016-5/abstract

154. Fu W, Fang Y, Liu DMS, Wang L, Ren S, Liu Y. Surface effects on in-shoe plantar pressure and tibial impact during running. *J Sport Heal Sci*. 2015;4(4):384-390. doi:10.1016/j.jshs.2015.09.001

155. Zadpoor AA, Nikooyan AA. Modeling muscle activity to study the effects of footwear on the impact forces and vibrations of the human body during running. *J Biomech*. 2010;43(2):186-193.

156. Butler RJ, Hamill J, Davis I. Effect of footwear on high and low arched runners' mechanics during a prolonged run. *Gait Posture*. 2007;26(2):219-225.

doi:10.1016/j.gaitpost.2006.09.015

157. Gholami M, Rezaei A, Cuthbert TJ, Napier C, Menon C. Lower Body Kinematics Monitoring in Running Using Fabric-Based Wearable Sensors and Deep Convolutional Neural Networks. *Sensors*. 2019;19(23):5325. doi:10.3390/s19235325

158. Clark RA, Bartold S, Bryant AL. Tibial acceleration variability during consecutive gait cycles is influenced by the menstrual cycle. *Clin Biomech*. 2010;25(6):557-562. doi:10.1016/j.clinbiomech.2010.03.002

159. Nedergaard NJ, Robinson MA, Eusterwiemann E, Drust B, Lisboa PJ, Vanrenterghem J. The Relationship Between Whole-Body External Loading and Body-Worn Accelerometry During Team Sports Movements. *Int J Sports Physiol Perform*. Published online 2016:1-44. doi:10.1123/ijspp.2015-0712

160. Cormack SJ, Smith RL, Mooney MM, Young WB, O'Brien BJ. Accelerometer load as a measure of activity profile in different standards of netball match play. *Int J Sports Physiol Perform*. 2014;9(2):283-291. doi:10.1123/ijspp.2012-0216

161. Polglaze T, Dawson B, Hiscock DJ, Peeling P. A comparative analysis of accelerometer and time-motion data in elite men's hockey training and competition. *Int J Sports Physiol Perform*. 2015;10(4):446-451. doi:10.1123/ijspp.2014-0233

162. Barreira P, Robinson MA, Drust B, Nedergaard N, Raja Azidin RMF, Vanrenterghem J. Mechanical Player Load™ using trunk-mounted accelerometry in football: Is it a reliable, task- and player-specific observation? *J Sports Sci*. 2017;35(17):1674-1681. doi:10.1080/02640414.2016.1229015

163. Cormack SJ, Mooney MG, Morgan W, McGuigan MR. Influence of neuromuscular

fatigue on accelerometer load in elite Australian football players. *Int J Sports Physiol Perform*. 2013;8(4):373-378. Accessed June 10, 2016. http://www.ncbi.nlm.nih.gov/pubmed/23170747

164. Boyd LJ, Ball K, Aughey RJ. The reliability of MinimaxX accelerometers for measuring physical activity in Australian football. *Int J Sports Physiol Perform*. 2011;6(3):311-321. Accessed June 10, 2016. http://www.ncbi.nlm.nih.gov/pubmed/21911857

165. Scott BR, Lockie RG, Knight TJ, Clark AC, Janse de Jonge XAK. A comparison of methods to quantify the in-season training load of professional soccer players. *Int J Sports Physiol Perform*. 2013;8(2):195-202. Accessed June 10, 2016. http://www.ncbi.nlm.nih.gov/pubmed/23428492

166. Dalen T, Aune TK, Hjelde GH, Ettema G, Sandbakk Ø, McGhie D. Player load in male elite soccer: Comparisons of patterns between matches and positions. Mourot L, ed. *PLoS One*. 2020;15(9):e0239162. doi:10.1371/journal.pone.0239162

167. Rogalski B, Dawson B, Heasman J, Gabbett TJ. Training and game loads and injury risk in elite Australian footballers. *J Sci Med Sport*. 2013;16(6):499-503. doi:10.1016/j.jsams.2012.12.004

168. Veugelers KR, Young WB, Fahrner B, Harvey JT. Different methods of training load quantification and their relationship to injury and illness in elite Australian football. *J Sci Med Sport*. 2016;19(1):24-28. doi:10.1016/j.jsams.2015.01.001

169. Fowles JR. Technical Issues in Quantifying Low-Frequency Fatigue in Athletes. 2006;1(2):169-171. doi:10.1123/ijspp.1.2.169

170. Keeton RB, Binder-Macleod SA. Low-Frequency Fatigue. *Phys Ther*. 2006;86(8):1146-

1150. doi:10.1093/ptj/86.8.1146

171. Komi P V. Stretch-shortening cycle: a powerful model to study normal and fatigued muscle. *J Biomech*. 2000;33(10):1197-1206. doi:10.1016/S0021-9290(00)00064-6

172. Boullosa DA, Abreu L, Nakamura FY, Muñoz VE, Domínguez E, Leicht AS. Cardiac Autonomic Adaptations in Elite Spanish Soccer Players During Preseason. *Int J Sports Physiol Perform*. 2013;8(4):400-409. doi:10.1123/ijspp.8.4.400

173. Rabbani A, Baseri MK, Reisi J, Clemente FM, Kargarfard M. Monitoring collegiate soccer players during a congested match schedule: Heart rate variability versus subjective wellness measures. *Physiol Behav*. 2018;194:527-531. doi:10.1016/j.physbeh.2018.07.001

174. Adams D, Pozzi F, Carroll A, Rombach A, Zeni J. Validity and Reliability of a Commercial Fitness Watch for Measuring Running Dynamics. *J Orthop Sport Phys Ther*. 2016;46(6):471-476. doi:10.2519/jospt.2016.6391

175. Leardini A, Sawacha Z, Paolini G, Ingrosso S, Nativo R, Benedetti MG. A new anatomically based protocol for gait analysis in children. *Gait Posture*. 2007;26(4):560-571. doi:10.1016/j.gaitpost.2006.12.018

176. Leardini A, Biagi F, Merlo A, Belvedere C, Benedetti MG. Multi-segment trunk kinematics during locomotion and elementary exercises. *Clin Biomech*. 2011;26(6):562-571. doi:10.1016/j.clinbiomech.2011.01.015

177. Needham R, Naemi R, Healy A, Chockalingam N. Multi-segment kinematic model to assess three-dimensional movement of the spine and back during gait. *Prosthetics Orthot Int*. 2016;40(5):624-635. doi:10.1177/0309364615579319

178. Pontzer H, Holloway JH, Raichlen DA, Lieberman DE. Control and function of arm swing in human walking and running. *J Exp Biol*. 2009;212(4):523-534. doi:10.1242/jeb.024927

179. Lee CR, Farley CT. Determinants of the center of mass trajectory in human walking and running. *J Exp Biol*. 1998;201(21):2935-2944. doi:10.1242/jeb.201.21.2935

180. Thorstensson A, Nilson J, Carlson H, Zomlefer MR. Trunk movements in human locomotion. *Acta Physiol Scand*. 1984;121(1):9-22. doi:10.1111/j.1748-1716.1984.tb10452.x

181. Kawabata M, Goto K, Fukusaki C, et al. Acceleration patterns in the lower and upper trunk during running. *J Sports Sci*. 2013;31(16):1841-1853. doi:10.1080/02640414.2013.805884

182. Lindsay TR, Yaggie JA, McGregor SJ. Contributions of lower extremity kinematics to trunk accelerations during moderate treadmill running. *J Neuroeng Rehabil*. 2014;11(1):162. doi:10.1186/1743-0003-11-162

183. Cronin NJ. Using deep neural networks for kinematic analysis: Challenges and opportunities. *J Biomech*. 2021;123:110460. doi:10.1016/j.jbiomech.2021.110460

184. Mihcin S. Simultaneous validation of wearable motion capture system for lower body applications: over single plane range of motion (ROM) and gait activities. *Biomed Eng / Biomed Tech*. 2022;67(3):185-199. doi:10.1515/bmt-2021-0429

185. Stetter BJ, Krafft FC, Ringhof S, Stein T, Sell S. A Machine Learning and Wearable Sensor Based Approach to Estimate External Knee Flexion and Adduction Moments During Various Locomotion Tasks. *Front Bioeng Biotechnol*. 2020;8.

doi:10.3389/fbioe.2020.00009

186. Mizrahi J, Verbitsky O, Isakov E, Daily D. Effect of fatigue on leg kinematics and impact acceleration in long distance running. *Hum Mov Sci*. 2000;19(2):139-151. doi:10.1016/S0167-9457(00)00013-0

187. RUDER M, JAMISON ST, TENFORDE A, MULLOY F, DAVIS IS. Relationship of Foot Strike Pattern and Landing Impacts during a Marathon. *Med Sci Sport Exerc*. 2019;51(10):2073-2079. doi:10.1249/MSS.0000000000002032

188. JOHNSON CD, OUTERLEYS J, JAMISON ST, TENFORDE AS, RUDER M, DAVIS IS. Comparison of Tibial Shock during Treadmill and Real-World Running. *Med Sci Sport Exerc*. 2020;52(7):1557-1562. doi:10.1249/MSS.0000000000002288

189. Blackah N, Bradshaw EJ, Kemp JG, Shoushtarian M. The Effect of Exercise-Induced Muscle Damage on Shock Dissipation during Treadmill Running. *Asian J Exerc Sport Sci*. 2013;10(1):16-30. http://ezproxy.staffs.ac.uk/login?url=http://search.ebscohost.com/login.aspx?direct=true&db=s3h&AN=94819599&site=ehost-live

190. Garcia MC, Gust G, Bazett-Jones DM. Tibial acceleration and shock attenuation while running over different surfaces in a trail environment. *J Sci Med Sport*. 2021;24(11):1161-1165. doi:10.1016/j.jsams.2021.03.006

191. Hamill J, Derrick TR, Holt KG. Shock attenuation and stride frequency during running. *Hum Mov Sci*. 1995;14(1):45-60. doi:10.1016/0167-9457(95)00004-C

192. Hesar NGZ, Van Ginckel A, Cools A, et al. A prospective study on gait-related intrinsic risk factors for lower leg overuse injuries. *Br J Sports Med*. 2009;43(13):1057-1061.

doi:10.1136/bjsm.2008.055723

193. Wundersitz DWT, Gastin PB, Robertson S, Davey PC, Netto KJ. Validation of a Trunk-mounted Accelerometer to Measure Peak Impacts during Team Sport Movements. *Int J Sports Med*. 2015;36(9):742-746. doi:10.1055/s-0035-1547265

194. Drillis R, Contini R, Bluestein M. Body Segment Parameters; a Survey of Measurement Techniques. *Artif Limbs*. 1964;25:44-66. doi:10.1049/ecej:19890011

195. Fukuchi RK, Fukuchi CA, Duarte M. A public dataset of running biomechanics and the effects of running speed on lower extremity kinematics and kinetics. *PeerJ*. 2017;5:e3298. doi:10.7717/peerj.3298

196. Brughelli M, Cronin J, Chaouachi A. Effects of Running Velocity on Running Kinetics and Kinematics. *J Strength Cond Res*. 2011;25(4):933-939. doi:10.1519/JSC.0b013e3181c64308

197. Saunders SW, Schache A, Rath D, Hodges PW. Changes in three dimensional lumbo-pelvic kinematics and trunk muscle activity with speed and mode of locomotion. *Clin Biomech*. 2005;20(8):784-793. doi:10.1016/j.clinbiomech.2005.04.004

198. Hendelman D, Miller K, Baggett C, Debold E, Freedson P. Validity of accelerometry for the assessment of moderate intensity physical activity in the field. *Med Sci Sports Exerc*. 2000;32(9 SUPPL.):S442-S449. https://www.scopus.com/inward/record.uri?eid=2-s2.0-0033817363&partnerID=40&md5=d0db786032ed1b93770cf0d1204e66a7

199. Bono R, Alarcón R, Blanca MJ. Report Quality of Generalized Linear Mixed Models in Psychology: A Systematic Review. *Front Psychol*. 2021;12.

doi:10.3389/fpsyg.2021.666182

200. Thiele J, Markussen B. Potential of GLMM in modelling invasive spread. *CABI Rev*. 2012;2012(5):1-10. doi:10.1079/PAVSNNR20127016

201. Quan W, Zhou H, Xu D, Li S, Baker JS, Gu Y. Competitive and Recreational Running Kinematics Examined Using Principal Components Analysis. *Healthcare*. 2021;9(10):1321. doi:10.3390/healthcare9101321

202. Hennig EM, Lafortune MA. Relationships Between Ground Reaction Force and Tibial Bone Acceleration Parameters. *Int J Sport Biomech*. 1991;7(3):303-309. http://ezproxy.staffs.ac.uk/login?url=http://search.ebscohost.com/login.aspx?direct=true&db=s3h&AN=20710067&site=ehost-live

203. Butler RJ, Crowell HP, Davis IM. Lower extremity stiffness: implications for performance and injury. *Clin Biomech*. 2003;18(6):511-517. doi:10.1016/S0268-0033(03)00071-8

204. Buttfield A, Ball K. The practical application of a method of analysing the variability of within-step accelerations collected via athlete tracking devices. *J Sports Sci*. 2020;38(3):343-350. doi:10.1080/02640414.2019.1699987

205. Rapp E, Shin S, Thomsen W, Ferber R, Halilaj E. Estimation of kinematics from inertial measurement units using a combined deep learning and optimization framework. *J Biomech*. 2021;116. doi:10.1016/j.jbiomech.2021.110229

206. Weygers I, Kok M, Konings M, Hallez H, De Vroey H, Claeys K. Inertial Sensor-Based Lower Limb Joint Kinematics: A Methodological Systematic Review. *Sensors*. 2020;20(3):673. doi:10.3390/s20030673

207. Barbour B, Brunel N, Hakim V, Nadal J-P. What can we learn from synaptic weight distributions? *Trends Neurosci*. 2007;30(12):622-629. doi:10.1016/j.tins.2007.09.005

208. BLACK MI, ALLEN SJ, FORRESTER SE, FOLLAND JP. The Anthropometry of Economical Running. *Med Sci Sport Exerc*. 2020;52(3):762-770. doi:10.1249/MSS.0000000000002158

209. De Wit B, De Clercq D, Aerts P. Biomechanical analysis of the stance phase during barefoot and shod running. *J Biomech*. 2000;33(3):269-278. doi:10.1016/S0021-9290(99)00192-X

210. Bernal-Orozco MF, Posada-Falomir M, Quiñónez-Gastélum CM, et al. Anthropometric and Body Composition Profile of Young Professional Soccer Players. *J Strength Cond Res*. 2020;34(7):1911-1923. doi:10.1519/JSC.0000000000003416

211. Varley MC, Fairweather IH, Aughey RJ. Validity and reliability of GPS for measuring instantaneous velocity during acceleration, deceleration, and constant motion. *J Sports Sci*. 2012;30(2):121-127. doi:10.1080/02640414.2011.627941

212. Hart JM, Kerrigan DC, Fritz JM, Ingersoll CD. Jogging Kinematics After Lumbar Paraspinal Muscle Fatigue. *J Athl Train*. 2009;44(5):475-481. doi:10.4085/1062-6050-44.5.475

213. Quan W, Ren F, Sun D, Fekete G, He Y. Do Novice Runners Show Greater Changes in Biomechanical Parameters? Ugbolue UC, ed. *Appl Bionics Biomech*. 2021;2021:1-8. doi:10.1155/2021/8894636

214. Hunter JP, Marshall RN, McNair PJ. Segment-interaction analysis of the stance limb in sprint running. *J Biomech*. 2004;37(9):1439-1446.

doi:10.1016/j.jbiomech.2003.12.018

215. Malinzak RA, Colby SM, Kirkendall DT, Yu B, Garrett WE. A comparison of knee joint motion patterns between men and women in selected athletic tasks. *Clin Biomech*. 2001;16(5):438-445. doi:10.1016/S0268-0033(01)00019-5

216. Lee JB, Sutter KJ, Askew CD, Burkett BJ. Identifying symmetry in running gait using a single inertial sensor. *J Sci Med Sport*. 2010;13(5):559-563. doi:10.1016/j.jsams.2009.08.004

217. Mercer JA, Devita P, Derrick TR, Bates BT. Individual effects of stride length and frequency on shock attenuation during running. *Med Sci Sports Exerc*. 2003;35(2):307-313. doi:10.1249/01.MSS.0000048837.81430.E7

218. Moran J, Liew B, Ramirez-Campillo R, Granacher U, Negra Y, Chaabene H. The effects of plyometric jump training on lower-limb stiffness in healthy individuals: A meta-analytical comparison. *J Sport Heal Sci*. 2023;12(2):236-245. doi:10.1016/j.jshs.2021.05.005

219. Brazier J, Bishop C, Simons C, Antrobus M, Read PJ, Turner AN. Lower Extremity Stiffness. *Strength Cond J*. 2014;36(5):103-112. doi:10.1519/SSC.0000000000000094

220. Myhill N, Weaving D, Robinson M, Barrett S, Emmonds S. Concurrent validity and between-unit reliability of a foot-mounted inertial measurement unit to measure velocity during team sport activity. *Sci Med Footb*. Published online July 2023:1-9. doi:10.1080/24733938.2023.2237493

221. Waldron M, Harding J, Barrett S, Gray A. A New Foot-Mounted Inertial Measurement System in Soccer: Reliability and Comparison to Global Positioning Systems for

Velocity Measurements During Team Sport Actions. *J Hum Kinet*. 2021;77:37-50. doi:10.2478/hukin-2021-0010

222. Sandmæl S, van den Tillaar R, Dalen T. Validity and Reliability of Polar Team Pro and Playermaker for Estimating Running Distance and Speed in Indoor and Outdoor Conditions. *Sensors*. 2023;23(19):8251. doi:10.3390/s23198251

223. Falbriard M, Meyer F, Mariani B, Millet GP, Aminian K. Accurate Estimation of Running Temporal Parameters Using Foot-Worn Inertial Sensors. *Front Physiol*. 2018;9. doi:10.3389/fphys.2018.00610

224. Lago-Peñas C, Rey E, Lago-Ballesteros J, Casais L, Domínguez E. Analysis of work-rate in soccer according to playing positions. *Int J Perform Anal Sport*. 2009;9(2):218-227. doi:10.1080/24748668.2009.11868478

225. Hands DE, Janse de Jonge X. Current time-motion analyses of professional football matches in top-level domestic leagues: a systematic review. *Int J Perform Anal Sport*. 2020;20(5):747-765. doi:10.1080/24748668.2020.1780872

226. Kanko RM, Laende EK, Davis EM, Selbie WS, Deluzio KJ. Concurrent assessment of gait kinematics using marker-based and markerless motion capture. *J Biomech*. 2021;127:110665. doi:10.1016/j.jbiomech.2021.110665

Appendices

Appendix 1: Ethical approval for conducting research.

Health Sciences

PROPORTIONATE REVIEW APPROVAL FEEDBACK

Researcher name:	Michael Lawson
Title of Study:	The ability of the GPS based IMU's to measure biomechanical responses to workload and their application in team sports
Status of approval:	Approved

Thank you for addressing the committee's comments. Your research proposal has now been approved by the Ethics Panel and you may commence the implementation phase of your study. You should note that any divergence from the approved procedures and research method will invalidate any insurance and liability cover from the University. You should, therefore, notify the Panel of any significant divergence from this approved proposal.

You should arrange to meet with your supervisor for support during the process of completing your study and writing your dissertation.

When your study is complete, please send the ethics committee an end of study report. A template can be found on the ethics BlackBoard site.

Signed: Dr Roozbeh Naemi **Date: 13.06.2018**

Chair of the Health Sciences Ethics Panel

Appendix 2: Category 1 fixed effect variables GLMM results for each dependent variable.

Table S1: Category 1 Peak RES Accelerations GLMM results

Plane of Motion	Joint/Segment	Gait Phase	F	df1	df2	Coefficient	Sig.
FLEX/EXT	ANKLE	IFC	0.801	1	78	0.011	0.374
ADD/ABD	ANKLE	MS	0.210	1	78	-0.018	0.648
FLEX/EXT	ANKLE	MS	10.046	1	78	-0.077	0.002
INT/EXT ROT	ANKLE	MS	6.376	1	78	0.063	0.014
ADD/ABD	FOOT	MS	0.213	1	78	-0.023	0.646
ADD/ABD	FOOT	TFC	0.074	1	78	0.006	0.787
FLEX/EXT	HIP	IFC	7.665	1	78	-0.048	0.007
ADD/ABD	HIP	MS	4.752	1	78	0.060	0.032
FLEX/EXT	HIP	MS	0.249	1	78	0.016	0.619
FLEX/EXT	HIP	TFC	8.929	1	78	0.079	0.004
FLEX/EXT	KNEE	IFC	11.589	1	78	0.049	0.001
INT/EXT ROT	KNEE	IFC	2.498	1	78	-0.027	0.118
ADD/ABD	KNEE	TFC	1.035	1	78	-0.041	0.312
FLEX/EXT	KNEE	TFC	1.350	1	78	0.044	0.249
INT/EXT ROT	KNEE	TFC	7.394	1	78	0.052	0.008
ADD/ABD	PELVIS	MS	1.566	1	78	-0.059	0.215
FLEX/EXT	PELVIS	MS	26.417	1	78	0.225	0.000
INT/EXT ROT	PELVIS	TFC	1.159	1	78	0.038	0.285
FLEX/EXT	SHANK	TFC	6.068	1	78	-0.105	0.016
ADD/ABD	THORAX	IFC	2.908	1	78	0.159	0.092
FLEX/EXT	THORAX	IFC	5.406	1	78	0.092	0.023
INT/EXT ROT	THORAX	IFC	5.769	1	78	0.118	0.019
ADD/ABD	THORAX	MS	0.046	1	78	0.021	0.830
FLEX/EXT	THORAX	MS	3.657	1	78	-0.071	0.060
ADD/ABD	THORAX	TFC	5.521	1	78	-0.243	0.021
INT/EXT ROT	THORAX	TFC	7.802	1	78	-0.149	0.007
Corrected Model			**54.181**	**26**	**78**	**5.167**	**0.000**

FLEX/EXT = Flexion/Extension angle; ADD/ABD = Adduction/Abduction angle; INT/EXT ROT = Internal/External Rotation angle

Table S2. Category 1 Peak VT Accelerations GLMM results

Plane of Motion	Joint/Segment	Gait Phase	F	df1	df2	Coefficient	Sig.
FLEX/EXT	ANKLE	IFC	0.027	1	76	0.004	0.869
ADD/ABD	ANKLE	MS	2.361	1	76	-0.072	0.129
FLEX/EXT	ANKLE	MS	18.208	1	76	-0.134	0.000
INT/EXT ROT	ANKLE	MS	6.116	1	76	0.074	0.016
ADD/ABD	ANKLE	TFC	0.138	1	76	-0.011	0.711
FLEX/EXT	FOOT	IFC	0.003	1	76	-0.001	0.955
ADD/ABD	FOOT	MS	0.023	1	76	-0.009	0.881
ADD/ABD	FOOT	TFC	0.263	1	76	0.013	0.610

FLEX/EXT	HIP	IFC	6.735	1	76	0.057	0.011
FLEX/EXT	HIP	MS	0.234	1	76	-0.020	0.630
FLEX/EXT	HIP	TFC	0.531	1	76	0.034	0.468
ADD/ABD	KNEE	IFC	0.156	1	76	-0.015	0.694
FLEX/EXT	KNEE	IFC	1.546	1	76	-0.035	0.217
INT/EXT ROT	KNEE	IFC	2.547	1	76	-0.034	0.115
ADD/ABD	KNEE	TFC	8.669	1	76	-0.134	0.004
FLEX/EXT	KNEE	TFC	0.053	1	76	0.012	0.818
INT/EXT ROT	KNEE	TFC	0.302	1	76	0.014	0.584
INT/EXT ROT	PELVIS	IFC	4.921	1	76	-0.146	0.030
ADD/ABD	PELVIS	MS	6.290	1	76	-0.132	0.014
FLEX/EXT	PELVIS	MS	12.961	1	76	0.189	0.001
INT/EXT ROT	PELVIS	TFC	4.225	1	76	0.137	0.043
FLEX/EXT	SHANK	TFC	1.170	1	76	-0.059	0.283
ADD/ABD	THORAX	IFC	3.883	1	76	-0.076	0.052
FLEX/EXT	THORAX	IFC	4.425	1	76	0.090	0.039
INT/EXT ROT	THORAX	IFC	0.537	1	76	0.044	0.466
FLEX/EXT	THORAX	MS	3.537	1	76	-0.081	0.064
INT/EXT ROT	THORAX	MS	0.458	1	76	0.042	0.501
INT/EXT ROT	THORAX	TFC	9.192	1	76	-0.112	0.003
Corrected Model			**48.064**	**28**	**76**	**4.357**	**0.000**

FLEX/EXT = Flexion/Extension angle; ADD/ABD = Adduction/Abduction angle; INT/EXT ROT = Internal/External Rotation angle

Table S3. Category 1 Peak AP Accelerations GLMM results

Plane of Motion	Joint/Segment	Gait Phase	F	df1	df2	Coefficient	Sig.
FLEX/EXT	ANKLE	IFC	3.905	1	63	0.018	0.053
INT/EXT ROT	ANKLE	IFC	0.248	1	63	-0.010	0.620
FLEX/EXT	ANKLE	MS	0.157	1	63	-0.019	0.694
INT/EXT ROT	ANKLE	MS	4.302	1	63	0.045	0.042
FLEX/EXT	ANKLE	TFC	1.304	1	63	0.016	0.258
ADD/ABD	FOOT	IFC	0.535	1	63	-0.010	0.467
FLEX/EXT	FOOT	MS	0.015	1	63	-0.006	0.902
FLEX/EXT	FOOT	TFC	10.875	1	63	-0.026	0.002
INT/EXT ROT	FOOT	TFC	0.219	1	63	0.007	0.641
ADD/ABD	HIP	IFC	0.039	1	63	-0.004	0.843
ADD/ABD	HIP	MS	0.575	1	63	0.015	0.451
FLEX/EXT	KNEE	IFC	0.001	1	63	0.001	0.970
FLEX/EXT	KNEE	MS	0.079	1	63	0.014	0.780
INT/EXT ROT	KNEE	MS	3.035	1	63	0.026	0.086
ADD/ABD	KNEE	TFC	0.341	1	63	0.018	0.561
ADD/ABD	PELVIS	IFC	4.908	1	63	-0.092	0.030
FLEX/EXT	PELVIS	IFC	6.221	1	63	-0.058	0.015
INT/EXT ROT	PELVIS	IFC	0.363	1	63	0.019	0.549
ADD/ABD	PELVIS	MS	0.001	1	63	0.001	0.977
FLEX/EXT	PELVIS	MS	3.929	1	63	0.038	0.052
INT/EXT ROT	PELVIS	MS	0.470	1	63	-0.020	0.496
ADD/ABD	SHANK	IFC	3.471	1	63	-0.046	0.067

FLEX/EXT	SHANK	IFC	0.582	1	63	-0.012	0.448
INT/EXT ROT	SHANK	IFC	0.498	1	63	-0.014	0.483
INT/EXT ROT	SHANK	TFC	0.255	1	63	0.007	0.615
FLEX/EXT	THIGH	MS	0.049	1	63	0.014	0.825
FLEX/EXT	THIGH	TFC	1.732	1	63	0.019	0.193
FLEX/EXT	THORAX	IFC	0.132	1	63	0.014	0.717
INT/EXT ROT	THORAX	IFC	1.997	1	63	0.034	0.162
ADD/ABD	THORAX	MS	0.249	1	63	-0.027	0.620
FLEX/EXT	THORAX	MS	6.238	1	63	0.063	0.015
INT/EXT ROT	THORAX	MS	0.708	1	63	-0.032	0.403
ADD/ABD	THORAX	TFC	1.628	1	63	0.064	0.207
FLEX/EXT	THORAX	TFC	0.859	1	63	-0.030	0.357
INT/EXT ROT	THORAX	TFC	0.039	1	63	-0.006	0.844
ADD/ABD	TRUNK	IFC	0.807	1	63	-8.071	0.372
INT/EXT ROT	TRUNK	IFC	0.164	1	63	2.730	0.687
ADD/ABD	TRUNK	MS	0.328	1	63	6.459	0.569
INT/EXT ROT	TRUNK	MS	1.488	1	63	5.425	0.227
ADD/ABD	TRUNK	TFC	0.060	1	63	1.833	0.807
INT/EXT ROT	TRUNK	TFC	2.764	1	63	-7.632	0.101
Corrected Model			**56.433**	**41**	**63**	**1.268**	**0.000**

FLEX/EXT = Flexion/Extension angle; ADD/ABD = Adduction/Abduction angle; INT/EXT ROT = Internal/External Rotation angle

Table S4. Category 1 Peak ML Accelerations GLMM results.

Plane of Motion	Joint/Segment	Gait Phase	F	df1	df2	Coefficient	Sig.
ADD/ABD	ANKLE	MS	0.540	1	72	0.043	0.465
FLEX/EXT	ANKLE	MS	0.436	1	72	0.010	0.511
INT/EXT ROT	ANKLE	MS	4.689	1	72	0.029	0.034
ADD/ABD	ANKLE	TFC	0.003	1	72	-0.002	0.959
INT/EXT ROT	ANKLE	TFC	0.475	1	72	0.025	0.493
FLEX/EXT	FOOT	IFC	0.487	1	72	0.005	0.487
ADD/ABD	FOOT	MS	0.786	1	72	-0.045	0.378
FLEX/EXT	FOOT	MS	1.019	1	72	0.024	0.316
ADD/ABD	FOOT	TFC	0.006	1	72	0.004	0.941
INT/EXT ROT	FOOT	TFC	1.133	1	72	-0.040	0.291
ADD/ABD	HIP	MS	0.877	1	72	-0.013	0.352
ADD/ABD	HIP	TFC	0.028	1	72	0.002	0.867
INT/EXT ROT	HIP	TFC	0.475	1	72	0.013	0.493
ADD/ABD	KNEE	TFC	2.780	1	72	-0.052	0.100
FLEX/EXT	KNEE	TFC	0.225	1	72	-0.004	0.636
INT/EXT ROT	KNEE	TFC	0.234	1	72	0.034	0.630
ADD/ABD	PELVIS	MS	1.177	1	72	-0.028	0.282
FLEX/EXT	PELVIS	MS	0.032	1	72	-0.002	0.858
FLEX/EXT	SHANK	IFC	1.953	1	72	-0.015	0.167
ADD/ABD	SHANK	MS	0.320	1	72	0.035	0.573
ADD/ABD	SHANK	TFC	5.275	1	72	0.104	0.025
INT/EXT ROT	SHANK	TFC	0.063	1	72	-0.017	0.803
ADD/ABD	THIGH	IFC	0.443	1	72	0.012	0.508

FLEX/EXT	THIGH	TFC	4.973	1	72	0.024	0.029
INT/EXT ROT	THIGH	TFC	0.262	1	72	0.036	0.610
INT/EXT ROT	THORAX	IFC	4.177	1	72	-0.024	0.045
ADD/ABD	THORAX	TFC	0.723	1	72	-0.013	0.398
FLEX/EXT	THORAX	MS	2.725	1	72	0.010	0.103
ADD/ABD	TRUNK	IFC	0.937	1	72	-5.823	0.336
FLEX/EXT	TRUNK	IFC	0.781	1	72	-8.119	0.380
ADD/ABD	TRUNK	MS	0.927	1	72	5.775	0.339
FLEX/EXT	TRUNK	MS	0.915	1	72	8.561	0.342
Corrected Model			**33.407**	**32**	**72**	**-0.796**	**0.000**

FLEX/EXT = Flexion/Extension angle; ADD/ABD = Adduction/Abduction angle; INT/EXT ROT = Internal/External Rotation angle

Appendix 3: Category 2 fixed effect variables GLMM results for each dependent variable.

Table S5. Category 2 Peak RES Accelerations GLMM results

Plane of Motion	Segment	Gait Phase	F	df1	df2	Coefficient	Sig.
ADD/ABD	FOOT	IFCMS	0.296	1	69	0.001	0.588
ADD/ABD	FOOT	MSTFC	0.051	1	69	0.000	0.821
FLEX/EXT	FOOT	MSTFC	0.131	1	69	0.000	0.718
ML	FOOT	IFCMS	1.249	1	69	0.841	0.268
VT	FOOT	IFCMS	0.185	1	69	-0.232	0.668
FLEX/EXT	PELVIS	IFCMS	7.083	1	69	-0.002	0.010
INT/EXT ROT	PELVIS	IFCMS	58.932	1	69	0.007	0.000
FLEX/EXT	PELVIS	MSTFC	17.954	1	69	-0.020	0.000
INT/EXT ROT	PELVIS	MSTFC	0.000	1	69	0.000	0.986
AP	PELVIS	IFCMS	58.028	1	69	5.694	0.000
AP	PELVIS	MSTFC	0.079	1	69	0.239	0.779
VT	PELVIS	MSTFC	0.024	1	69	-0.194	0.877
ADD/ABD	SHANK	IFCMS	129.176	1	69	-0.029	0.000
FLEX/EXT	SHANK	IFCMS	0.513	1	69	-0.002	0.476
INT/EXT ROT	SHANK	IFCMS	6.054	1	69	0.002	0.016
ADD/ABD	SHANK	MSTFC	17.843	1	69	0.016	0.000
INT/EXT ROT	SHANK	MSTFC	17.866	1	69	-0.007	0.000
VT	SHANK	IFCMS	8.084	1	69	-2.925	0.006
FLEX/EXT	THIGH	IFCMS	6.988	1	69	-0.007	0.010
ADD/ABD	THIGH	IFCMS	0.599	1	69	-0.001	0.442
ADD/ABD	THIGH	MSTFC	0.012	1	69	0.000	0.914
FLEX/EXT	THIGH	MSTFC	50.753	1	69	0.023	0.000
INT/EXT ROT	THIGH	MSTFC	1.125	1	69	-0.001	0.293
AP	THIGH	IFCMS	4.750	1	69	-1.618	0.033
ML	THIGH	IFCMS	2.990	1	69	-2.523	0.088

VT	THIGH	IFCMS	9.134	1	69	3.143	0.004
AP	THIGH	MSTFC	3.919	1	69	1.213	0.052
ML	THIGH	MSTFC	0.354	1	69	-0.953	0.554
VT	THIGH	MSTFC	0.553	1	69	-0.661	0.460
AP	THORAX	IFCMS	2.961	1	69	-2.055	0.090
VT	THORAX	IFCMS	9.551	1	69	3.448	0.003
AP	THORAX	MSTFC	8.038	1	69	-3.921	0.006
ML	THORAX	MSTFC	16.764	1	69	-5.004	0.000
VT	THORAX	MSTFC	6.395	1	69	2.787	0.014
Corrected Model			**720.828**	**34**	**69**	**1.540**	**0.000**

FLEX/EXT = Flexion/Extension angular velocity; ADD/ABD = Adduction/Abduction angular velocity; INT/EXT ROT = Internal/External Rotation angular velocity; VT = Vertical linear velocity; AP = Anterior/Posterior linear velocity; ML = Medial/Lateral linear velocity

Table S6. Category 2 Peak VT Accelerations GLMM results

Plane of Motion	Segment	Gait Phase	F	df1	df2	Coefficient	Sig.
ML	FOOT	IFCMS	1.164	1	77	0.813	0.284
VT	FOOT	IFCMS	2.648	1	77	0.878	0.108
ML	FOOT	MSTFC	0.123	1	77	-0.263	0.727
FLEX/EXT	PELVIS	IFCMS	2.669	1	77	0.003	0.106
INT/EXT ROT	PELVIS	IFCMS	1.580	1	77	-0.002	0.213
FLEX/EXT	PELVIS	MSTFC	10.356	1	77	-0.015	0.002
INT/EXT ROT	PELVIS	MSTFC	7.135	1	77	0.010	0.009
AP	PELVIS	IFCMS	28.251	1	77	4.621	0.000
AP	PELVIS	MSTFC	20.643	1	77	4.226	0.000
VT	PELVIS	MSTFC	4.242	1	77	-2.383	0.043
INT/EXT ROT	SHANK	MSTFC	0.494	1	77	-0.001	0.484
FLEX/EXT	SHANK	IFCMS	3.668	1	77	0.007	0.059
VT	SHANK	IFCMS	12.028	1	77	-4.843	0.001
FLEX/EXT	THIGH	IFCMS	7.207	1	77	-0.009	0.009
FLEX/EXT	THIGH	MSTFC	13.276	1	77	0.011	0.000
INT/EXT ROT	THIGH	MSTFC	1.290	1	77	0.002	0.260
ADD/ABD	THIGH	IFCMS	1.099	1	77	-0.002	0.298
AP	THIGH	IFCMS	9.691	1	77	-2.322	0.003
ML	THIGH	IFCMS	0.557	1	77	-1.521	0.458
VT	THIGH	IFCMS	15.197	1	77	5.872	0.000
VT	THIGH	MSTFC	15.551	1	77	-3.043	0.000
AP	THORAX	IFCMS	21.838	1	77	-8.697	0.000
AP	THORAX	MSTFC	3.289	1	77	-3.362	0.074
ML	THORAX	MSTFC	6.072	1	77	-3.362	0.016
VT	THORAX	MSTFC	21.601	1	77	5.061	0.000
VT	THORAX	IFCMS	2.984	1	77	2.802	0.088
Corrected Model			**149.788**	**26**	**77**	**0.448**	**0.000**

FLEX/EXT = Flexion/Extension angular velocity; ADD/ABD = Adduction/Abduction angular velocity; INT/EXT ROT = Internal/External Rotation angular velocity; VT = Vertical linear velocity; AP = Anterior/Posterior linear velocity; ML = Medial/Lateral linear velocity

Table S7. Category 2 Peak AP Accelerations GLMM results

Plane of Motion	Segment	Gait Phase	F	df1	df2	Coefficient	Sig.
ADD/ABD	FOOT	MSTFC	3.211	1	77	0.002	0.077
FLEX/EXT	FOOT	IFCMS	0.035	1	77	0.000	0.853

INT/EXT ROT	FOOT	MSTFC	9.761	1	77	-0.004	0.003
VT	FOOT	IFCMS	0.146	1	77	-0.188	0.703
AP	FOOT	MSTFC	17.064	1	77	-0.497	0.000
ML	FOOT	MSTFC	25.803	1	77	2.314	0.000
VT	FOOT	MSTFC	2.754	1	77	-0.419	0.101
INT/EXT ROT	PELVIS	IFCMS	4.280	1	77	0.001	0.042
FLEX/EXT	PELVIS	MSTFC	10.811	1	77	0.007	0.002
INT/EXT ROT	PELVIS	MSTFC	1.162	1	77	0.002	0.284
AP	PELVIS	IFCMS	0.364	1	77	-0.270	0.548
ML	PELVIS	IFCMS	0.167	1	77	-0.322	0.684
AP	PELVIS	MSTFC	2.723	1	77	-0.818	0.103
ML	PELVIS	MSTFC	2.735	1	77	-1.356	0.102
FLEX/EXT	SHANK	MSTFC	1.013	1	77	-0.001	0.317
ML	SHANK	MSTFC	2.777	1	77	-1.160	0.100
AP	SHANK	IFCMS	0.426	1	77	-0.130	0.516
INT/EXT ROT	THIGH	IFCMS	20.197	1	77	0.003	0.000
ADD/ABD	THIGH	MSTFC	1.206	1	77	0.001	0.275
FLEX/EXT	THIGH	MSTFC	13.545	1	77	0.004	0.000
AP	THIGH	IFCMS	0.008	1	77	0.037	0.930
VT	THIGH	IFCMS	0.006	1	77	-0.037	0.939
ML	THIGH	MSTFC	2.816	1	77	1.760	0.097
AP	THORAX	IFCMS	22.669	1	77	4.412	0.000
VT	THORAX	IFCMS	40.150	1	77	3.336	0.000
ML	THORAX	MSTFC	12.792	1	77	2.872	0.001
Corrected Model			**53.932**	**26**	**77**	**0.138**	**0.000**

FLEX/EXT = Flexion/Extension angular velocity; ADD/ABD = Adduction/Abduction angular velocity; INT/EXT ROT = Internal/External Rotation angular velocity; VT = Vertical linear velocity; AP = Anterior/Posterior linear velocity; ML = Medial/Lateral linear velocity

Table S8. Category 2 Peak ML Accelerations GLMM results.

Plane of Motion	Segment	Gait Phase	F	df1	df2	Coefficient	Sig.
FLEX/EXT	FOOT	IFCMS	0.370	1	76	0.000	0.545
ADD/ABD	FOOT	MSTFC	9.472	1	76	0.002	0.003
INT/EXT ROT	FOOT	MSTFC	34.960	1	76	-0.005	0.000
INT/EXT ROT	FOOT	IFCMS	27.337	1	76	-0.003	0.000
ADD/ABD	FOOT	IFCMS	19.251	1	76	0.003	0.000
VT	FOOT	IFCMS	4.126	1	76	0.421	0.046
ML	FOOT	MSTFC	0.579	1	76	0.130	0.449
ADD/ABD	PELVIS	IFCMS	1.528	1	76	-0.001	0.220
INT/EXT ROT	PELVIS	IFCMS	0.310	1	76	0.000	0.580
ADD/ABD	PELVIS	MSTFC	16.599	1	76	0.004	0.000
INT/EXT ROT	PELVIS	MSTFC	1.554	1	76	0.001	0.216
AP	PELVIS	MSTFC	1.617	1	76	-0.302	0.207
ML	PELVIS	MSTFC	14.879	1	76	-1.769	0.000
ADD/ABD	SHANK	IFCMS	49.245	1	76	-0.009	0.000
FLEX/EXT	SHANK	IFCMS	3.291	1	76	-0.002	0.074
ADD/ABD	SHANK	MSTFC	1.249	1	76	0.001	0.267
FLEX/EXT	SHANK	MSTFC	1.710	1	76	0.000	0.195

INT/EXT ROT	SHANK	MSTFC	3.193	1	76	0.002	0.078
VT	SHANK	IFCMS	0.702	1	76	0.245	0.405
ADD/ABD	THIGH	IFCMS	2.788	1	76	-0.001	0.099
ADD/ABD	THIGH	MSTFC	2.199	1	76	0.001	0.142
FLEX/EXT	THIGH	MSTFC	15.719	1	76	0.004	0.000
INT/EXT ROT	THIGH	MSTFC	12.536	1	76	-0.002	0.001
ML	THIGH	IFCMS	2.087	1	76	-0.806	0.153
ML	THIGH	MSTFC	0.005	1	76	-0.032	0.944
ML	THORAX	IFCMS	3.922	1	76	0.971	0.051
VT	THORAX	IFCMS	3.900	1	76	0.721	0.052
Corrected Model			**55.376**	**27**	**76**	**0.612**	**0.000**

FLEX/EXT = Flexion/Extension angular velocity; ADD/ABD = Adduction/Abduction angular velocity; INT/EXT ROT = Internal/External Rotation angular velocity; VT = Vertical linear velocity; AP = Anterior/Posterior linear velocity; ML = Medial/Lateral linear velocity

Appendix 4: Comparison between the actual and predicted peak accelerometer accelerations from each GLMM.

Table S9. Actual Peak RES Accelerations vs GLMM predicted for Category 1 &2 variables.

		Category 1 GLMM variables				Category 2 GLMM variables			
Speed	**Actual (g)**	**Predicted (g)**	**Difference (g)**	**Lower 95% LOA (g)**	**Upper 95% LOA (g)**	**Predicted (g)**	**Difference (g)**	**Lower 95% LOA (g)**	**Upper 95% LOA (g)**
10 km/h	3.964	3.987	0.023	-0.50	0.55	3.973	0.009	-0.53	0.54
11 km/h	4.096	4.079	-0.017	-0.28	0.25	4.058	-0.038	-0.48	0.41
12 km/h	4.192	4.233	0.041	-0.48	0.56	4.229	0.037	-0.21	0.28
13 km/h	4.414	4.407	-0.007	-0.36	0.34	4.381	-0.033	-0.83	0.76
14 km/h	4.439	4.470	0.031	-0.21	0.28	4.471	0.033	-0.32	0.39
15 km/h	4.534	4.480	-0.054	-0.40	0.29	4.517	-0.017	-0.21	0.17
16 km/h	4.609	4.644	0.035	-0.25	0.32	4.679	0.070	-0.26	0.40
17 km/h	4.651	4.564	-0.088	-0.62	0.44	4.625	-0.026	-0.54	0.48
18 km/h	4.754	4.741	-0.013	-0.64	0.62	4.750	-0.005	-0.08	0.07
AVG	**4.406**	**4.401**	**-0.005**	**-0.416**	**0.405**	**4.409**	**0.003**	**-0.383**	**0.389**
STDev	**0.806**	**0.759**	**0.216**	**0.155**	**0.140**	**0.785**	**0.217**	**0.230**	**0.204**

Table S10. Actual Peak VT Accelerations vs GLMM predicted for Category 1 & 2 variables.

		Category 1 GLMM variables				Category 2 GLMM variables			
Speed	Actual (g)	Predicted (g)	Difference (g)	Lower 95% LOA (g)	Upper 95% LOA (g)	Predicted (g)	Difference (g)	Lower 95% LOA (g)	Upper 95% LOA (g)
10 km/h	3.768	3.799	0.031	-0.60	0.67	3.880	0.112	-0.53	0.75
11 km/h	3.893	3.898	0.005	-0.23	0.24	3.891	-0.003	-0.03	0.02
12 km/h	3.962	4.004	0.042	-0.48	0.57	3.973	0.011	-0.39	0.41
13 km/h	4.199	4.126	-0.072	-0.47	0.33	4.206	0.007	-0.75	0.76
14 km/h	4.174	4.197	0.023	-0.35	0.39	4.207	0.033	-0.57	0.63
15 km/h	4.259	4.174	-0.086	-0.51	0.34	4.188	-0.071	-0.78	0.63
16 km/h	4.284	4.359	0.075	-0.41	0.56	4.416	0.132	-0.44	0.70
17 km/h	4.308	4.199	-0.109	-0.60	0.39	4.338	0.030	-0.66	0.72
18 km/h	4.416	4.413	-0.003	-0.64	0.63	4.262	-0.154	-1.01	0.70
AVG	**4.140**	**4.130**	**-0.010**	**-0.478**	**0.457**	**4.151**	**0.011**	**-0.571**	**0.593**
STDev	**0.872**	**0.841**	**0.245**	**0.131**	**0.150**	**0.822**	**0.319**	**0.278**	**0.238**

Table S11. Actual Peak AP Accelerations vs GLMM predicted for Category 1 & 2 variables.

		Category 1 GLMM variables				Category 2 GLMM variables			
Speed	Actual (g)	Predicted (g)	Difference (g)	Lower 95% LOA (g)	Upper 95% LOA (g)	Predicted (g)	Difference (g)	Lower 95% LOA (g)	Upper 95% LOA (g)
10 km/h	1.356	1.351	-0.004	-0.14	0.13	1.340	-0.016	-0.28	0.25
11 km/h	1.384	1.375	-0.010	-0.12	0.10	1.393	0.009	-0.20	0.21
12 km/h	1.436	1.440	0.003	-0.16	0.17	1.413	-0.024	-0.22	0.17
13 km/h	1.452	1.498	0.046	-0.22	0.31	1.477	0.024	-0.21	0.25
14 km/h	1.543	1.558	0.015	-0.20	0.24	1.547	0.004	-0.14	0.14
15 km/h	1.618	1.608	-0.009	-0.10	0.09	1.647	0.030	-0.17	0.23
16 km/h	1.709	1.687	-0.022	-0.18	0.13	1.651	-0.058	-0.28	0.16
17 km/h	1.722	1.729	0.007	-0.14	0.15	1.737	0.015	-0.22	0.25
18 km/h	1.738	1.743	0.006	-0.14	0.16	1.739	0.001	-0.17	0.18
AVG	**1.551**	**1.554**	**0.004**	**-0.155**	**0.162**	**1.549**	**-0.002**	**-0.209**	**0.206**
STDev	**0.446**	**0.438**	**0.084**	**0.038**	**0.069**	**0.435**	**0.107**	**0.048**	**0.043**

Table S12. Actual Peak ML Accelerations vs GLMM predicted for Category 1 & 2 variables.

		Category 1 GLMM variables				Category 2 GLMM variables			
Speed	Actual (g)	Predicted (g)	Difference (g)	Lower 95% LOA (g)	Upper 95% LOA (g)	Predicted (g)	Difference (g)	Lower 95% LOA (g)	Upper 95% LOA (g)
10 km/h	0.773	0.771	-0.002	-0.19	0.19	0.766	-0.006	-0.08	0.06
11 km/h	0.768	0.800	0.032	-0.19	0.26	0.806	0.038	-0.16	0.23

12 km/h	0.844	0.849	0.005	-0.13	0.13	0.839	-0.006	-0.06	0.04
13 km/h	0.907	0.885	-0.022	-0.16	0.11	0.915	0.009	-0.03	0.05
14 km/h	0.958	0.956	-0.001	-0.17	0.17	0.957	-0.001	-0.19	0.19
15 km/h	0.977	0.970	-0.007	-0.13	0.12	0.991	0.013	-0.14	0.17
16 km/h	1.045	1.046	0.001	-0.16	0.16	1.040	-0.005	-0.21	0.20
17 km/h	1.076	1.057	-0.019	-0.14	0.11	1.060	-0.016	-0.22	0.19
18 km/h	1.164	1.076	-0.088	-0.41	0.23	1.129	-0.035	-0.32	0.25
AVG	**0.946**	**0.934**	**-0.011**	**-0.186**	**0.164**	**0.945**	**-0.001**	**-0.155**	**0.153**
STDev	**0.269**	**0.255**	**0.096**	**0.086**	**0.053**	**0.258**	**0.087**	**0.091**	**0.080**